

Louisiana State University

LSU Scholarly Repository

LSU Master's Theses

Graduate School

2004

Kinetic analysis of *Kluyveromyces marxianus* yeast strain

Erika Guimaraes Madeira Reeves

Louisiana State University and Agricultural and Mechanical College

Follow this and additional works at: https://repository.lsu.edu/gradschool_theses



Part of the [Engineering Commons](#)

Recommended Citation

Reeves, Erika Guimaraes Madeira, "Kinetic analysis of *Kluyveromyces marxianus* yeast strain" (2004). *LSU Master's Theses*. 917.

https://repository.lsu.edu/gradschool_theses/917

This Thesis is brought to you for free and open access by the Graduate School at LSU Scholarly Repository. It has been accepted for inclusion in LSU Master's Theses by an authorized graduate school editor of LSU Scholarly Repository. For more information, please contact gradetd@lsu.edu.

KINETIC ANALYSIS OF *KLUYVEROMYCES MARXIANUS* YEAST STRAIN

A Thesis

Submitted to the Graduate Faculty of the
Louisiana State University and
Agricultural and Mechanical College
in partial fulfillment of the
requirements for the degree of
Master of Science in Biological and
Agricultural Engineering

in

The Department of Biological and Agricultural Engineering

by

Erika Guimarães Madeira Reeves
B.S., Louisiana State University, 2001
May 2004

*Dedicated to my sister, the late Camila Guimarães Madeira and my husband Edward
Patrick Reeves for loving and supporting me throughout my life.*

ACKNOWLEDGEMENTS

First and foremost, I would like to thank God for giving me the strength and persistence to complete this research. I would also like to acknowledge the many people whose advice and support was invaluable throughout the pursuit of this thesis.

I want to express great thanks and appreciation to my major advisors Dr. Caye Drapcho and Dr. Terry Walker, and my committee member Dr. James Geaghan for their guidance and great efforts in encouraging and supporting me in accomplishing this research. I would also like to express my gratitude to Dr. Richard Bentgson for accepting me into this graduate program, and to the department head Dr. Daniel Thomas for committing to my thesis. Acknowledgments and thanks are also extended to all of the people that have helped me in ways that they will never know; Shufang Liu, Hui Zhu, Tom Bride, Brian White, Lee Madsen, Timothy Moran, and the BAE office staff and faculty.

I would like to acknowledge my beautiful family in Zachary, LA and my parents in Campinas, S.P. Brazil for their appreciation and everlasting love.

I would like to thank my wonderful husband, Edward Patrick Reeves (“Pat”), and my wonderful friend, Laure Capouya, for their prayers, strength, amazing encouragement, and help throughout my research with their unconditional love. Thanks to all my friends in America and in Brazil that have continued to pray for my strength and ongoing success in life.

TABLE OF CONTENTS

	Page
ACKNOWLEDGEMENTS	iii
LIST OF TABLES.....	vi
LIST OF FIGURES.....	vii
ABSTRACT.....	xii
CHAPTER 1. INTRODUCTION.....	1
CHAPTER 2. REVIEW OF LITERATURE.....	6
2.1 Introduction.....	6
2.2 Sweet Potato Waste.....	6
2.3 Ethanol Production.....	8
2.4 Ethanol Producing Yeast.....	10
2.5 Fermentors.....	12
2.6 Simultaneous Saccharification and Fermentation Process.....	13
2.7 Summary of Journal Articles.....	13
CHAPTER 3. KINETIC STUDIES OF KLUYVEROMYCES MARXIANUS UNDER AEROBIC AND ANAEROBIC CONDITIONS.....	19
3.1 Materials and Methods.....	19
3.1.1 Preparation of Yeast and Medium.....	19
3.1.1.1 Culture Storage Procedure.....	19
3.1.1.2 Agar Growth.....	20
3.1.1.3 Glucose Media.....	21
3.1.2 Fermentation Reactors.....	22
3.1.2.1 Orbital Shaker Bed.....	22
3.1.2.2 Bioflo [®] 2000 Fermentors.....	23
3.1.2.3 Batch Reactor Experiments.....	23
3.1.3 Analytical Methods.....	26
3.1.3.1 COD (Chemical Oxygen Demand) Measurement.....	26
3.1.3.2 TSS (Total Suspended Solids) Measurement.....	27
3.1.3.3 OD (Optical Density) Measurement.....	27
3.1.3.4 HPLC (High Performance Liquid Chromatography) Measurement.....	27
3.1.3.5 GC (Gas Chromatography) Measurement.....	31
3.1.4 Kinetic Parameter Determination.....	35
3.1.4.1 Monod Model.....	35
3.1.4.2 Linearization Methods.....	36
3.1.4.2.1 Lineweaver-Burk Plot.....	37
3.1.4.2.2 Hanes Plot.....	38
3.1.4.3 Nonlinear Method.....	38

3.2 Results and Discussion.....	40
3.2.1 Aerobic Environment.....	40
3.2.1.1 Orbital Shaker Bed.....	40
3.2.1.1.1 Substrate Concentration Comparison with Tap Water.....	41
3.2.1.2 Two-Liter Bioflo® 2000 Fermentors.....	44
3.2.1.2.1 Water Comparison with 1,000 mg/L Glucose Media.....	44
3.2.1.2.2 Substrate Comparison Using Tap Water.....	46
3.2.1.2.3 The Linearization Methods for the Laboratory Data Set.....	50
3.2.1.2.4 The Nonlinear Method Approach for the Laboratory Data Set using Statistics Analysis Software (SAS).....	52
3.2.2 Anaerobic Environment.....	53
3.2.2.1 Two-Liter Bioflo® 2000 Fermentors.....	53
3.2.2.1.1 Substrate Concentration Comparisons.....	54
3.2.2.1.2 Soluble Substrate Determination Using HPLC Method.....	59
3.2.2.1.3 Product Quantification Using GC Method.....	64
3.3 Conclusions.....	66
3.4 References.....	69
 CHAPTER 4. BIOLOGICAL GROWTH KINETIC PARAMETER DETERMINATION ANALYSIS USING MONTE CARLO SIMULATIONS.....	73
4.1 Introduction.....	73
4.2 Materials and Methods.....	77
4.2.1 Data Generation.....	78
4.2.2 Data Simulation.....	79
4.2.3 Monte Carlo Fitting the Models.....	80
4.2.3.1 Nonlinear Method.....	81
4.2.3.2 Linear Method.....	82
4.3 Results and Discussion.....	84
4.3.1 Results from the Data Generation and Simulation.....	84
4.3.2 Results for the Nonlinear Models.....	88
4.3.3 Results for the Linear Models.....	99
4.3.4 Comparison between Nonlinear and Linear Models.....	102
4.4 Conclusions.....	103
4.5 Future Recommendations.....	106
4.6 References.....	107
 CHAPTER 5. SUMMARY AND CONCLUSIONS.....	109
 REFERENCES.....	112
 APPENDIX A SWEET POTATO WASTE PRELIMINARY EXPERIMENT.....	119

APPENDIX B DIONEX DX-600 HPLC (HIGH PERFORMANCE LIQUID CHROMATOGRAPHY) METHOD.....	136
APPENDIX C GLUCOSE BROTH MEDIA AND SWEET POTATO ANALYSIS.....	139
APPENDIX D SHIMADZU GC 17-A GAS CHROMATOGRAPHY, CLASS VP CHROMATOGRAPHY DATA SYSTEM.....	144
APPENDIX E THE PICTURES OF THE <i>KLUYVEROMYCES MARXIANUS</i> YEAST STRAIN.....	147
APPENDIX F THE CALIBRATION CURVES FOR <i>KLUYVEROMYCES</i> <i>MARXIANUS</i>	149
APPENDIX G AEROBIC AND ANAEROBIC CONDITIONS USING THE TWO-LITER BIOFLO® 2000 FERMENTORS.....	151
APPENDIX H SAS CODE FOR THE AEROBIC EXPERIMENTAL DATA SET USING THE TWO-LITER BIOFLO® 2000 FERMENTORS.....	156
APPENDIX I SAS (VERSION 9.0) PROGRAM FOR THE “BIOLOGICAL GROWTH KINETIC PARAMETER DETERMINATION ANALYSIS USING MONTE CARLO SIMULATIONS”.....	160
APPENDIX J THE SAS PROGRAM DEVELOPED TO PLOT THE HISTOGRAMS FOR THE MEANS OF μ_{\max} AND K_s AND THE HISTOGRAMS OF μ_{\max}	171
VITA.....	179

LIST OF TABLES

	Page
Table 2.1 Summary of Journal Articles for the Growth Kinetic Parameters.....	15
Table 3.1.1 Summary of the Overall Reactor Experiments.....	24
Table 3.1.2 Summary of the Probes Performance for the Experiments using the 2-L Bioflo® 2000 Reactor (KC-25 D New Brunswick Scientific)..	26
Table 3.1.3 Sample Dilutions for the Anaerobic Experiments.....	30
Table 3.2.1 The Comparison of the Specific Growth Rates for Different Substrates.....	43
Table 3.2.2 Water Comparison for the 1,000 mg/L Glucose Concentration.....	46
Table 3.2.3 Summary for the Different Substrate Concentrations during Exponential Growth Phase.....	49
Table 3.2.4 Summary of the Kinetic Parameters from the Linearization Methods.....	51
Table 3.2.5 The Kinetic Parameter Results from the Nonlinear Model using SAS for the Aerobic Experiments.....	53
Table 3.2.6 Summary of the Anaerobic Experiments for the Exponential Growth Phase.....	58
Table 4.2.1 The Twelve Combinations for the Nonlinear Method.....	82
Table 4.2.2 The Combinations for the Linear Method.....	83
Table 4.3.1 The Nonlinear Models Output for K_s and μ_{max} without errors.....	88
Table 4.3.2 The Nonlinear Models Output for K_s and μ_{max} with errors.....	89
Table 4.3.3 The Hanes Equation Output for each Combinations.....	100
Table 4.3.4 The Lineweaver-Burk Equation Output for each Combinations.....	101

LIST OF FIGURES

	Page
Fig. 1.1 The enzyme process configured as separate hydrolysis and fermentation (Biofuels program (http://www.ott.doe.gov/biofuels/enzymatic.html)).....	2
Fig. 1.2 The enzyme process configured for simultaneous saccharification and Fermentation (Biofuels program(http://www.ott.doe.gov/biofuels/enzymatic.html)).....	3
Fig. 3.1.1 <i>Kluyveromyces marxianus</i> yeast cells from the agar petri dish, used to inoculate the glucose media.....	21
Fig. 3.1.2 <i>Kluyveromyces marxianus</i> yeast cells from the Orbital Shaker bed grown aerobically in glucose media.....	22
Fig. 3.1.3 Two-Liter Bioflo [®] 2000 Fermentor (New Brunswick Scientific).....	25
Fig. 3.1.4 Picture of the actual HPLC setup and computer from our Biological Engineering Laboratory, LSU.....	29
Fig. 3.1.5 Typical Chromatogram of External Sugar Standards for 50 ppm (mg/L)..	29
Fig. 3.1.6 Typical Chromatogram of Sugar Results from ‘Sample-7t103’ (Reactor 7,500mg/L for time 35 hours, third replicate).....	30
Fig. 3.1.7 The actual Shimadzy GC 17-A version 3.0 Gas Chromatography System Used to evaluate ethanol production from the anaerobic experiment.....	31
Fig. 3.1.8 Typical Chromatogram for the External Alcohol Standards of 50 ppm (mg/L) Concentration (plotted in mVolts versus minutes).....	33
Fig. 3.1.9 Typical Batch Growth Curve.....	35
Fig. 3.2.1 The Calibration Curve for 1,000 mg/L glucose media for <i>Kluyveromyces</i> <i>marxianus</i> yeast strain.....	41
Fig. 3.2.2 The Natural log of biomass versus time for 500 mg/L glucose media....	42
Fig. 3.2.3 The specific growth rate determination during exponential phase for 500 mg/L glucose media.....	42
Fig. 3.2.4 Natural log of biomass versus time for 1,000 mg/L glucose media.....	43
Fig. 3.2.5 Specific growth rate for 1,000 mg/L glucose media.....	43

Fig. 3.2.6 Natural log of biomass versus time for 1,000 mg/L glucose media with either de-ionized or tap water.....	45
Fig. 3.2.7 Specific growth rate for 1,000 mg/L glucose media with either de-ionized or tap water.....	45
Fig. 3.2.8 The Ln(biomass) versus time for the Bioflo® 2000 fermentors first run.....	47
Fig. 3.2.9 Specific growth rate for 200, 400, and 1,000 mg/L glucose media during the exponential growth phase for the first run.....	47
Fig. 3.2.10 The Ln(biomass) versus time for the Bioflo® 2000 fermentors second run.....	48
Fig. 3.2.11 Specific growth rate for 200, 400, and 800 mg/L glucose media during the exponential growth phase.....	48
Fig. 3.1.12 Hanes Plot for the averaged substrate over the specific growth rate versus averaged substrate concentrations.....	50
Fig. 3.1.13 Lineweaver-Burk Plot for the averaged substrate over the specific growth rate versus averaged substrate concentrations.....	51
Fig. 3.2.14 Medium Range COD Standard Curve	54
Fig. 3.2.15 High Range COD Standard Curve.....	54
Fig. 3.2.16 The natural log of biomass versus time grown on 200, 400, and 1,000 mg/L initial substrate concentrations.....	55
Fig. 3.2.17 The natural log of biomass versus time grown on 1,000, 2,000, and 3,000 mg/L initial substrate concentrations.....	56
Fig. 3.2.18 The exponential growth phase for 1,000, 2,000, and 3,000 mg/L initial substrate concentrations and linear regression fits.....	56
Fig. 3.2.19 The natural log of biomass versus time grown on 3,000, 10,000, and 80,000 mg/L initial substrate concentrations.....	57
Fig. 3.2.20 The exponential growth phase for 3,000, and 10,000 mg/L initial substrate concentrations and linear regression fits.....	57
Fig. 3.2.21 The natural log of biomass versus time for 5,000, 7,500, and 15,000 mg/L initial substrate concentrations.....	57

Fig. 3.2.22 The exponential growth phase for 5,000, 7,500, and 15,000 mg/L initial substrate concentrations and linear regression fits.....	58
Fig. 3.2.23 Glucose Standard Curve.....	60
Fig. 3.2.24 Fructose Standard Curve.....	60
Fig. 3.2.25 Glucose concentration for the third anaerobic experiment.....	61
Fig. 3.2.26 Fructose concentration for the third anaerobic experiment.....	61
Fig. 3.2.27 Total sugar substrate concentration for the third anaerobic experiment (glucose and fructose added together).....	62
Fig. 3.2.28 Glucose concentration for the fourth anaerobic experiment.....	62
Fig. 3.2.29 Fructose concentration for the fourth anaerobic experiment.....	63
Fig. 3.2.30 Total sugar substrate concentration for the fourth anaerobic experiment (glucose and fructose added together).....	63
Fig. 3.2.31 Ethanol concentration for the anaerobic experiment.....	65
Fig. 4.3.1 Biomass (mg/L) for the high substrate concentration versus time.....	84
Fig. 4.3.2 Biomass (mg/L) for the medium substrate concentration versus time.....	85
Fig. 4.3.3 Biomass (mg/L) for the low substrate concentration versus time.....	85
Fig. 4.3.4 The high substrate concentration (mg/L) versus time.....	86
Fig. 4.3.5 The medium substrate concentration (mg/L) versus time.....	86
Fig. 4.3.6 The low substrate concentration (mg/L) versus time.....	87
Fig. 4.3.7 Lee Equation-Fixed-Given.....	92
Fig. 4.3.8 Lee Equation-Fixed-Not Given.....	92
Fig. 4.3.9 Lee Equation-Float-Given.....	93
Fig. 4.3.10 Lee Equation-Float-Not Given.....	93
Fig. 4.3.11 Robinson Equation-Fixed-Given.....	94
Fig. 4.3.12 Robinson Equation-Fixed-Not Given.....	94

Fig. 4.3.13 Robinson Equation-Float-Given.....	95
Fig. 4.3.14 Robinson Equation-Float-Not Given.....	95
Fig. 4.3.15 Shuler & Kargi Equation-Fixed-Given.....	96
Fig. 4.3.16 Shuler & Kargi Equation-Fixed-Not Given.....	96
Fig. 4.3.17 Shuler & Kargi Equation-Float-Given.....	97
Fig. 4.3.18 Shuler & Kargi Equation-Float-Not Given.....	97

ABSTRACT

This research investigated the growth kinetic parameters (K_s and μ_{\max}) of the *Kluyveromyces marxianus* yeast strain for a batch process under aerobic and anaerobic conditions at 45°C using the Two-Liter Bioflo[®] 2000 Fermentors and the Orbital Shaker Bed with 250mL flasks (New Brunswick Scientific). This yeast strain was grown in twelve different glucose media concentrations (Anderson et al. 1986), ranging from 200 mg/L to 80,000 mg/L. Several analytical techniques were used, such as COD measurement to determine soluble and total substrate concentrations, TSS and OD measurements to determine biomass formation, HPLC measurements to determine carbohydrate concentrations, and GC measurements to determine alcohol concentrations. The growth kinetic parameters were investigated using the Monod Model which accounts for microbial growth in any environmental condition, assuming decay a constant for the microorganism negligible during the exponential growth phase. The nonlinear (the ‘Lee’ equation) and linear (the ‘Hanes’ and the ‘Lineweaver-Burk’ equations) methods were used to estimate the kinetic parameters (K_s and μ_{\max}) for the aerobic and the anaerobic conditions. Neither the nonlinear nor the linear method succeeded with reasonable estimations for the growth kinetic parameters (K_s and μ_{\max}). The lack of information and investigation on the nonlinear and the linear models in the literature, concerning *Kluyveromyces marxianus* kinetic analysis initiated an investigation of these nonlinear and linear models using a mathematical simulation technique called the ‘Monte Carlo method’ with the SAS (Statistical Analysis Software) program (version 9). The sweet potato waste was used as substrate for a preliminary experiment which was designed to determine the growth kinetic parameters at 40°C, 45°C, and 50°C and the Arrhenius

parameters for the *Kluyveromyces marxianus* yeast strain (Appendix A). This preliminary experiment used the three Two-Liter Bioflo[®] 2000 fermentors (New Brunswick Scientific) for a batch process under anaerobic conditions.

CHAPTER 1

INTRODUCTION

Louisiana and North Carolina are the two largest sweet potato producing states in the United States, accounting for 57 percent of the 1993 output (USDA, 1993). Sweet potato industries in these states, as throughout the world, generate large amounts of sweet potato waste. Approximately 40% of the sweet potato waste ends up in wastewaters and as waste solids (Hill et al. 1992). Therefore, certain techniques have been developed to use sweet potato waste to produce usable substances that will benefit society.

Ethanol production has been investigated since 1972, when the price of oil increased and this scarcity prompted the development of an extensive evaluation of alternative technologies for the production of liquid fuels (Jones et al.1983). Any biological materials, such as crops, grains, woods, food processing wastes, or any waste materials from agriculture, can be bioconverted to useful products such as energy, chemicals and feedstock (Tan et al. 1986). These biological materials provide amounts of carbohydrates, proteins and biopolymers, which can be converted to usable sugars for microorganisms to utilize and then produce useful products.

The current method of producing ethanol from sweet potato waste in industry is by a non-simultaneous saccharification followed by fermentation process (NSSF). In the NSSF process, starches are broken down into glucose by high temperature acid or enzyme treatments, and then this glucose is cooled down for the yeast cells to use the glucose for growth and alcohol production (Figure 1.1). This current method (NSSF) has many disadvantages such as high operation and maintenance costs, high-energy costs,

high capital costs, large volume of reactors are needed, and many unit operations are required.

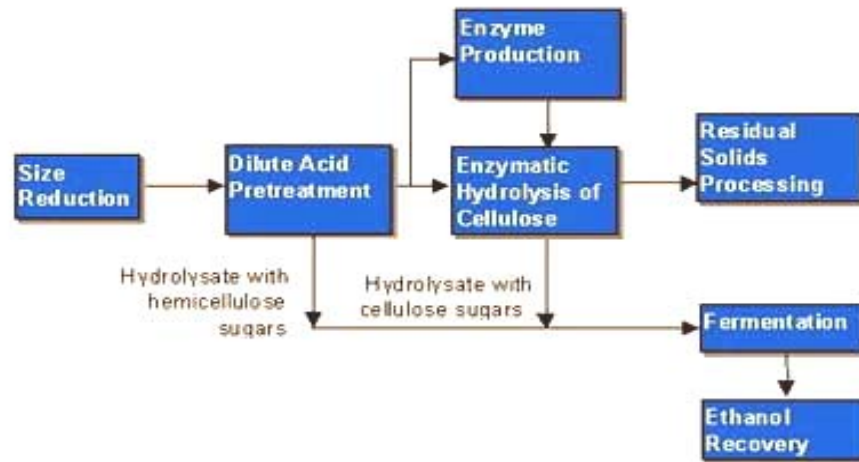


Figure 1.1 The enzyme process configured as separate hydrolysis and fermentation (Biofuels program (<http://www.ott.doe.gov/biofuels/enzymatic.html>)).

A possible way for the industries to increase their economic efficiency would be by combining in one reactor the enzymatic step with the fermentation step. The optimal temperature suitable for enzymatic activity and ethanol production to occur simultaneously has been determined to be 35°C with a pH of 5.8 (Suresh et al. 1999). However, when the temperature increases above 35°C, then the amylase activity increases, but this temperature is not suitable for the organism *Saccharomyces cerevisiae* (currently used by industries) to grow exponentially (Suresh et al. 1999). Some industries have proposed to use a simultaneous saccharification and fermentation (SSF) process to produce ethanol from raw starch using the *Saccharomyces cerevisiae* yeast strain, but genetic modification of this yeast strain may be necessary for growth at high temperatures (above 40°C). Therefore, one of the emergent problems associated with the

SSF process is the difference in optimum temperature for saccharification and fermentation which must be performed simultaneously in this technology. As a consequence of the higher temperature requirement for saccharification, there are endeavors to use thermotolerant yeasts in the SSF process (Bollok et al. 2000). Figure 1.2 shows the schematic of SSF process available for industries.

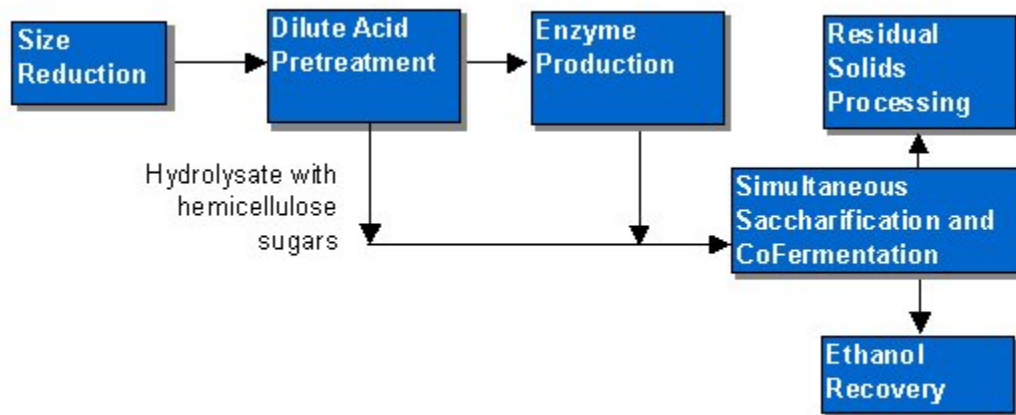


Figure 1.2 The enzyme process configured for simultaneous saccharification and fermentation (Biofuels program <http://www.ott.doe.gov/biofuels/enzymatic.html>)).

The NSSF and SSF processes are both able to produce high yields of ethanol, but these ethanol yields could be even greater if a thermally tolerant system were designed. In other words, to design a system to accommodate thermotolerant yeast cells to enhance the yield of ethanol in SSF process. The problem with *Saccharomyces cerevisiae* yeast and *Zymomonas mobilis* bacteria is that both have an optimum temperature requirement of 35°C for growth, while the enzymes optimum temperature in the range of 45°C to 60°C (Morrison 1990). As renewable materials are used for ethanol production with inexpensive lignocellulosic substrates (such as sweet potato skins or softwoods), when lignocellulosic materials are used as a substrate in a SSF process, the fermenting yeast

must be adapted to inhibitors. Therefore the most frequently investigated thermotolerant yeast strains are the *Kluyveromyces sp.* (Bollok et al. 2000). The advantage of the heat-tolerant yeast, such as species from *Kluyveromyces sp.*, is that its optimum temperature for growth is from 45 to 50°C, which is not very different from the enzymes' optimum activity temperature range (45-60°C). The SSF process can reduce bioreactor volume, resulting in greater decrease of capital costs and energy expenses for industries. Even though there are several journals published on ethanol production using *Kluyveromyces sp.* yeast strains, those journals have not shown complete results on growth kinetic parameter determinations under either aerobic or anaerobic conditions.

The priorities of this research were to define the growth characteristics of the *Kluyveromyces marxianus* yeast strain, and to use statistical analysis software (SAS program) to model these growth characteristics from differential equations.

The specific objectives of this research were as follows:

1. To determine the growth kinetic parameters for the *Kluyveromyces marxianus* yeast strain under aerobic and anaerobic conditions from the laboratory experimental data sets using nonlinear and linear equations.
2. To determine ethanol production from the *Kluyveromyces marxianus* yeast strain using Gas Chromatography (GC) under anaerobic conditions.
3. To fit and evaluate the nonlinear and the linear equations using the 'Monte Carlo' simulation method with SAS software (Statistical Analysis Software) to determine the growth kinetic parameters during exponential growth phase for microorganisms following Monod kinetic behavior.

The following chapters of this thesis are as follows: Chapter 2 is the literature review on bioprocess engineering with several topics, such as ‘Sweet Potato Waste’, ‘Ethanol Production’, ‘Ethanol Producing Yeast’, ‘Fermentors’, ‘Simultaneous Saccharification and Fermentation’, and a summary table (2.1) of some important journal articles; Chapter 3 is kinetic studies of *Kluyveromyces marxianus* under aerobic and anaerobic conditions, with detailed materials and methods, results and conclusions; Chapter 4 is the biological growth kinetic parameter determination analysis using Monte Carlo simulations with detailed information on how we performed this simulation; along with overall conclusions; references, and several appendices that were used in this thesis.

The chapters 3 and 4 are constructed in way to satisfy the intent to publish these in referred journals.

CHAPTER 2

REVIEW OF LITERATURE

2.1 Introduction

Many opportunities may be explored using different costless renewable waste materials with a lot of usable substrate for microorganisms to grow upon, and then produce useful products for society (for example, agricultural food waste, wood chips, molasses, whey permeate, rice straw, and newspaper waste). Most renewable energy source (carbon source) can be used in a fermentation process with microorganisms to produce bio-ethanol. Ethanol production benefits the society and the environment and may be easily produced from thermotolerant yeast strains with a capacity to withstand high temperatures and different types of fermentation processes. There are a lot of ways to maximize ethanol production, such as through continuous SSF process with either two-stages in sequence (first aerobic and then anaerobic stages) or with a two-stage anaerobic fermentation process with cell recycling (Banat et al. 1996). Therefore, we have summarized some important topics to illustrate the importance of how to use renewable waste to produce useful products.

2.2 Sweet Potato Waste

One of the most promising energy producing crops is sweet potato because it has a long growing season, does not need to be immediately harvested, (unlike corn), is drought tolerant, and grows in deep sand. In addition, six different sweet potato cultivars have already been studied under various cultural conditions to characterize their potential for ethanol production (Jones et al.1983). Sweet potato cultivars containing $\geq 40\%$ dry

matter (DM), and have the capacity to produce ethanol (which averaged 10 mt/ha over three years), were developed by Clemson University. Different anaerobic environments in sweet potato root metabolisms were studied among four different sweet potato cultivars to observe ethanol production in those roots, which turned out to be directly related to the rate-limiting reaction of pyruvate decarboxylase and alcohol dehydrogenase enzymes (Chang et. al. 1983). Thus, in the North Carolina State University study, that submerged storage roots under water to replace the O₂ and N₂ gases with CO₂ gas, this process was found to increase the CO₂ concentration in the roots and resulted in greater ethanol production (Chang et. al. 1983).

Sweet potato waste has a high content of starch and cellulose, which is a suitable substrate for ethanol production. By fermenting this sweet potato waste, we can not only generate new sources of energy (bio-ethanol), but also help to clear our wastewaters from the solids of sweet potato waste (Hill et al., 1992).

Kim and Hamdy (1985) studied the acid hydrolysis of sweet potato, which was conducted for maximal ethanol production using 1N HCl at 110°C. They concluded that 1N HCl concentration at 110°C temperature was the most effective for maximizing reduced sugar levels to 84.2 DE (dextrose equivalent, % dry weight), with a minimum amount of HMF (Hydroxymethylfurfural) formation. They used *Saccharomyces cerevisiae* at 37°C to ferment the acid hydrolyzed SPS, and this fermentation lasted more than 24 hours, producing 41.6g (200 proof) alcohol from 1400mL media, containing 8% total solids prepared from 400g of fresh sweet potato (Kim et. al., 1984).

2.3 Ethanol Production

Currently, ethanol blended in fuels represents more than 12% of the U.S. motor gasoline sales. Ethanol blended fuel is also widely marketed across the country as a high-octane enhancer and oxygenate that reduces air pollution and improves automobile performance (BBI Inc.). Ethanol production reduces our energy costs for petroleum fuel, which reduces the overall gasoline prices that benefits consumers. Ethanol can also be blended up to 10% under the warranties of all the major auto manufacturers, domestic and foreign, marketed in the U.S.A. BBI Inc. has discovered that 80% of all revenue generated by an ethanol facility is spent within a 50 mile radius of the plant, thereby creating substantial rural economic development.

The National Renewable Energy Laboratory (NREL) has also been researching other ways that ethanol can be used as a fuel additive, as it can reduce vehicles' carbon monoxide and other smog-causing emissions. "Flexible-fuel vehicles", which run on mixtures of gasoline and up to 85% of ethanol, are now available on the market, which show the public that alternative vehicles do exist and have better qualities for our environment (NREL).

The U.S. Department of Energy (DOE) has found that the ethanol industry is responsible for approximately 200,000 jobs, and that ethanol production creates domestic jobs in plant construction, plant operation, plant maintenance, and plant support in the communities where ethanol is being produced (DOE). This has a tremendous impact on rural America where a decline in employment has placed increasing burdens on our cities, infrastructure and tax structures. The federal tax receipt is increased by \$3.6

billion annually as the economic activities created by the ethanol industry stay at high level productivity.

The development of high-productivity ethanol processes and reactors can potentially reduce capital costs associated with new construction and expansion of existing facilities (Mahesh et al., 1999). The proper selection of reactor configuration and fermentative microorganisms can also be used to increase productivity, ethanol yields, and tolerance to inhibitors (Mahesh et al., 1999).

The cost of energy to produce ethanol via fermentation is only \$0.08 to \$0.16/gallon (\$0.02 to \$0.04/L), significantly less than that of petroleum based production (National Renewable Energy Laboratory, CO). The retrieved ethanol, which is primarily used as a fuel additive in automobiles, will significantly diminish fuel costs and the amount of air pollution normally produced from petroleum alone.

Ethanol can replace MTBE (methyl tertiary butyl ether), which is used to produce reformulated gasoline. MTBE was introduced to reduce carbon monoxide and volatile organic compounds released into the atmosphere. However, MTBE has already contaminated drinking water, which has caused tremendous damage to our public health. Substituting ethanol for MTBE would not cause any adverse impact to public health or to the environment (State of California).

The following are several more reasons why processing sweet potato waste into ethanol may prove beneficial:

(1) The uses of raw materials, such as sweet potato waste, are important for the production of ethanol from renewable energy resources.

- (2) Decreasing the amount of wastewater to be processed will reduce the cost of wastewater treatment, which will also increase the quality of the discharged water.
- (3) Large amounts of solid sweet potato waste used as landfill that cause several environmental problems such as odor and uncontrolled biogas production from compost mounds can be lessened through sweet potato waste processing.
- (4) The byproducts produced by fermentation have extensive uses such as in animal feed and fertilizers.

2.4 Ethanol Producing Yeast

The necessity to isolate and select thermotolerant yeasts in nature without genetic modifications was researched by many investigators to ascertain if those yeast strains were suitable for high bio-ethanol production.

Eighteen yeast strains from six genera were tested by Saigal D. (1994) to verify their ability to grow on 20% glucose media at 40°C. Subsequently, seven strains, primarily *Kluyveromyces* sp. and *Hansenula* sp. were further studied to investigate if they presented any capability to ferment in 12-20% total sugars substrate (diluted molasses) at temperature ranges of 35-43°C, to produce ethanol, and to tolerate ethanol concentrations of 5% and 7.5% (v/v). When the kinetic parameters were determined for the eight best strains at 43°C with 200g/L total sugars, *Kluyveromyces* species were considered the best strains with total reducing sugars of 4.50g/100mL/24 hours and 0.90g/100mL/48 hour, and an alcohol theoretical yield of 41% in 72 hours with a specific growth rate of 0.130 hr⁻¹. *Saccharomyces cerevisiae* was used as a control strain which was not genetically modified to withstand high temperature (Saigal D. 1994).

A total of six strains were selected among 55 strains because they could grow at 45°C, but not all could produce as high amounts of ethanol as the *Saccharomyces* and *Candida* strains. Therefore, those strains were evaluated at 40°C in batch fermentations, and only *Saccharomyces* and *Candida* were able to meet the minimum commercial ethanol production of 8% (v/v) to 14%(v/v) from 14.6 %(w/v) of glucose (Hacking et. al. 1984).

The Institute of Renewable Energy of Madrid selected 27 yeast strains among *Candida*, *Saccharomyces*, and *Kluyveromyces* species to screen their capability to grow and ferment at 32-45°C. The best yeast strains were *Kluyveromyces marxianus* and *Kluyveromyces fragilis* because they produced the highest ethanol concentration (38g/L) in a simultaneous saccharification and fermentation system (SSF) at 42-45°C in a cellulolytic system for 78 hours (Ballesteros et. al. 1991).

A thermotolerant yeast strain, *Kluyveromyces marxianus* IMB3, was studied by the University of Ulster, which found this strain capable of producing 10g/L of ethanol during growth at 45°C on a media containing milled paper and commercial cellulase. Thus, this yeast strain proved to be a candidate in simultaneous saccharification and fermentation (SSF) to convert the substrate to ethanol in a batch system (Barron et. al. 1995).

The kinetics for the thermotolerant strain of the yeast *Kluyveromyces marxianus* were obtained in glucose media for five different temperatures from 30°C to 48°C, and the maximum growth rate was 0.38 hr⁻¹ at 45°C. The highest overall ethanol yield was 92.2 % theoretical yield at 40°C, and when molasses media were used, the highest overall ethanol yield was 83% theoretical yield at 40°C (Hughes et. al. 1984).

2.5 Fermentors

Two different types of reactors for fermentation were compared: a packed-bed external circulating reactor with gel beads and one with yeast entrapped in modified calcium alginate thin gel slices, using mash of dried sweet potato as the substrate for the immobilized yeast cells. The cells presented a maximum specific growth rate of 0.536 hr^{-1} , and alcohol production for these two reactors averaged 9.5 g (EtOH)/L at 35°C (Yu et al. 1996). Banat et al. (1996) investigated *Kluyveromyces marxianus* IMB3 and found it capable of producing ethanol from different carbon sources such as lactose, cellobiose, xylose, and whey permeate, at 45°C . A batch experiment was done to find out the growth rate, ethanol production, and conversion efficiency at 45°C using 10g/L of different carbon sources. The growth rate in glucose media was 0.63 hr^{-1} , producing 5.10g/L of ethanol and 100% conversion efficiency. Then, they performed different continuous fermentation experiments. One of these experiments was conducted under anaerobic chemostat condition at 45°C , with 75g/L of initial glucose and produced less than 1g/L of biomass and 1.8% of ethanol levels. The second experiment used two fermenters in series (aerobic-anaerobic). The third experiment used a two-stage anaerobic fermenter with cell recycling and was able to achieve 10 g/L greater biomass formation, and 4.3% (v/v) higher in ethanol production using 150 g/L of initial glucose concentration at 40°C , than using the batch experiment. Unfortunately, this research had some problems keeping the large amount of glucose inside the reactors without being “washed out” faster than the product was formed this led to a lower level of product formation, which in turn led to the conclusion that the results were due to the rapid switch of the yeast cells from aerobic conditions to anaerobic conditions. They also noticed with

the cell recycle step an increase in ethanol formation up to 7.7% (v/v) at 40°C, but eventually, over a period of weeks, cell viability reduced. This reduction was not believed to be due to high levels of ethanol because found that final levels of ethanol reached by thermotolerant yeasts were highest at 16.5 – 20.3% (v/v) with 8% of ethanol initially (Freitas et al. 1998). This yeast strain was capable of producing around 10.5 – 12.3% (v/v) of ethanol and could withstand up to 8% (v/v) of additional external ethanol.

2.6 Simultaneous Saccharification and Fermentation Process

Currently, one of the most investigated processes to produce bio-ethanol from starch and cellulose sources is called simultaneous saccharification and fermentation (SSF). The SSF process, which was first used in 1977, gives high rates and yields for ethanol production from biomass, when the organic substrates hydrolyzed by enzymes into glucose are coupled with yeast fermentation in one reactor (Mohagheghi et al. 1991). To operate an SSF system, an optimum temperature is required with respect to the saccharification enzymes, which are activated between 45-55°C. Therefore, research on thermophilic microorganisms has been steadily increasing because they are capable of growth up to 49°C and capable of producing alcohol at and above 40°C (Banat et al. 1992). Some yeasts of the genus *Kluyveromyces* were found to be more thermotolerant than *Saccharomyces* or *Candida* strains (Hacking et al. 1984).

2.7 Summary of Journal Articles

Table 2.1 shows the summary of the few journal articles which were able to determine the growth kinetic parameters, such as μ_{\max} (the maximum specific growth rate, hr^{-1}), Y_{xb} (the biomass yield, mg/L/mg/L), K_s (the half saturation constant, mg/L),

and the product formation (maximum ethanol formed, g/L) using thermotolerant yeast strains. Those articles addressed different microorganism species with different substrate types under aerobic or anaerobic conditions. The information from these articles yielded helpful comparative data for reference growth kinetic parameters.

The *Kluyveromyces* species used in many of these experiments under aerobic condition at 45°C showed a range for the maximum specific growth rate from 0.18 to 0.63 hr⁻¹, and a biomass yield of 0.2 (g/g). The *Kluyveromyces* species under anaerobic condition at 45°C showed a range for the maximum specific growth rate from 0.09 to 0.93 hr⁻¹, for the biomass yield from 0.022 to 0.1 (g/g), for the half saturation constant (K_s) of 0.065 g/L, and for the maximum ethanol production from 0.8 to 95 g/L.

The *Zygosaccharomyces* species under anaerobic condition at 43°C had a range for the maximum specific growth rate from 0.175-0.180 hr⁻¹, for the biomass yield from 0.0683-0.0731 (g/g), and for the maximum ethanol production from 29.56-28.54 g/L. The *Candida* species under anaerobic condition at 43°C had a range for the maximum specific growth rate of 0.190 hr⁻¹, for the biomass yield of 0.0934 (g/g), and for the maximum ethanol production of 31.74 g/L. The *Hansenula* species under anaerobic condition at 43°C had a range for the maximum specific growth rate from 0.180-0.160 hr⁻¹, for the biomass yield from 0.0736-0.0775 (g/g), and for the maximum ethanol production of 35.10 g/L. The *Saccharomyces* species under anaerobic condition at 43°C had a range for the maximum specific growth rate from 0.09-0.536 hr⁻¹, for the biomass yield of 0.049 (g/g), and for the maximum ethanol production from 2.79-28.54 g/L.

Table 2.1 Summary of journal articles for the growth kinetic parameters.

Authors	Microbes	Substrates	Systems	μ_{\max} (hr ⁻¹)	Y_{xb}	K_s	Maximum Ethanol (g/L)
Banat et al. 1992	Kluyveromyces marxianus IBM3	Glucose medium (10% glucose (w/v))	Batch Orbital Shaker bed at 45°C (Anaerobic condition)	0.93	-	-	59
Banat et al. 1995	Kluyveromyces marxianus IBM3	Lactose medium 10g/L	Batch Orbital Shaker bed at 45°C (Aerobic condition)	0.43- 0.5	-	-	-
		Whey permeate 10g/L		0.38- 0.43			
		Cellobiose medium 10g/L		0.18- 0.3			
		Xylose medium 10g/L		0.18- 0.26			
		Glucose medium 10g/L		0.58- 0.63			
		Glucose medium 10g/L	Batch Orbital Shaker bed at 45°C (Anaerobic condition)	0.09- 0.14			95

Table 2.1 continued

Authors	Microbes	Substrates	Systems	μ_{\max} (hr ⁻¹)	Y _{xb}	K _s	Maximum Ethanol (g/L)
Banat et al. 1996	Kluyveromyces marxianus IBM3	YFM medium (10g/L of glucose, lactose, cellobiose, or xylose)	Batch Orbital Shaker bed at 45°C (Anaerobic condition)	0.19- 0.63	-	-	0.80-16.80
			Continuous Fermentation at 45°C (Anaerobic chemostat)	-			0.7-1.8 (% v/v)
			Continuous two fermenter in a series (aerobic- anaerobic) at 45°C				3.8-4.3 (% v/v)
			Continuous two- stage anaerobic fermenter with cell recycle at 45°C				5.3-7.7 (% v/v)
Barron et al. 1995	Kluyveromyces marxianus IBM3	Cellulose medium (0.75% cellulase and 5% cellulose)	Batch Orbital Shaker bed at 45°C (Anaerobic condition)	-	-	-	6.6
Fleming et al. 1993	Kluyveromyces marxianus IBM3	Yeast sucrose medium (YSM) (10% sucrose (w/v))	Batch Orbital Shaker bed at 45°C (Anaerobic condition)	0.7	-	-	35

Table 2.1 continued

Authors	Microbes	Substrates	Systems	μ_{\max} (hr ⁻¹)	Y_{xb}	K_s	Maximum Ethanol (g/L)
Hack et al. 1998	Kluyveromyces marxianus Kluyveromyces marxianus IMB3	MYFM Glucose medium (from 15 to 300g/L)	4-Liter Braun Biostat-B Batch Fermenter at 45°C (Aerobic condition)	-	0.2 (g/g)	-	-
			Continuous Fermentation with cell recycle at 45°C (Anaerobic condition)	0.60	0.1 (g/g)	0.065 g/L	14.6
Hughes et al. 1984	Kluyveromyces marxianus	Glucose medium (140 – 160 g/L total sugars)	Batch Orbital Shaker bed at 45°C (Anaerobic condition)	0.38	0.022	-	51.0 (% theoretical yield)
		Diluted Molasses medium (140 – 160 g/L total sugars)		-	-		51.9 (% theoretical yield)

Table 2.1 continued

Authors	Microbes	Substrates	Systems	μ_{\max} (hr ⁻¹)	Y_{xb}	K_s	Maximum Ethanol (g/L)
Saigal, 1994	Zygosaccharomyces sp.	Diluted Molasses 200 g/L total sugars	Batch fermentation at 43°C (Anaerobic condition)	0.175 - 0.180	0.0683- 0.0731	-	29.56 - 28.54
	Kluyveromyces sp.			0.125 - 0.130	0.0393- 0.0453	-	50.54 - 44.14
	Candida sp.			0.190	0.0934	-	31.74
	Hansenula sp.			0.180 - 0.160	0.0736- 0.0775	-	35.10
	Saccharomyces sp.			0.125	0.049	-	28.54
Szczodrak et al. 1987	Kluyveromyces fragilis	Glucose medium (140g/L total sugars)	Batch Orbital Shaker bed at 45°C (Anaerobic condition)	0.21- 0.33	-	-	35.0-56.0
	Saccharomyces cerevisiae			0.09			19.0
	S. carlsbergensis			0.07			15.0
	S. muciparus			0.20			26.4
	S. marxianus			0.23			30.4
Yu et al. 1996	Saccharomyces cerevisiae K	Saccharified Mash of Dried Sweet Potato (12.5- 13.5% total sugars)	Batch with Immobilized cells at 35°C (Aerobic condition)	0.536	-	-	0.8 (g/L*hr)
			Immobilized cells in a packed-bed reactor with an external circulating apparatus at 35°C	-			2.79-2.35 (g/L*hr)

CHAPTER 3

KINETIC STUDIES OF *KLUYVEROMYCES MARXIANUS* UNDER AEROBIC AND ANAEROIC CONDITIONS

The yeast strain *Kluyveromyces marxianus* was studied under aerobic and anaerobic batch conditions using glucose media in the Orbital Shaker Bed and Two-Liter Bioflo[®] 2000 Fermentors to determine the kinetic parameters for this yeast growth. Biomass formation and substrate utilization over time were determined with methods including COD total and soluble, TSS, OD, and HPLC. Ethanol formed during the anaerobic environment was determined for the last experiment using GC equipment. The kinetic parameters were determined for the laboratory experimental data using the linearization method derived from Monod Model. The nonlinear, or logistic method, was unsuccessful for the laboratory experiment data sets.

3.1 Materials and Methods

3.1.1 Preparation of Yeast and Medium

3.1.1.1 Culture Storage Procedure

- Materials

Several 250mL flasks were used to grow the yeast strain in 100 mL of glucose media (Appendix C). After twelve hours of aerobic growth the cells were pipette into the 2mL sterile cryogenic vials (Nalgene Cryoware) with the sterile glycerol (Glycerin Certified A.C.S by Fisher Scientific).

- Procedures

Flasks (250mL Erlenmeyer) containing 100mL glucose media were autoclaved according to the method described by Anderson et al. (1986) using the flask cycle for 30 minutes. Autoclaved glucose media was inoculated with yeasts from the stored cryogenic vials at room temperature. A flask (250mL Erlenmeyer) with 30 g of glycerol was autoclaved using the wet cycle for 20 minutes. Under the laminar flow hood, 1.05 mL of the yeast culture was aseptically transferred into each cryogenic vial and 0.45mL of the cooled-down autoclaved glycerol was pipette into each cryogenic vial (70% yeast and 30% glycerol). The cryogenic vials were stored at -20°C freezer.

3.1.1.2 Agar Growth

- Materials

Flasks (250mL Erlenmeyer) with PDA (potato dextrose agar) media were autoclaved and poured into the petri dishes (VWR – Polystyrene disposable sterile, 100x15 mm) under the laminar flow hood to solidify.

- Procedure

The PDA media was autoclaved in 250mL flasks using the flask cycle for 20 minutes, and poured into the petri dishes. After the agar has hardened, the yeast culture was spread from the cryogenic vials into the petri dishes using a sterile metal inoculum loop. Then, the petri dishes were incubated for 2 days at room temperature. Figure 3.1.1 shows the picture of the yeast cells from a sterile petri dish using a light-phase microscope.

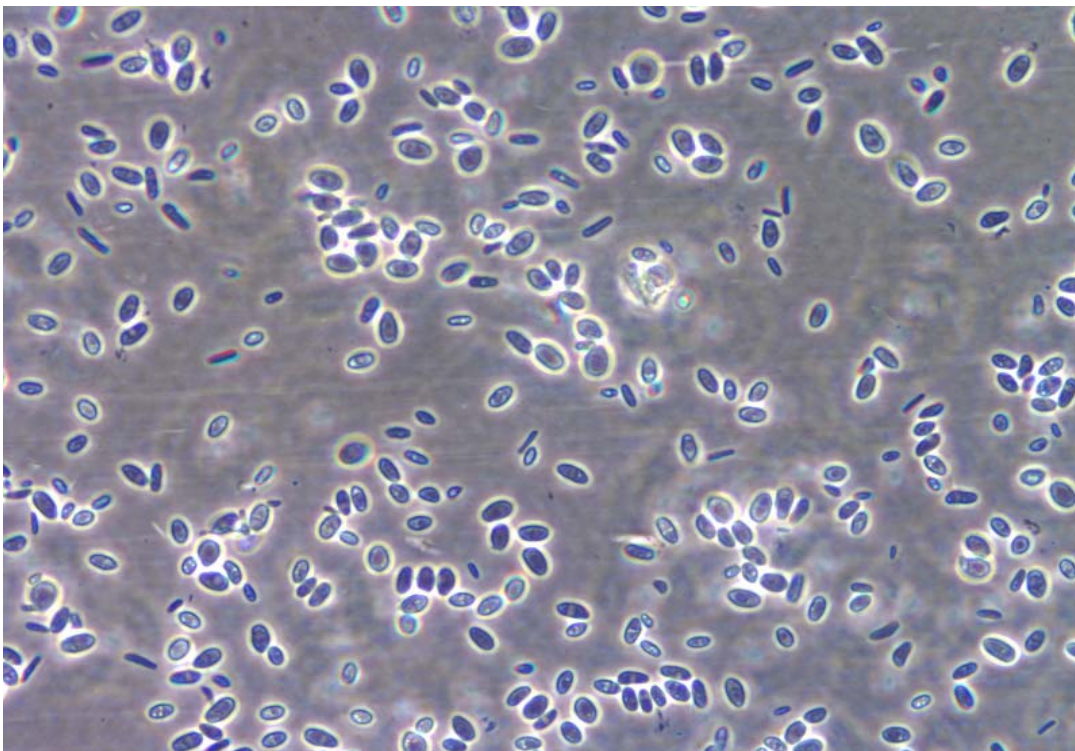


Figure 3.1.1 *Kluveromyces marxianus* yeast cells from agar petri dish, used to inoculate the glucose media.

3.1.1.3 Glucose Media

Glucose media for each pre-culture (seed) was made according to the glucose concentrations used in the reactors for either the “Orbital Shaker Bed” or the “Two-Liter Bioflo[®] 2000 Fermentors” experiments. The glucose concentrations range from 200 to 15,000 mg/L.

- Materials

The glucose media chemicals used in this procedure (Anderson et al. 1986) are available in Appendix C.

- Procedures

The pre-cultures were made in flasks (250mL Erlenmeyer) according to the designated glucose concentration, and autoclaved. After the cool-down period, the flasks

were inoculated from a single colony of the petri dishes. Then, the inoculated flasks were placed in the Orbital Shaker bed to grow for 24 hours at 45°C and 120 rpm. Figure 3.1.2 shows the picture of the yeast cells from glucose media using a light-phase microscope.

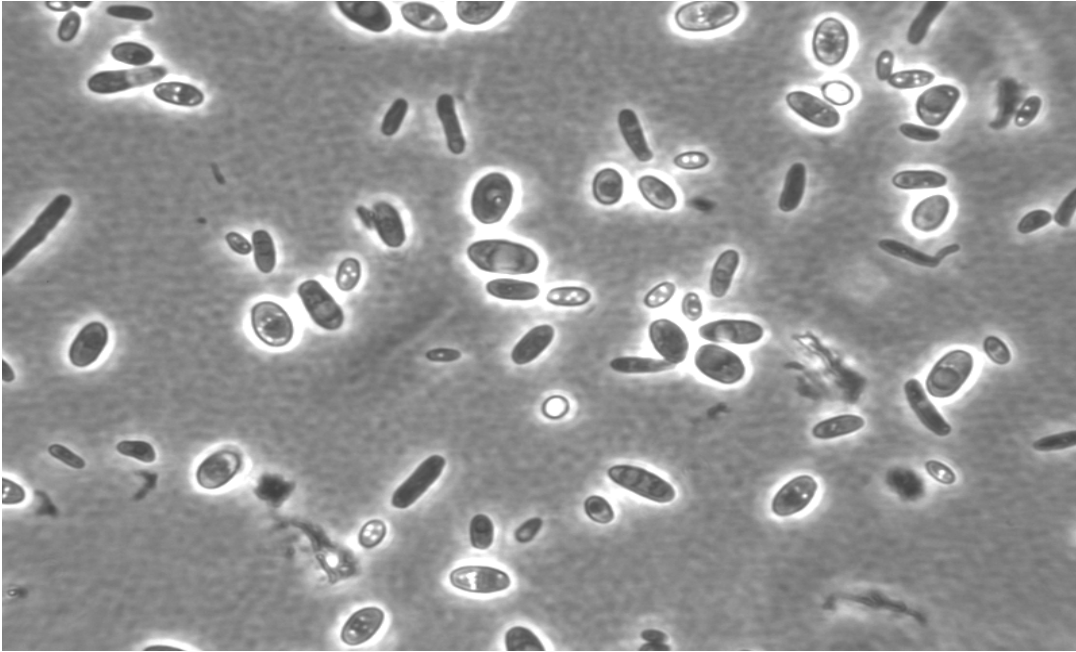


Figure 3.1.2 *Kluyveromyces marxianus* yeast cells from of the Orbital Shaker bed grown aerobically in glucose media.

3.1.2 Fermentation Reactors

3.1.2.1 Orbital Shaker Bed

The Orbital Shaker Bed (KC-25D, New Brunswick Scientific) was operated at 45°C, 120rpm, from 0 to 12 hours, or from 0 to 70 hours for aerobic batch experiments. Flasks with 250mL volume were used with glucose media with sponges on top of the flasks to allow air to pass through. The substrate concentrations used in the Orbital Shaker Bed were 500 mg/L and 1,000 mg/L glucose media.

3.1.2.2 Bioflo[®] 2000 Fermentors

Three Two-Liter Bioflo[®] 2000 Fermentors (New Brunswick Scientific CO., INC, Brunswick, NJ) were used to grow the yeast strain *Kluyveromyces marxianus*, at 45°C, and stirred speed of 150 rpm. The air pump and a nitrogen gas tank were connected to the Two-Gas Mixer (NBS-New Brunswick Scientific CO.), which contained a 0.2 µm filter connected to the air/gas inlet tubing, where a filter was used to sterilize the air before reaching the autoclaved glucose media in the vessels. For the aerobic condition experiments, the air pump line was set at 1 vvm (vessel volume per minute), while the nitrogen gas line was off. For the anaerobic condition experiments, the nitrogen gas line was set on 1 vvm, while the air pump line was off. The AFS – BioCommand, a powerful software package for NBS fermentors, windows[®] based, with graphical interface and automated data archival system which was connected to record pH, temperature, stir speed, and D.O. (dissolved oxygen). The three D.O. probes were placed in each of the Bioflo[®] 2000 vessels with the glucose media. The three pH probes were calibrated before autoclaving the vessels, while the D.O. probes were polarized for more than six hours and then calibrated after being autoclaved. After the calibration of the probes was completed, the air pump was turned off, and nitrogen gas was turned on at 1 vvm, until the vessels' environment was completely anaerobic. Nitrogen gas was then turned down to 0.5 vvm for the anaerobic experiments.

3.1.2.3 Batch Reactor Experiments

Three Two-Liter Bioflo[®] 2000 fermentors were inoculated with 5% of each substrate concentration from the pre-culture yeast (also called seed). The seed cultures were grown in flasks in the Orbital Shaker Bed (KC-25D, New Brunswick Scientific) for

24 hours, at 45°C with the speed of 150 rpm for either aerobic or anaerobic, according to the experiments conducted. The seeds were grown with the desired substrate concentration of 200 mg/L, 400 mg/L, 800 mg/L, 1,000 mg/L, 3,000 mg/L, 5,000 mg/L, 7,500 mg/L, 10,000mg/L, 15,000 mg/L and 80,000 mg/L to be used as inoculum of the same substrate concentrations already in the Bioflo[®] reactors.

A variety of experiments were conducted using the three Two-Liter Bioflo[®] 2000 reactors and the Orbital Shaker Bed. Table 3.1.1 describes the experiments conducted in this research.

Table 3.1.1 Summary of the Overall Reactor Experiments.

	Orbital shaker bed	
	Aerobic environment	
	Specific growth rate and Kinetic parameters	
	500 mg/L glucose media	Tap water
	1,000 mg/L glucose media	Tap and De-ionized water
	Bioflo[®] 2000 fermentors	
	Aerobic environment	Anaerobic environment
Kinetic Parameters	Specific growth rate	Specific growth rate
	1,000mg/L glucose media	Tap water
		De-ionized water
	Glucose media made with tap water:	Glucose media made with tap water:
	200 mg/L, 400 mg/L, 1,000mg/L	200 mg/L, 400 mg/L, 1,000mg/L
	200 mg/L, 400 mg/L, 800 mg/L	1,000 mg/L, 2,000 mg/L, 3,000 mg/L
		3,000 mg/L, 10,000 mg/L, 80,000 mg/L
		5,000 mg/L, 7,500 mg/L, 15,000 mg/L
Linear Method	Hanes Plot and Lineweaver-Burk Plot	Hanes Plot and Lineweaver-Burk Plot
Non-linear Method	Monte Carlo technique	Glucose determination using “HPLC” Alcohol determination using “GC”

The following Figure 3.1.3 is the actual picture of one Bioflo[®] 2000 fermentor used for aerobic and anaerobic experiments during this research.



Figure 3.1.3 Two-Liter Bioflo[®] 2000 Fermentor (New Brunswick Scientific)

Table 3.1.2 shows the averaged initial, maximum, and minimum values recorded by the AFS – BioCommand software for the D.O., and temperature probes for the aerobic and anaerobic experiments. The average of the pH values were from 4.5 to 5.5 (using the pH paper) throughout the aerobic and anaerobic experiments for this research.

Table 3.1.2 Summary of the Probes Performance for the Experiments using the 2-L Bioflo[®] 2000 Reactors (New Brunswick Scientific).

Aerobic Condition	Average D.O. (Dissolved Oxygen)			Average Temperature, °C		
Bioflo [®] 1	Initial 103.067	Maximum 103.733	Minimum 93.733	Initial 45.075	Maximum 45.375	Minimum 44.5
Bioflo [®] 2	Initial 109.9	Maximum 103.033	Minimum 97.366	Initial 44.575	Maximum 45.875	Minimum 43.225
Bioflo [®] 3	Initial 84.1	Maximum 100.3	Minimum 72.4	Initial 44.825	Maximum 45.125	Minimum 44.5
Anaerobic Condition	Average D.O. (Dissolved Oxygen)			Average Temperature, °C		
Bioflo [®] 1	Initial 86.36	Maximum 43.16	Minimum 0	Initial 39.18	Maximum 47.36	Minimum 44.76
Bioflo [®] 2	Initial 76.28	Maximum 36.78	Minimum 0	Initial 39.32	Maximum 47.78	Minimum 43.4
Bioflo [®] 3	Initial 99.58	Maximum 37.32	Minimum 1.42	Initial 39.64	Maximum 47.74	Minimum 44.86

3.1.3 Analytical Methods

3.1.3.1 COD (Chemical Oxygen Demand) Measurement

The COD (Chemical Oxygen Demand) procedure used for this research followed Method 5220D, Standard Methods (APHA, 1995). COD is a measure of the amount of oxygen that is required to completely oxidize an organic compound to CO₂ and H₂O, representing substrate and biomass from a bioreactor as an equivalent mass of COD.

Samples were analyzed for chemical oxygen demand (COD) analysis (Standard Method 5220 D, APHA, 1995) using the standard range (from 0 to 900 mg/L) and the high range (from 0 to 4,500 mg/L) in micro COD vials (Bioscience, Inc.). The total COD and soluble COD were tested in this study. The soluble COD was determined by filtering the samples through 0.45µm Millipore filter (mixed cellulose esters, sterile) prior to analysis. The total COD and soluble COD vials' contents were digested using the COD Reactor from HACH[®] for two hours at 302°F.

3.1.3.2 TSS (Total Suspended Solids) Measurement

The TSS procedure was used (Method 2540D, Standard Methods (APHA, 1995)) to prepare the 0.45 µm Millipore filters (mixed cellulose esters; sterile) to determine biomass concentration throughout each experiment.

3.1.3.3 OD (Optical Density) Measurement

The Optical Density (OD) for the yeast strain was measured at 680nm. The spectrophotometer used was from Spectronic Instruments, model Spectronic 20D+.

3.1.3.4 HPLC (High Performance Liquid Chromatography) Measurement

The Dionex DX-600 high performance liquid chromatography (HPLC) was equipped with; ED50 electrochemical detector (integrated pulsed amperometry detection (PAD), working electrode of gold, and reference pH electrode), vials used to analyze sugars, auto sampler AS40, GP50 gradient pump, CarboPac™ PA10 column, a mobile phase for conductivity detection of 200mM carbonate-free sodium hydroxide (NaOH), and high-quality water of high resistivity (18MΩ-cm) as free of dissolved carbon dioxide as possible.

- Carbohydrate Method

High performance liquid chromatography (HPLC) has been applied to the characterization and quantization of the simple sugars (glucose, fructose, sucrose, maltose and lactose) present in a broad variety of food items, both fresh and processed (Hurst et al. 1979). High-performance anion-exchange chromatography (HPAE) capable of separating complex mixtures of carbohydrates was used to determine the carbohydrates presented in the fermentation broth. PAD detection is a powerful

technique with a broad linear range and very low detection limits. This coupled with HPAE, permits direct quantification of nonderivatized carbohydrates. The HPAE takes advantage of the weakly acidic nature of carbohydrates to give highly selective separations at a high pH using a strong anion exchange phase (Dionex technical note 20). The anion-exchange column used was Dionex CarboPac PA-10 4 mm (10-32), which is highly sensitive for the separation of mixtures of sugar alcohol monosaccharides and disaccharides, using strong eluents such as carbonate-free sodium hydroxide (Dionex product manual, document no.031824-03). A Dionex AS40 automated sampler was used to inject 25 µl volumes of each sample poly-vial into a mobile phase running a gradient method with two eluents over a period of eighteen minutes. The mobile phase eluents were composed of carbonate-free sodium hydroxide at 200mM, and high-quality de-ionized water (18MΩ-cm), with which sodium hydroxide makes an excellent mobile phase for anion exchange. The eluents (%) and flows (ml/min) used to expedite this method are found in Appendix B. Figure 3.1.4 is the overall pictures of the Dionex DX-600 system used in this research. Concentrations of the anions were calculated from peak areas (Figure 3.1.6) and calibrated against the external sugar standards of 50, 100, and 200 ppm (Figure 3.1.5) using the Dionex Peaknet System (version 6.0) software.



Figure 3.1.4 Picture of the actual HPLC setup and computer from our Biological Engineering Laboratory, LSU.

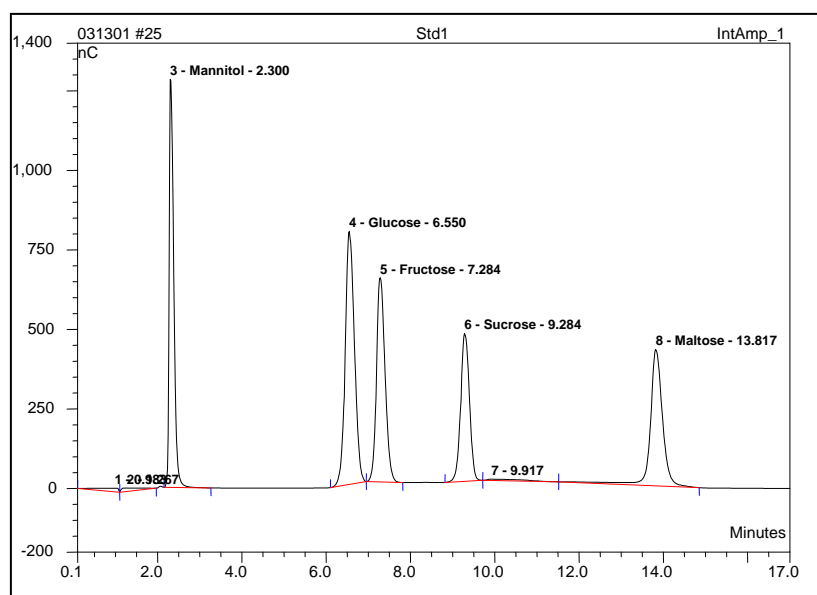


Figure 3.1.5 Typical Chromatogram of External Sugar Standards for 50ppm (mg/L).

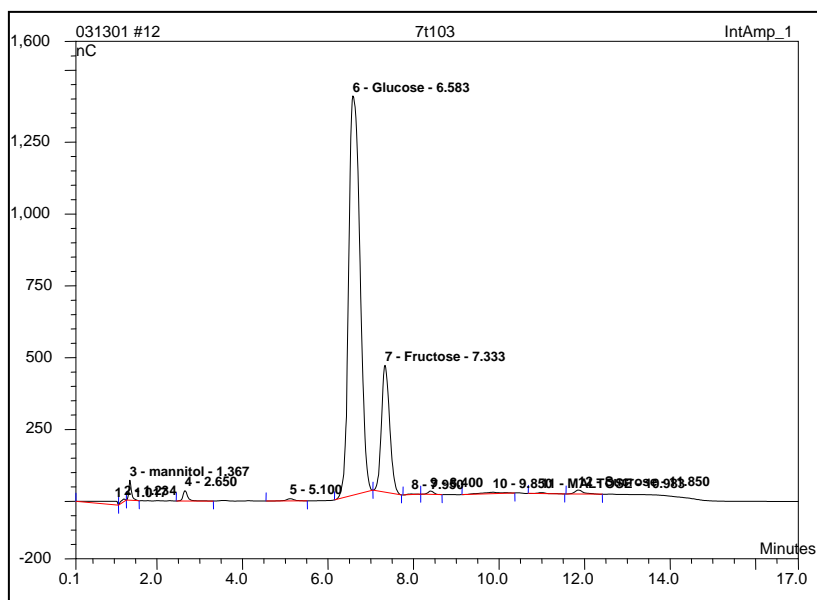


Figure 3.1.6 Typical Chromatogram of Sugar Results from ‘Sample-7t103’ (Reactor 7,500mg/L for time 35 hours, third replicate).

- Samples Method

Table 3.1.3 shows the concentrations from anaerobic experiments where samples were diluted and filtered with 0.22µm syringe filters before being analyzed for sugar content by the HPLC. Several replicates of the diluted samples were analyzed using the carbohydrates method.

Table 3.1.3 Sample Dilutions for the Anaerobic Experiments.

Reactors original concentration	Diluted samples saved from the reactors	Second dilution needed for the HPLC
5000 mg/L	$\frac{1}{2} = 2500$ mg/L	$\frac{1}{10} = 250$ mg/L $\Rightarrow \frac{1}{2} = 125$ mg/L
7500 mg/L	$\frac{1}{2} = 3750$ mg/L	$\frac{1}{10} = 375$ mg/L $\Rightarrow \frac{1}{2} = 187.5$ mg/L
15000 mg/L	$\frac{1}{5} = 3000$ mg/L	$\frac{1}{10} = 300$ mg/L $\Rightarrow \frac{1}{2} = 150$ mg/L
Reactors original concentration	Diluted samples saved from the reactors	Second dilution needed for the HPLC
3,000 mg/L	No dilution	$3,000 \Rightarrow \frac{1}{10} = 300$ mg/L
10,000 mg/L	$\frac{1}{2.5} = 4,000$ mg/L	$4,000 \Rightarrow \frac{1}{10} = 400$ mg/L
80,000 mg/L	$\frac{1}{20} = 4,000$ mg/L	$4,000 \Rightarrow \frac{1}{10} = 400$ mg/L

3.1.3.5 GC (Gas Chromatography) Measurement

The Shimadzu's GC-17A version 3.0 Gas Chromatography was equipped with; Shimadzu's FID (Flame Ionization Detector) detector; Agilent Technology Capillary HP-FFAP (polyethylene glycol (PEG)) Column; Gas supplies of Helium (700~800 kPa) (carrier gas), of Nitrogen (300~800 kPa) (make-up gas), of Hydrogen (300~500 kPa), and of Air (300~500 kPa); AOC-20i Auto Injector; National Scientific's autosampler vials 12x32 mm with septa; Fisher Scientific's internal standard n-Propanol (C_3H_7OH), and external standards of ethanol, butanol, n-propanol, and methanol. Figure 3.1.7 is the actual Shimadzu instrument from our Biological Engineering Laboratory, LSU.



Figure 3.1.7 The actual Shimadzu GC 17-A version 3.0 Gas Chromatography System used to evaluate ethanol production from the anaerobic experiments.

- Alcohol Methods

The Shimadzu GC 17-A version 3.0 equipped with a FID detector (output mVolts) and a HP-FFAP capillary column (Agilent technologies with 25m x 0.35mm) was used to determine the content of alcohol in the fermentation samples. The samples, previously filtered through 0.45µm Millipore filters, were then filtered through 0.20µm Nalgene® nylon syringe filters and 0.5ml was added to the 2ml autosampler vials (National Scientific) with 0.5 ml of 50 ppm n-Propanol (C₃H₇OH). The n-propanol (Fisher Scientific) was used as the internal standard for all samples. The AOC-20i auto injector was used to inject 0.5~2.0µl of sample to the split injection system, when said injected sample is partially split to the capillary column at an oven temperature from 40°C to 200°C, increased at a rate of 20°C per minute. The total program time was 15 minutes per sample. The method chosen was the most frequently used capillary analysis method to achieve highly efficient separation (Shimadzu user's manual GC-17A). The FID sensitivity changes according to the mixture ratio of the carrier gas. Helium was used as the carrier gas at 600 kPa with the total flow rate of 19 ml/min. The Shimadzu Class-VP version 3.0 chromatography software was used providing a complete data acquisition, instrument control, and analysis of the samples. The complete alcohol setup parameters method may be found in Appendix D. Figure 3.1.8 shows peaks of external standards (50ppm), used to calibrate unknown samples.

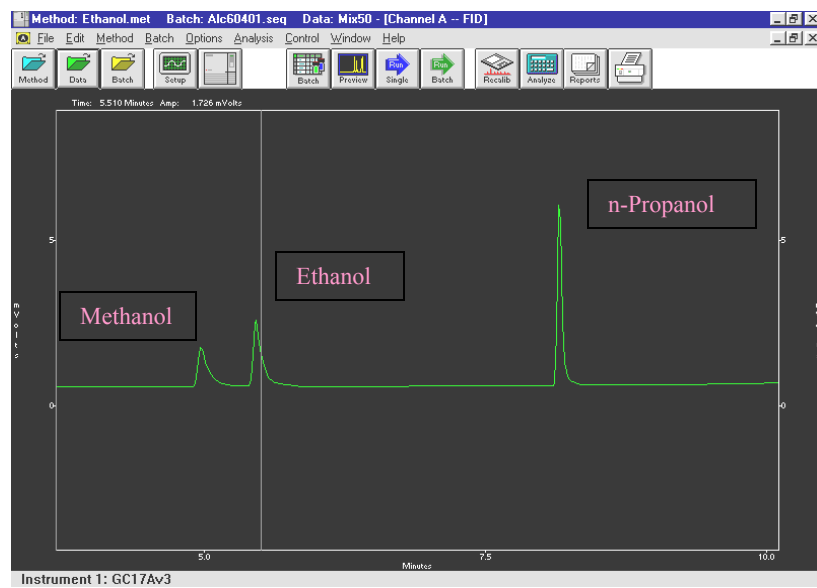


Figure 3.1.8 Typical Chromatogram for External Alcohol Standards of 50ppm (mg/L) Concentration (plotted in mVolts versus minutes).

- Alcohol Quantification

The quantification of alcohol was accomplished using the internal standard method as follows:

$$C_s = \frac{(C_{is} * A_s * RR_f * D_f)}{(A_{is})}$$

Where:

C_s = Concentration of sample

C_{is} = Concentration of internal standard

A_s = Area of sample

A_{is} = Area of internal standard

RR_f = Relative response factor for individual alcohol to internal standard

D_f = Dilution factor of the samples (In this research D_f was equal to one).

The concentration of internal standard C_{is} , equal to the total volume added into the autosampler vials, was 0.5ml of sample plus 0.5ml of 50ppm internal standard.

Therefore, the total C_{is} was 25ppm for the internal standard.

The RR_f was calculated using external standards of ethanol (ethyl alcohol USP absolute, 200 proof from AAPER Alcohol and Chemical, Co) and n-propanol with the following

RR_f definition equation:

$$RR_f = \frac{\left[\frac{C_x}{A_x} \right]}{\left[\frac{C_{is}}{A_{is}} \right]}$$

C_x = Average concentration of the external standard component (Ethanol),

A_x = Averaged area of the external standard component (Ethanol),

C_{is} = Averaged concentration of the internal standard component (n-Propanol),

A_{is} = Averaged area of the internal standard component (n-Propanol).

The RR_f used in this alcohol determination was 1.42. The RR_f calculations are found in Appendix D.

3.1.4 Kinetic Parameter Determination

Several phases of cell growth are observed in batch culture; a typical growth curve is shown in Figure 3.1.9 from Doran, 1997.

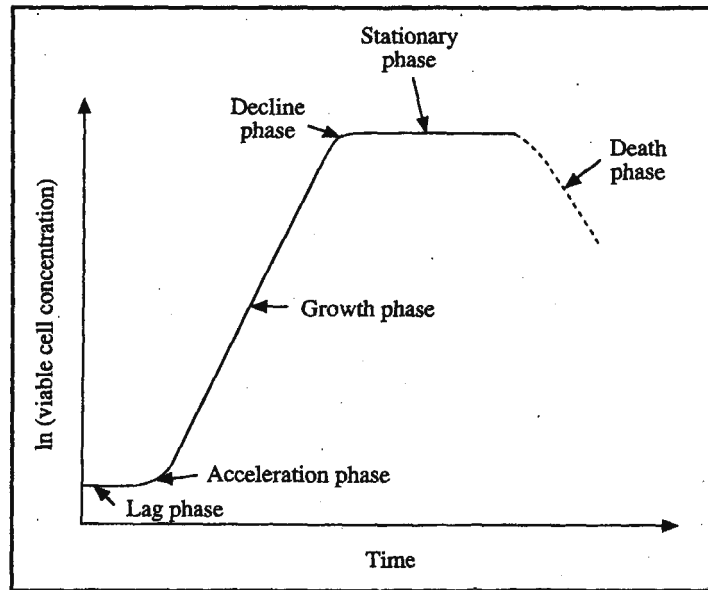


Figure 3.1.9 Typical Batch Growth Curve.

The growth kinetic parameters are calculated from the acceleration phase and continued through the growth and decline phases. The parameters estimated were maximum specific growth rates, half saturation constants, and biomass yields. The rate of growth is influenced by the nutrient concentration, the environmental conditions, and the nature of the organism itself. The experiments were conducted under batch conditions based on the following methods.

3.1.4.1 Monod Model

The relationship of specific growth rate to substrate concentration often assumes the form of saturation kinetics. In this case we assumed a single chemical species, S

(Substrate) that was growth rate limiting for the microorganisms. Therefore, an increase in substrate influences the growth rate of the microbes, while changes in other nutrient concentrations have minimal to no effect on microbial growth. These kinetic parameters are similar to the Langmuir-Hinshelwood, or Hougen-Watson, kinetics in traditional chemical kinetics or Michaelis-Menten kinetics for enzyme reactions (Shuler and Kargi, 1992). The Monod model is stated as:

$$\mu = \frac{(\mu_{\max} * S_t)}{(K_s + S_t)} \quad (3.1.1)$$

where:

μ = Specific growth rate, time⁻¹;

μ_{\max} = Maximum specific growth rate when $S \gg K_s$;

S_t = Substrate, mg/L;

K_s = Saturation constant or half-velocity constant, mg/L. Where $K_s = S$, when

$\mu = (1/2) * (\mu_{\max})$.

3.1.4.2 Linearization Methods

With the linearized method; the specific growth rate (μ) is determined by calculating the difference in the natural log of the biomass concentrations over time (equation 3.1.2).

$$\mu = \left(\frac{(\ln(X_{bt}) - \ln(X_{bo}))}{t} \right) \quad (3.1.2)$$

The specific growth rate coefficient (μ) is the slope determined by plotting the natural log of biomass versus time for each substrate concentration during the initial phase of exponential growth before the substrate concentration decreases significantly.

Then, the determined values of specific growth rate and substrate concentration determined are used to estimate the kinetic parameters, maximum specific growth rate (μ_{\max}) and half saturation constant (K_s), with either the Lineweaver-Burk or Hanes, linear methods.

3.1.4.2.1 Lineweaver-Burk Plot

The Lineweaver-Burk equation is obtained by taking the inverse of the Monod Model.

$$\left(\frac{1}{\mu}\right) = \left[\left(\frac{K_s}{\mu}\right) * \left(\frac{1}{S_t}\right) + \left(\frac{1}{\mu_{\max}}\right)\right] \quad (3.1.3)$$

The slope is $\left(\frac{K_s}{\mu_{\max}}\right)$ and the intercept is $\left(\frac{1}{\mu_{\max}}\right)$ from plotting $\left(\frac{1}{\mu}\right)$ versus $\left(\frac{1}{S_t}\right)$.

The Lineweaver – Burk method has been widely used to determine the kinetic parameter values. However, transforming the variables often distorts the errors associated with

variables, because with small errors for S (substrate), the errors for $\left(\frac{1}{S_t}\right)$ become

relatively larger. Whenever $\left(\frac{1}{\mu}\right)$ versus $\left(\frac{1}{S_t}\right)$ are plotted, the error values may influence

the slope significantly. This transformation is dependent on the value of the variable; therefore it is not the most recommended method.

3.1.4.2.2 Hanes Plot

The Hanes plot is obtained by multiplying the Lineweaver-Burk equation by the substrate concentration.

$$\left(\frac{S_t}{\mu} \right) = \left[\left(\frac{K_s}{\mu_{\max}} \right) + \left(\frac{1}{\mu_{\max}} \right) * S_t \right] \quad (3.1.4)$$

The slope is $\left(\frac{1}{\mu_{\max}} \right)$ and the intercept is $\left(\frac{K_s}{\mu_{\max}} \right)$ of the plot $\left(\frac{S_t}{\mu} \right)$ versus S_t .

This method is the most recommended for many different situations, because it minimizes the distortions in experimental error.

3.1.4.3 Nonlinear Method

This method takes into consideration the change in substrate concentrations in a batch reactor as the microorganisms grow over time.

To perform any reactor design modeling specific kinetic parameters for the microbial organism of interest is often necessary. The specific growth kinetic parameters for any microbe are found by performing the mass balance around the biological reactor with respect to biomass (X_b).

$$\left(\frac{dX_b}{dt} \right) = (\mu * X_b) - (b * X_b) \quad (3.1.5)$$

where:

μ = Specific growth rate, time^{-1} ;

b = Decay constant, time^{-1} ;

X_b = Biomass concentration, mg/L ;

Equation (3.1.5) is applied to the exponential growth phase also known as the logarithmic growth phase. Assuming b is negligible during the exponential growth phase, equation (3.1.5) can be integrated, thus yielding:

$$\mu = \left[\frac{\ln(X_{bt}) - \ln(X_{bo})}{t - t_o} \right] \quad (3.1.6)$$

X_{bt} and X_{bo} = the biomass concentration at time t and at time t_o .

Equation (3.1.6) may be used to determine the specific growth rate over time for a given substrate concentration.

Equation (3.1.6) may also be rearranged to result in an equation that describes the biomass concentration in the reactor at time t (Equation 3.1.7):

$$X_{bt} = \left(X_{bo} * \left(e^{(\mu * (t - t_o))} \right) \right) \quad (3.1.7)$$

Equation 3.1.8 was formulated by substituting the Monod model into the mass balance equation for a batch reactor with respect to biomass (Equation 3.1.5).

$$\left(\frac{dX_b}{dt} \right) = \left(\left(\frac{\mu_{\max} * S_t}{K_s + S_t} \right) * X_b \right) \quad (3.1.8)$$

The relationship between microbial growth yield and substrate consumption is determined by biomass yield, which is the cell mass yield based on the limiting nutrient:

$$Y_{xb} = \left(\frac{(X_{bt} - X_{bo})}{(S_o - S_t)} \right) \quad (3.1.9)$$

Y_{xb} = (mg/L of X_b / mg/L of S).

The biomass yield by definition is the rate of biomass formation over the rate of substrate utilization, during the exponential growth phase of the microorganism.

Then, after the Monod model was substituted into the mass balance equation with respect to biomass, Equation 3.1.8 was integrated and the biomass yield equation was substituted, yielding the Lee equation (Lee, 1992).

$$(time) = \left(\left(\frac{K_S Y_{xb}}{X_{bo} + S_o Y_{xb}} + 1 \right) \ln \left(\frac{X_{bt}}{X_{bo}} \right) + \left(\frac{K_S Y_{xb}}{X_{bo} + S_o Y_{xb}} \right) \ln \left(\frac{S_o}{S_t} \right) / \mu_{\max} \right) - t_o \quad (3.1.10)$$

Equation 3.1.10 describes how the biomass and substrate concentrations change with respect to time during exponential growth, as a sigmoidal-shaped batch growth curve. The Monod model applies at every point in time to the batch reactor (as the substrate concentration decreases, the specific growth rate decreases). Equation 3.1.10 may be used as a design equation and as a method to estimate growth kinetic parameters (μ_{\max} and K_S).

3.2 Results and Discussion

3.2.1 Aerobic Environment

Preliminary work was elaborated upon to determine the kinetic parameters for the yeast strain *Kluyveromyces marxianus* grown in aerobic conditions.

3.2.1.1 Orbital Shaker Bed

For each experiment pre-cultures of yeast were grown on glucose media with the same glucose concentration, used in the experimental run. Five percent (volume of the experimental flasks) of the pre-culture was used to inoculate the experiments. Each experiment had four replicates per time.

Figure 3.2.1 shows the calibration curve for 1,000 mg/L glucose media with the regression equation of $y=718.0489x$ and $R^2=0.989$, which was used to determine the TSS from OD for the following experiments.

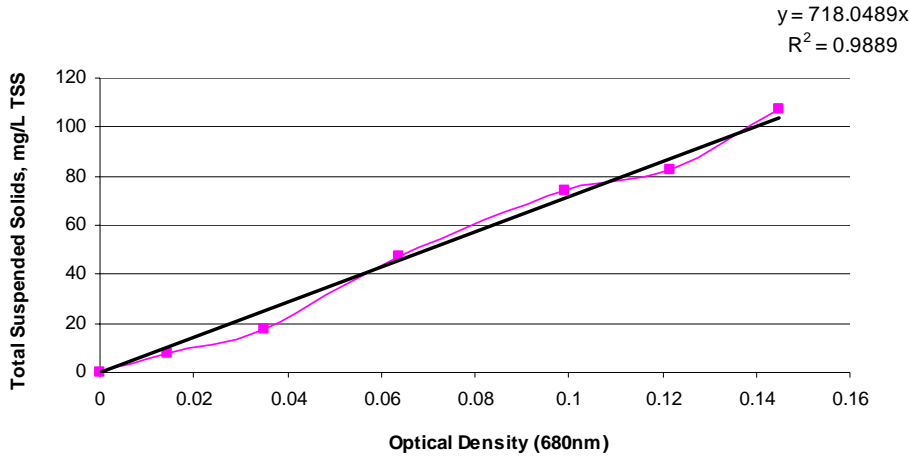


Figure 3.2.1 The Calibration Curve for 1,000 mg/L glucose media for *Kluyveromyces marxianus* yeast strain.

3.2.1.1.1 Substrate Concentration Comparison with Tap Water

Two glucose media concentrations of 500 mg/L, and 1,000 mg/L made with tap water were investigated to determine the specific growth rate. The specific growth rate of the exponential growth phase was calculated from the slope of the regression line of natural log biomass versus time for each substrate concentration. The calibration curve equation from Figure 3.2.1 shown above was used to calculate TSS from OD. Figure 3.2.2 shows the entire natural log of biomass versus time for 500 mg/L glucose media. Figure 3.2.3 shows the exponential phase only for the specific growth rate determination.

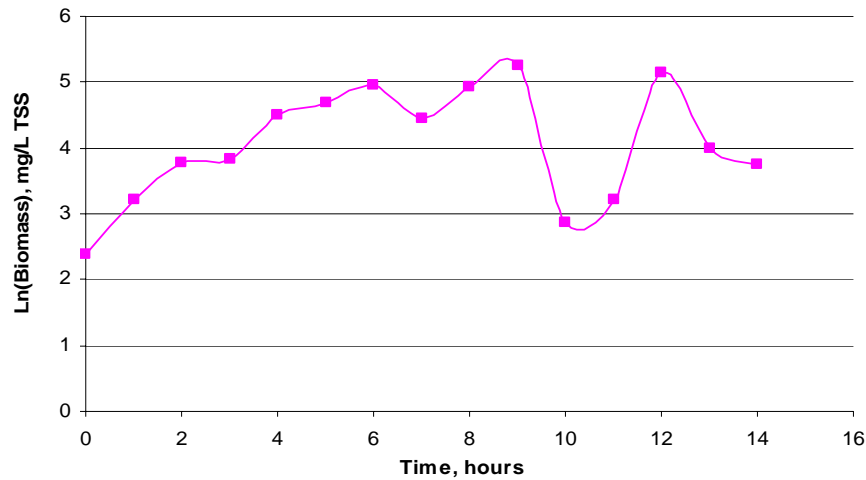


Figure 3.2.2 The Natural log of biomass versus time for 500 mg/L glucose media.

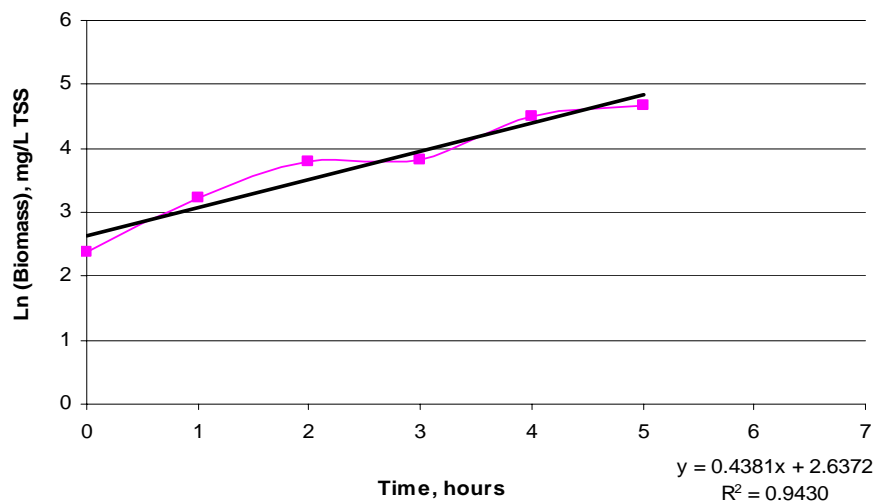


Figure 3.2.3 The specific growth rate determination during exponential phase for 500 mg/L initial substrate concentration.

Figure 3.2.4 shows the entire natural log biomass versus time for the 1,000mg/L glucose concentration. Figure 3.2.5 shows the specific growth rate determination from the exponential phase only, for 1,000 mg/L glucose media.

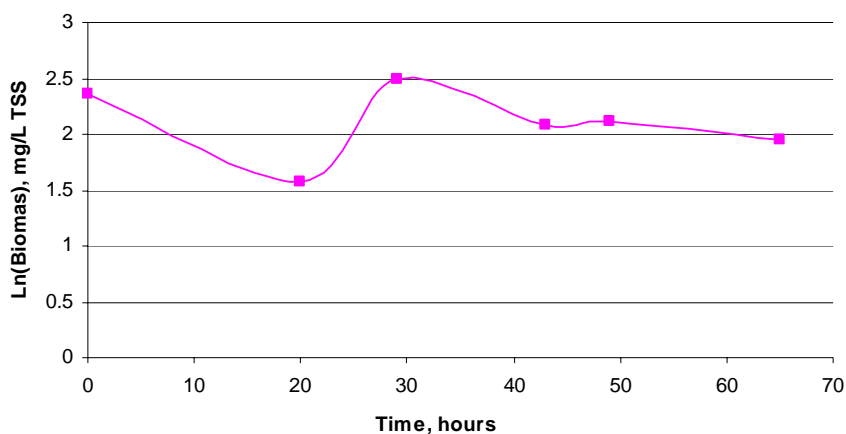


Figure 3.2.4 Natural log of biomass versus time for 1,000 mg/L glucose media.

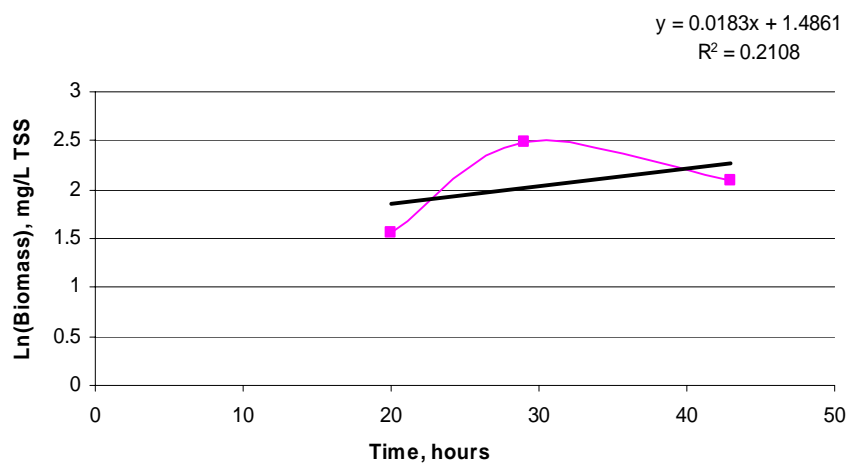


Figure 3.2.5 Specific growth rate for 1,000 mg/L glucose media.

Table 3.2.1 shows the regression equations for 500 mg/L and 1,000 mg/L, for the exponential growth phases.

Table 3.2.1 The Comparison of Specific Growth Rates for Different Substrates.

Glucose Concentrations (mg/L)	Specific Growth Rate (1/hr)	Equation	R ²
500 mg/L	0.438	$y=0.438x+2.637$	0.943
1,000 mg/L	0.0183	$y=0.0183x+1.486$	0.21

Figure 3.2.4 showed the entire experimental data for biomass formed over time with an unreliable initial value of biomass at time zero. The initial biomass value exceeded the final biomass value due to human sampling error.

Table 3.2.1 showed for the 500 mg/L initial substrate concentration a specific growth rate of 0.438/hr, and for the 1,000 mg/L initial substrate concentration a specific growth rate of 0.0183/hr. This experiment has been contradictory to some literature which has shown that the specific growth rate of *Kluyveromyces marxianus* is larger with higher substrate concentrations under aerobic conditions, such as 0.63 hr^{-1} with 40 g/L glucose media (Banat et al. 1996). The R^2 of 0.21 for the 1,000 mg/L initial substrate concentration was a very low regression fitting compared to the 500 mg/L initial substrate concentration with a R^2 of 0.943. Even though the 1,000 mg/L glucose media had more time for growth, it did not show an exponential period where the cells doubled during that time. The yeast cells in the 1,000 mg/L glucose media experiment did not actually grow as expected, perhaps due to contamination.

3.2.1.2 Two-Liter Bioflo[®] 2000 Fermentors

3.2.1.2.1 Water Comparison with 1,000 mg/L Glucose Media

Due to the unexpected results from the orbital shaker bed water experiments, different water types were studied using the Two-Liter Bioflo[®] 2000 Fermentors.

Two different water types (tap and de-ionized) were studied at a 1,000 mg/L glucose media concentration, using the Two-Liter Bioflo[®] 2000 reactors. The TSS for this experiment was calculated using the calibration curve equation already mentioned.

Figure 3.2.6 gives the entire natural log of biomass versus time for tap and de-ionized

water. Figure 3.2.7 gives the specific growth rate μ (1/hr), the regression equations, and R^2 for both tap and de-ionized waters during the exponential growth phase only.

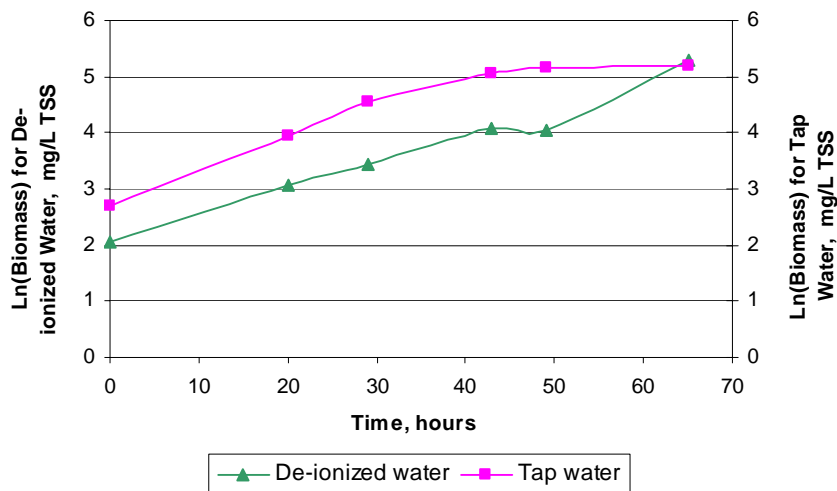


Figure 3.2.6 Natural log of biomass versus time for 1,000 mg/L initial substrate concentration using de-ionized and tap water.

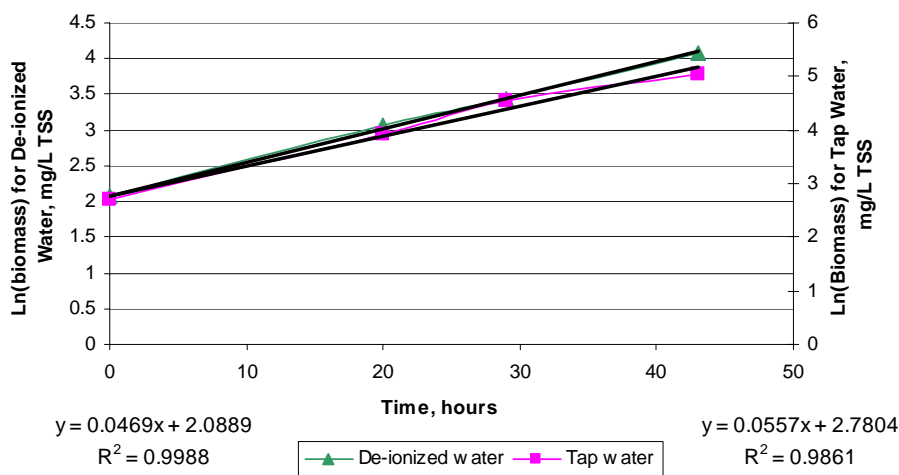


Figure 3.2.7 Specific growth rate for 1,000 mg/L initial substrate concentration using de-ionized and tap water.

Table 3.2.2 shows that the tap water media had a slightly higher specific growth rate than de-ionized water when using the two-liter Bioflo[®] 2000 reactors.

Table 3.2.2 Water Comparison for the 1,000 mg/L Glucose Concentration.

Glucose Concentration 1,000 mg/L	Equation	R ²	Specific Growth Rate, hr ⁻¹
Tap Water	y=0.055+2.78	0.986	0.055
De-ionized Water	y=0.047+2.08	0.998	0.047

The R² of 0.998 for de-ionized water and the R² of 0.986 for tap water showed a good regression fit of the data set. Even though the Bioflo[®] reactors are well sealed and decontaminated after autoclaving, something in the glucose environment did not allow the cells to double during the exponential growth phase. We did not expect the cells to only grow 0.055 per hour while the substrate was not limiting growth. We either had problems maintaining pH or temperature constant during the experiment. All further experiments for this research were done with the Two-Liter Bioflo[®] 2000 Fermentors using tap water.

3.2.1.2.2 Substrate Comparison Using Tap Water

The substrate comparison experiment was accomplished with three two-liter Bioflo[®] 2000 reactors, in duplicate. During the first run, we evaluated substrate concentrations of 200, 400, and 1,000 mg/L glucose media. In the second run, we evaluated substrate concentrations of 200, 400, and 800 mg/L glucose media.

Figure 3.2.8 shows the natural log of biomass versus time for the entire growth phase using the three two-liter Bioflo[®] 2000 reactors with different substrate concentrations. The initial substrate concentrations were as follows: 200, 400, and 1,000 mg/L.

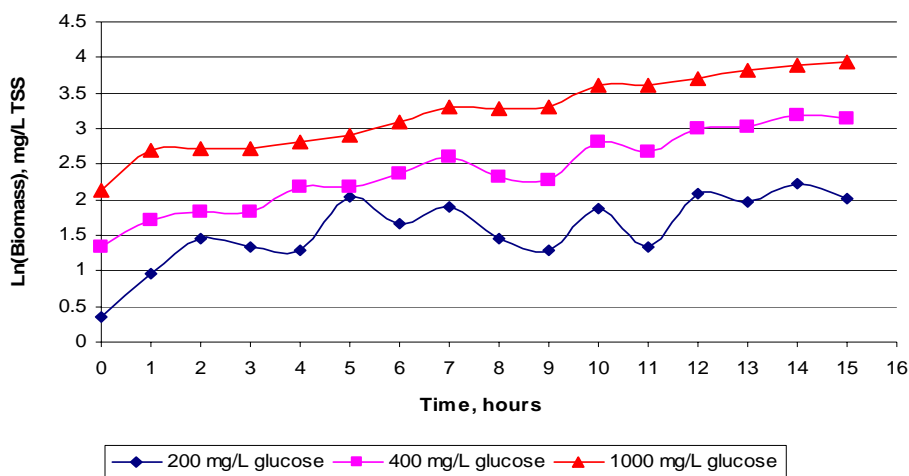


Figure 3.2.8 The Ln(biomass) versus time for the Bioflo[®] 2000 fermentors first run.

Figure 3.2.9 shows the regression equations and the specific growth rates during the exponential phase for the natural log of biomass versus time for the initial substrate concentrations of 200, 400, and 1,000 mg/L.

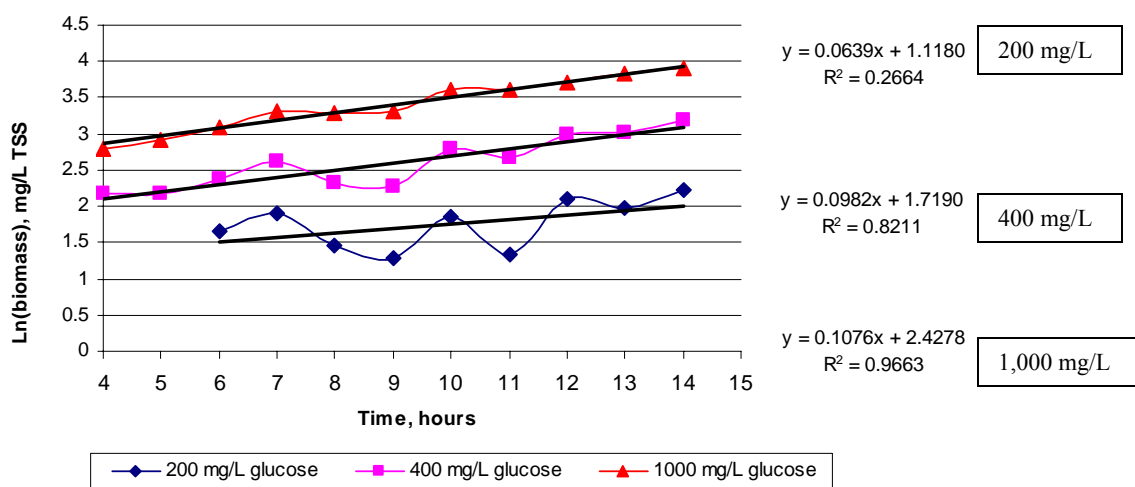


Figure 3.2.9 Specific growth rate for 200, 400, and 1,000 mg/L glucose media during the exponential growth phase for the first run.

Figure 3.2.10 shows the entire growth phase for the second run using the three two-liter Bioflo[®] reactors for 200, 400, and 800 mg/L glucose media.

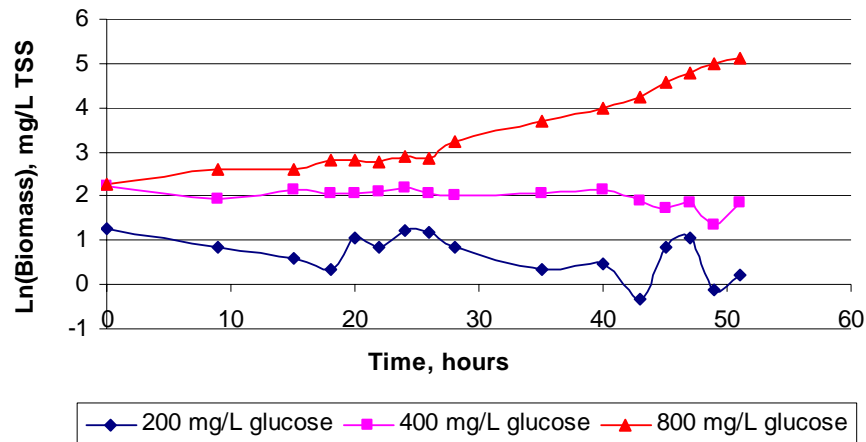


Figure 3.2.10 The Ln(biomass) versus time for the Bioflo[®] 2000 fermentors second run.

Figure 3.2.11 shows the regression equations during the exponential growth phase for the 800 mg/L initial substrate concentration.

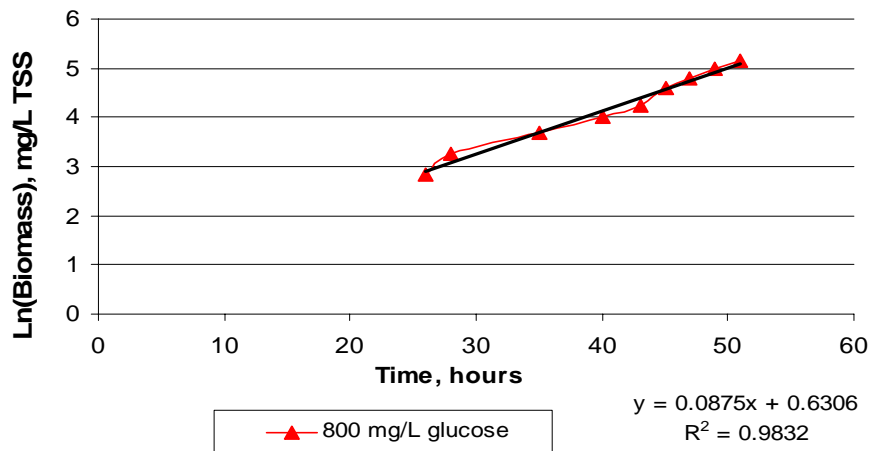


Figure 3.2.11 Specific growth rate for the 800 mg/L initial substrate concentration during the exponential growth phase.

Table 3.2.3 shows the regression equations, R^2 , specific growth rates, biomass yields calculated from COD measurements for four reactors. The 200 mg/L and 400 mg/L initial substrate concentrations from the second run were cancelled due to undetermined growth.

Table 3.2.3 Summary for the Different Substrate Concentrations during Exponential Growth Phase.

Original Substrate (glucose concentration, mg/L)	Regression Equation	R ²	Biomass Yield, Y _b (mg/L TSS/mg/LCOD)	Specific Growth Rate, μ (1/hr)
200 mg/L	y = 0.0639*x + 1.1180 (first run)	0.2664	0.111	0.0639
400 mg/L	y = 0.0982*x + 1.7190 (first run)	0.8211	0.303	0.0982
800 mg/L	y = 0.0875*x + 0.6306 (second run)	0.9832	0.81	0.0875
1,000 mg/L	y = 0.1076*x + 2.4278 (first run)	0.9663	0.285	0.1076

The biomass yield for every reactor was calculated by dividing the time into five parts, also called “time frames”. For each of the five time frames biomass formed (mg/L TSS) was averaged for the substrate utilized (mg/L COD). Further details on biomass yields are found in Appendix G, part G1.

The 800 mg/L glucose concentration had the highest biomass yield of 0.81 (mg/L TSS/ mg/L COD), and the 200 mg/L glucose concentration had the lowest biomass yield of 0.111 (mg/L TSS / mg/L COD). The other substrate concentrations (400 mg/L and 1,000 mg/L) calculated the biomass yields of 0.303 and 0.285 (mg/L TSS/ mg/L COD).

The specific growth rate for the first run of the 200 mg/L initial substrate concentration was 0.0639 (1/hr). The specific growth rate for the first run of the 400 mg/L initial substrate concentration was 0.0982 (1/hr).

The kinetic parameters for the maximum specific growth rate, and the half saturation constant were both calculated from these experimental data using the linear and the nonlinear methods.

3.2.1.2.3 The Linearization Methods for the Laboratory Data Set

The Linearization method was explained in the Materials and Methods section with use of the Monod equation.

The Linearization method was applied with the “Hanes Plot” and the “Lineweaver-Burk Plot” utilizing the averaged soluble substrate concentration (mg/L COD) and the specific growth rate column from Table 3.2.3. Figure 3.2.12 shows the Hanes plot and Figure 3.2.13 shows the Lineweaver-Burk Plot for the aerobic experiments from the summary Table 3.2.3.

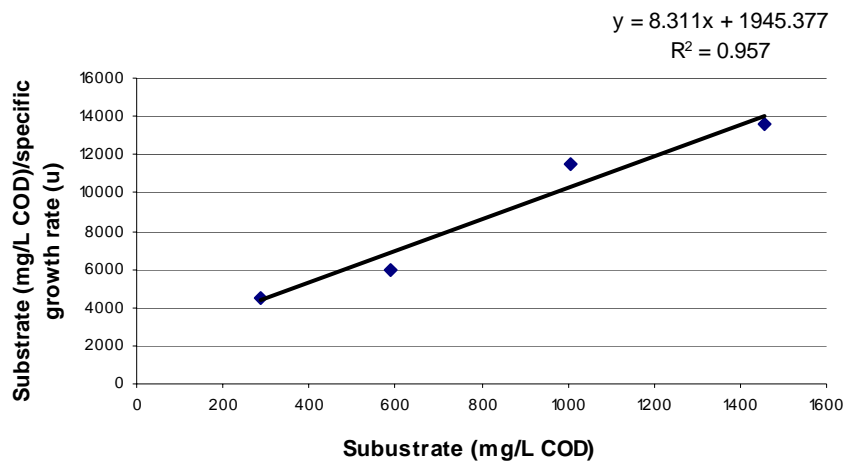


Figure 3.2.12 Hanes plot for the averaged substrate over the specific growth rate versus averaged substrate concentrations.

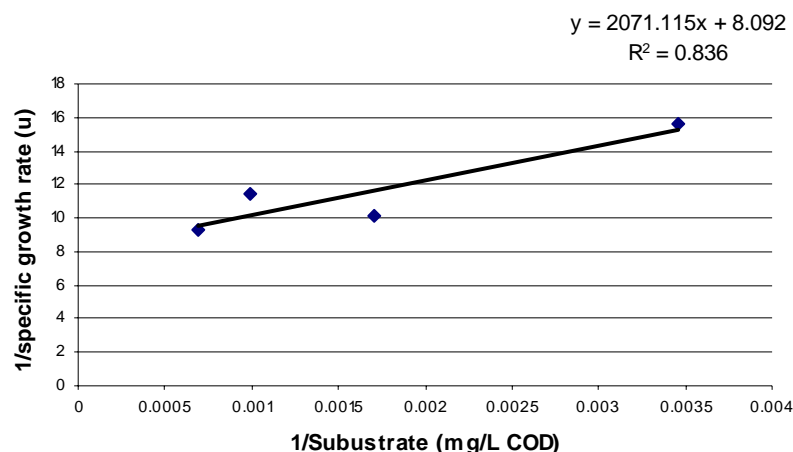


Figure 3.2.13 Lineweaver-Burk plot for the averaged substrate over the specific growth rate versus averaged substrate concentrations.

Table 3.2.4 shows the values used by the Hanes and Lineweaver-Burk plots to determine the growth kinetic parameters.

Table 3.2.4 Summary of the Kinetic Parameters from the Linearization Methods.

Glucose Media, mg/L	Averaged Soluble Substrate, mg/L COD	Specific Growth Rate, 1/hr	Linearization Method	Regression Equations	R^2	Half Saturation Constant, (K_s) mg/L COD	Maximum Specific Growth Rate, (μ_{max}) 1/hr
200	288.76	0.067	Hanes	$y=8.311x+1945.377$	0.957	234.073	0.120
400	586.81	0.053					
800	1004.64	0.088					
1,000	1456.73	0.108	Lineweaver-Burk	$y=2071.115x+8.092$	0.836	255.946	0.124

From the regression equations we were able to determine the growth kinetic parameters (K_s and the μ_{max}). The half saturation constant (K_s) was 234.073 mg/L COD, and the maximum specific growth rate (μ_{max}) was 0.120/hr for the Hanes method, and the half saturation constant (K_s) was 255.946 mg/L COD, and the maximum specific growth rate (μ_{max}) was 0.124/hr for the Lineweaver-Burk method. The maximum specific growth rates and the half saturation constants for both methods gave similar results. But

the Hanes method gave a much better regression fit for the data set of an $R^2 = 0.957$.

The values predicted using the Hanes method is considered a more reasonable prediction which confirms that the Lineweaver-Burk method is not as reliable as the Hanes method most of the times (Robinson, 1985).

3.2.1.2.4 The Nonlinear Method Approach for Laboratory Data Set Using Statistics Analysis Software (SAS)

Statistics Analysis Software (SAS) was used to perform a nonlinear analysis on the aerobic experiments (200, 400, 1,000 mg/L initial substrate concentrations) and (800 mg/L initial substrate concentration) using the two-liter Bioflo[®] Fermentors. The SAS code for this analysis can be found in Appendix H. The nonlinear equation (Lee, 1992) was used by the “proc model” from the SAS program to estimate the growth kinetic parameters. The first experiment had a time period from 0 to 15 hours and the second experiment had a time period from 0 to 51 hours. The initial soluble substrate (S_0), biomass yield (Y_{xb}), and biomass (X_{b0}) values used to find the kinetic parameters are shown in Table 3.2.5. Soluble substrate was calculated from COD measurements, biomass was calculated from TSS measurements, and biomass yield was calculated from the biomass formed (mg/L TSS) divided by the substrate utilized (mg/L COD).

Table 3.2.5 shows the output for the kinetic parameters determined using the nonlinear equation (Lee, 1992).

Table 3.2.5 The Kinetic Parameters Results from the Nonlinear Model using SAS for the Aerobic Experiments.

Glucose Media, mg/L	Initial Conditions for S_o , X_{bo} , and Y_{xb}			Half Saturation Constant, (K_s) mg/L COD	Maximum Specific Growth Rate, (μ_{max}) 1/hr
First Bioflo [®] experiment	(S_o) Soluble Substrate, mg/L COD	(X_{bo}) Biomass mg/L TSS	(Y_{xb}) Biomass Yield		
200	288.77	0.72	0.11	-296	-0.0028
400	586.82	3.11	0.30	-484	0.016
1000	1456.73	8.14	0.29	-1329	0.014
Second Bioflo [®] experiment					
800	946.01	9.87	0.81	-906	0.0039

The K_s and μ_{max} values for each glucose media concentration were not expected to be worse than the linear methods. Either experiment did not show any improvement on the half saturation constants or the maximum specific growth rate; negative K_s values and very small μ_{max} values were estimated in some cases. These estimations need better experimental data sets without significant errors, or nearly perfect data sets to obtain reasonable results from the logistic equation. Further investigations of the nonlinear and linear methods by developing a computer simulation using SAS were conducted to explain the unreasonable kinetic parameter determinations in Chapter 4 of this thesis.

3.2.2 Anaerobic Environment

All the following anaerobic experiments were done in the two-liter Bioflo[®] 2000 fermentors. The orbital shaker bed was only used to grow the pre-cultures (seed) anaerobically to be used as inoculums for the two-liter Bioflo[®] 2000 fermentors.

3.2.2.1 Two-Liter Bioflo[®] 2000 Fermentors

The three two-liter Bioflo[®] 2000 fermentors were used simultaneously for each of the anaerobic experiments conducted.

3.2.2.1.1 Substrate Concentration Comparisons

Figures 3.2.14 and 3.2.15 shows the medium and high range COD standard curves used to determine the soluble substrate for each experiment. The soluble substrate for the exponential growth phase was averaged for each experiment to determine the growth kinetic parameters under anaerobic condition for the *Kluyveromyces marxianus* yeast strain.

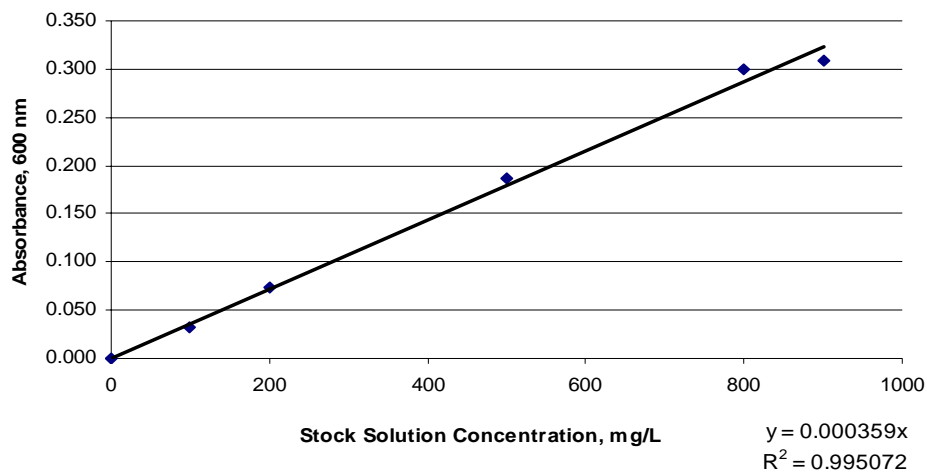
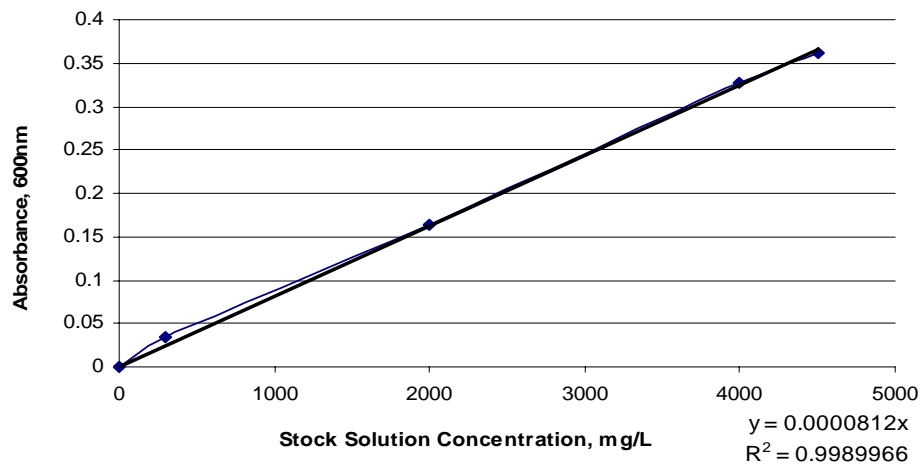


Figure 3.2.14 Medium Range COD Standard Curve.



Figures 3.2.15 High Range COD Standard Curve.

Figures 3.2.16 to 3.2.22 show results from four experiments conducted using three reactors simultaneously per experiment. Figures 3.2.16, 17, 19 and 3.2.21 plot the natural log of biomass versus time for each experiment. Figures 3.2.18, 20 and 3.2.22 show the exponential growth phase of the natural log of biomass versus time for each experiment. Figure 3.2.16 shows measurements for the first experiment, Figures 3.2.17 and 3.2.18 show values for the second experiment, Figures 3.2.19 and 3.2.20 show data for the third experiment, and Figures 3.2.21 and 3.2.22 show data for the fourth experiment. The experiments with the initial substrate concentrations from 200 mg/L to 3,000 mg/L used the 1,000 mg/L calibration curve equation, $y(\text{TSS}) = 718.04893 * x(\text{OD})$, to determine biomass concentration. The experiments with the initial substrate concentrations from 5,000 mg/L to 80,000 mg/L used the 100 g/L glucose media calibration curve equation, $y(\text{TSS}) = 17.8400097e^{(3.4083693 * x(\text{OD}))}$, to determine biomass concentration. These calibration curves are shown in Appendix F.

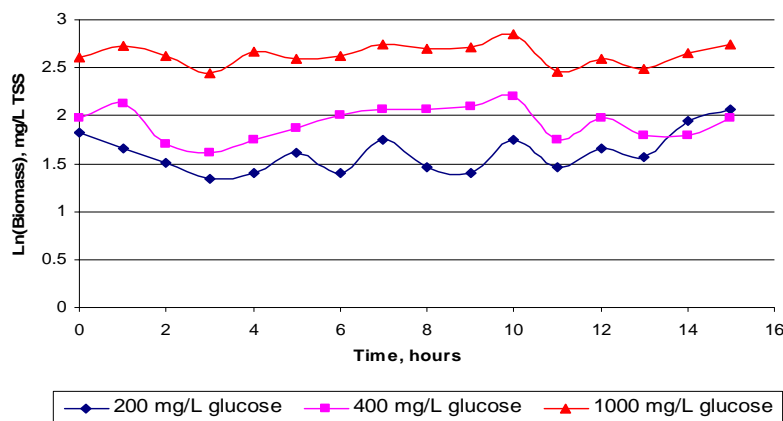


Figure 3.2.16 The natural log of biomass versus time grown on 200, 400, and 1,000 mg/L initial substrate concentrations.

The exponential growth phase for the anaerobic reactors 200, 400, and 1,000 mg/L (Figure 3.2.16) was not calculated due to inconsistent growth measured for this experiment.

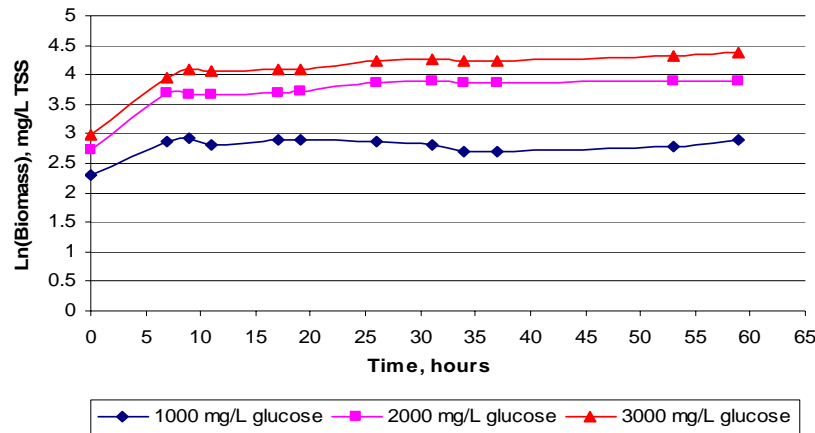


Figure 3.2.17 The natural log of biomass versus time grown on 1,000, 2,000, and 3,000 mg/L initial substrate concentrations.

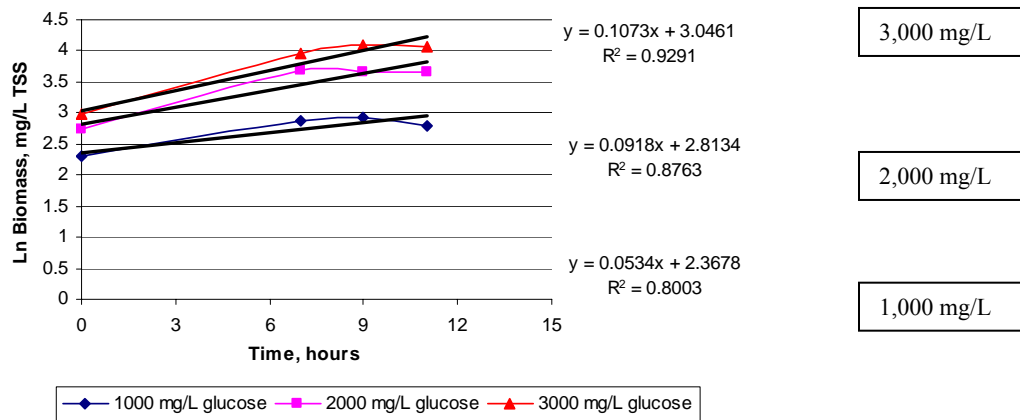


Figure 3.2.18 The exponential growth phase for 1,000, 2,000, and 3,000 mg/L initial substrate concentrations and linear regression fits.

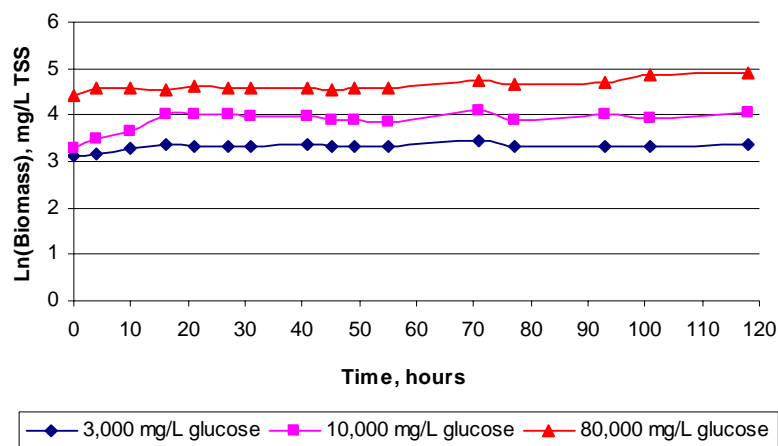


Figure 3.2.19 The natural log of biomass versus time grown on 3,000, 10,000, and 80,000 mg/L initial substrate concentrations.

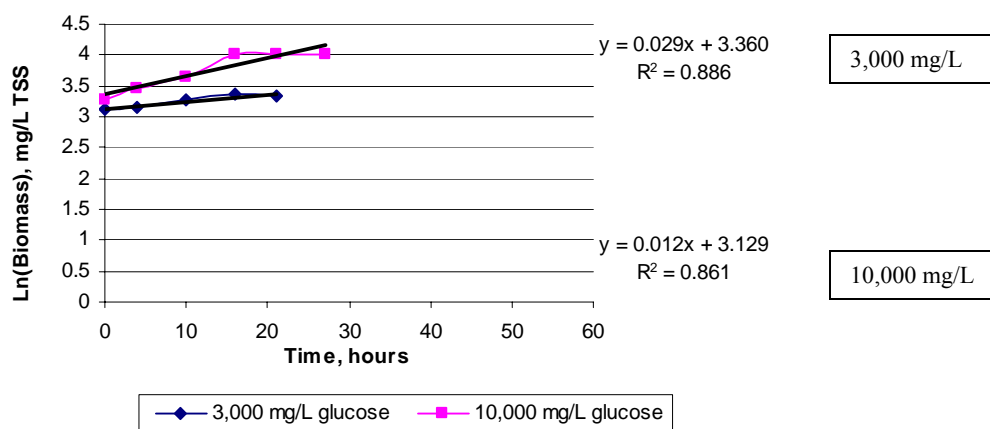


Figure 3.2.20 The exponential growth phase for 3,000, and 10,000 mg/L initial substrate concentrations and linear regression fits.

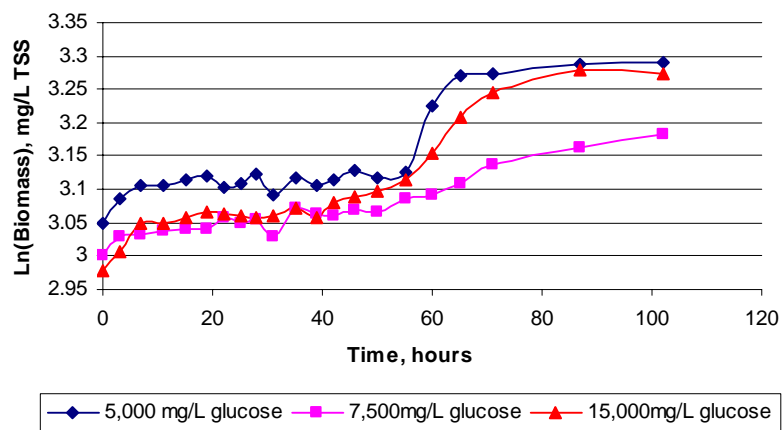


Figure 3.2.21 The natural log of biomass versus time grown on 5,000, 7,500, and 15,000 mg/L initial substrate concentrations.

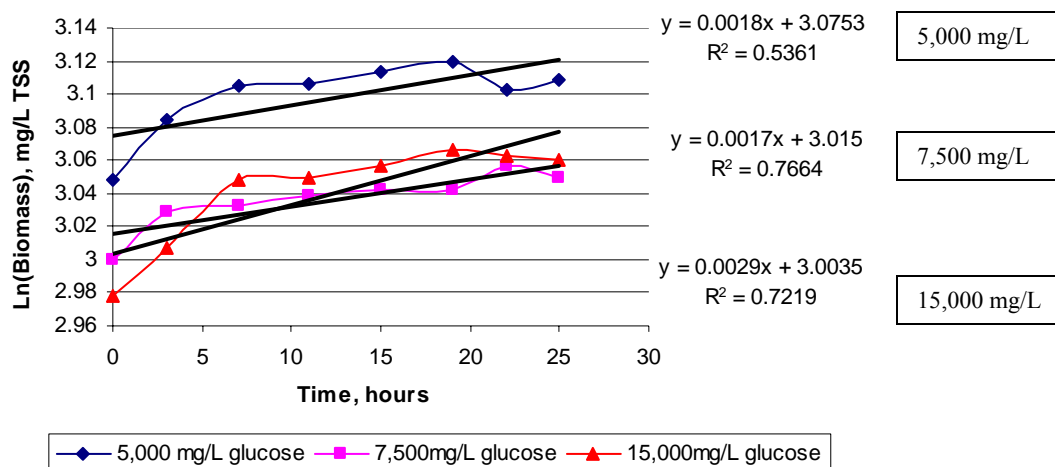


Figure 3.2.22 The exponential growth phase for 5,000, 7,500, and 15,000 mg/L initial substrate concentrations and linear regression fits.

Table 3.2.6 shows the regression equations, biomass yields, R^2 , and specific growth rates for the four experiments conducted under anaerobic conditions.

Table 3.2.6 Summary of the Anaerobic Experiments for the Exponential Growth Phase.

Original Glucose Media, mg/L	Regression Equation	Biomass Yield, Y_b (mg/L TSS/mg/LCOD)	R^2	Specific growth rate, (1/hr)
Second Experiment				
1,000	$y=0.053x+2.367$	0.1837	0.8	0.053
2,000	$y=0.091x+2.813$	0.1518	0.87	0.091
3,000	$y=0.107x+3.046$	0.1592	0.92	0.107
Third Experiment				
3,000	$y=0.029x+3.360$	0.0734	0.88	0.029
10,000	$y=0.012x+3.129$	0.1563	0.86	0.012
Fourth Experiment				
5,000	$y=0.0018x+3.075$	0.0031	0.53	0.0018
7,500	$y=0.0017x+3.015$	0.0057	0.76	0.0017
15,000	$y=0.0029x+3.003$	0.0263	0.72	0.0029

On the third experiment, 80,000 mg/L glucose media reactor was cancelled because it did not show any growth throughout the entire experiment. It was peculiar that the lower substrate concentrations showed higher specific growth rates compared to the

higher substrate concentrations. Even though not much growth was expected in the anaerobic environment, the growth rate of this organism under anaerobic condition was lower than expected. Since the experiments yielded erroneous results, where a lower specific growth rate was obtained at the higher substrate concentrations, there was not a point to attempt the linear and nonlinear methods.

3.2.2.1.2 Soluble Substrate Determination Using HPLC Method

HPLC (High Performance Liquid Chromatography) equipment was used to determine the glucose concentration for the two runs for samples collected during the fermentation experiment, filtered, and stored at -20°C. Figures 3.2.23 and 3.2.24 are the calibration curves for the external sugar standards used to determine the sugar concentrations for the two anaerobic experiments. Figure 3.2.23 shows the external glucose standard made from 50ppm, 100ppm, and 200ppm. Figure 3.2.24 show the external fructose standard made from 50ppm, 100ppm, and 200ppm. The glucose and fructose external standards were the only ones used in the calculations for our experimental data because our samples predominantly showed chromatograms with glucose and fructose peaks. Figure 3.2.23 had a regression equation of $y=3.391x+6.188$ with R^2 equaled to 0.995, and Figure 3.2.24 had a regression equation of $y=3.0596x-15.88$ with R^2 equaled to 0.996.

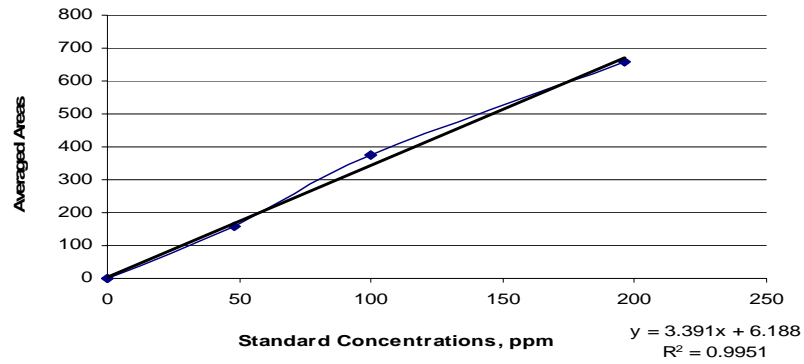


Figure 3.2.23 Glucose Standard Curve.

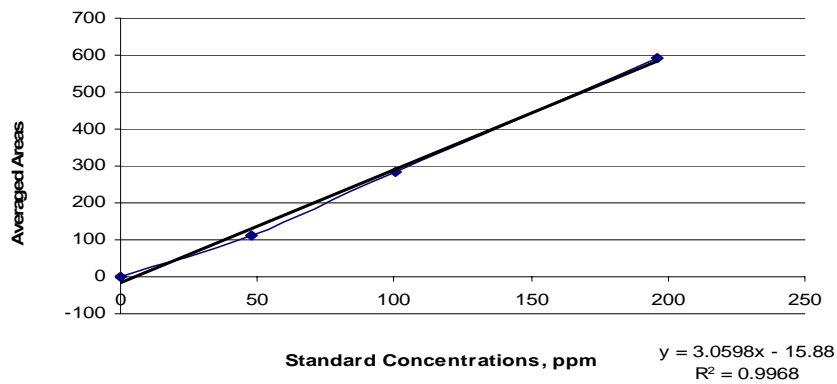


Figure 3.2.24 Fructose Standard Curve.

Figures 3.2.25, 3.2.26 and 3.2.27 show the sugar concentrations for the third anaerobic experiment. Figures 3.2.28, 3.2.29 and 3.2.30 show the sugar concentrations for the fourth anaerobic experiment. Figures 3.2.25 and 3.2.28 show the glucose concentration changing over time for both anaerobic experiments, and Figures 3.2.26 and 3.2.29 show the fructose concentration changing over time for both anaerobic experiments. Figures 3.2.27 and 3.2.30 show the glucose and fructose substrate concentrations added together yielding one substrate concentration changing over time for each experiment.

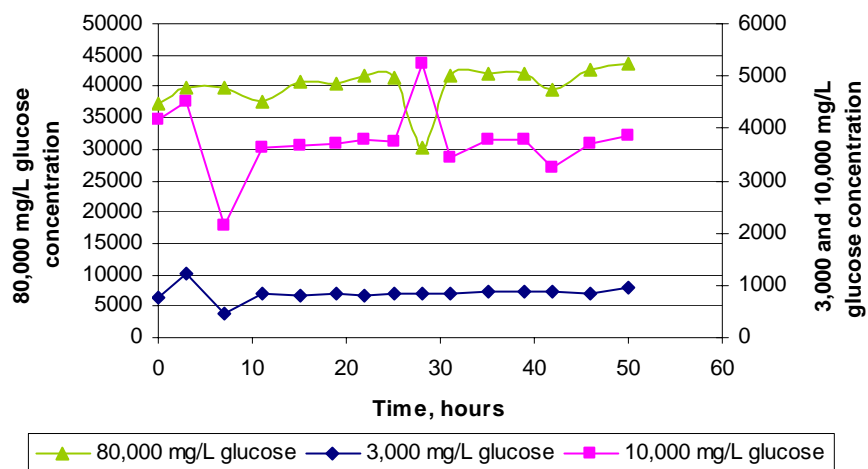


Figure 3.2.25 Glucose concentration for the third anaerobic experiment.

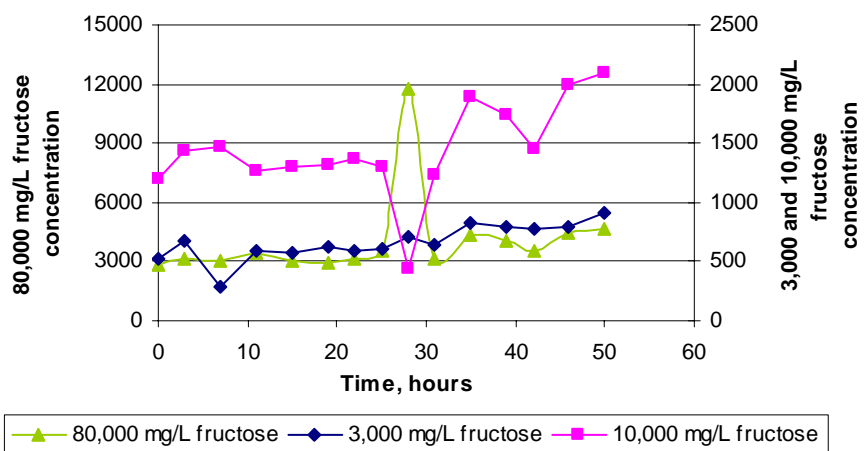


Figure 3.2.26 Fructose concentration for the third anaerobic experiment.

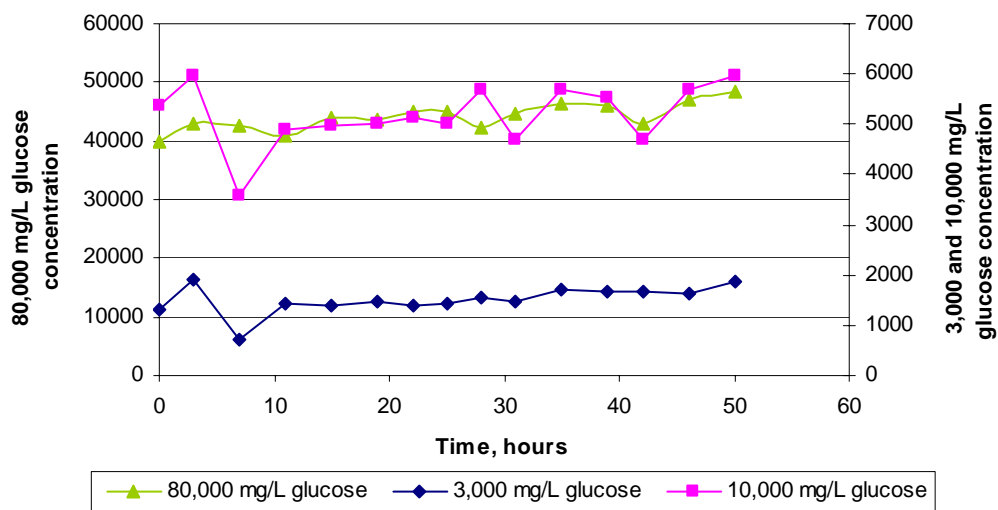


Figure 3.2.27 Total sugar substrate concentration for the third anaerobic experiment (glucose and fructose added together).

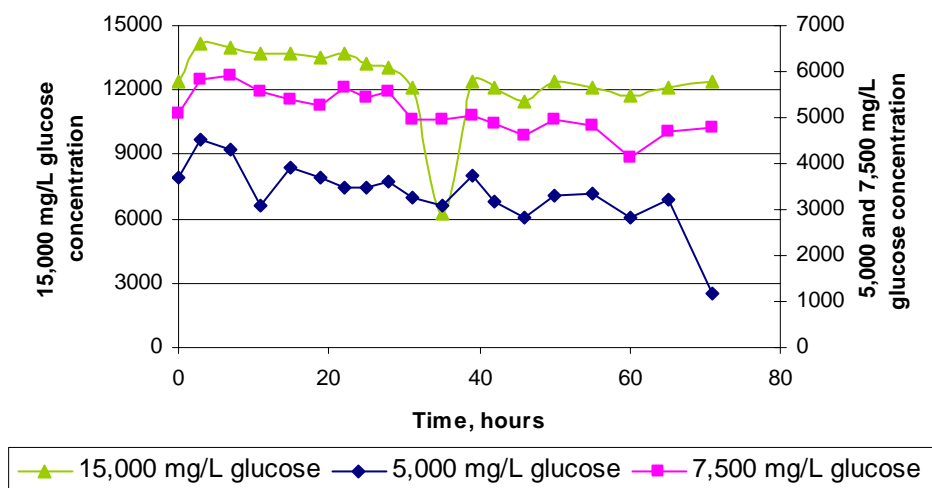


Figure 3.2.28 Glucose concentration for the fourth anaerobic experiment.

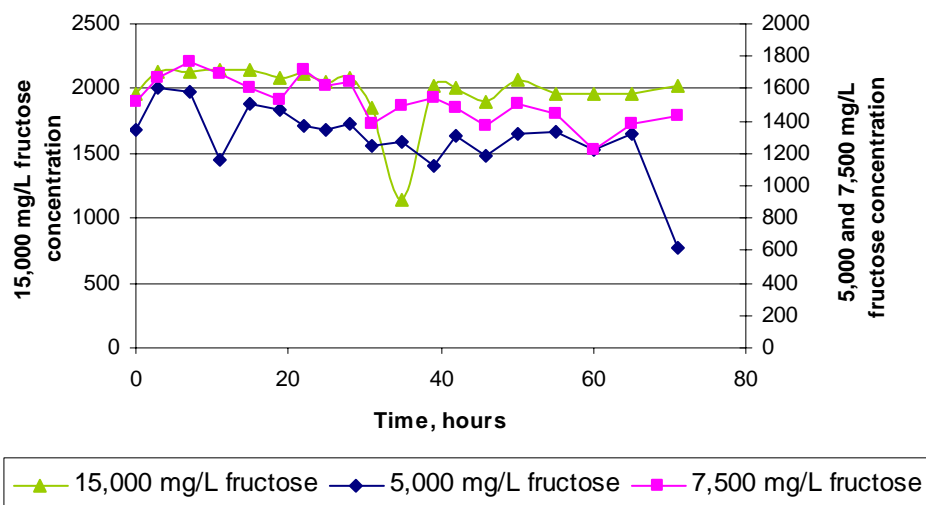


Figure 3.2.29 Fructose concentration for the fourth anaerobic experiment.

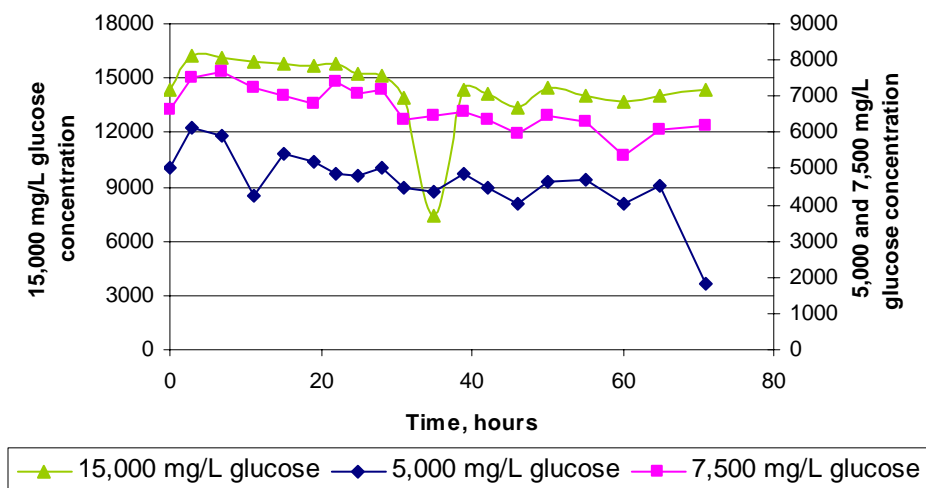


Figure 3.2.30 Total sugar substrate concentration for the fourth anaerobic experiment (glucose and fructose added together).

The soluble substrate concentrations were determined for both experiments using the HPLC method. These soluble substrate concentrations were not used to calculate the growth kinetic parameters with the linear and nonlinear methods, due to unreliable specific growth rates calculated (Table 3.2.6). Figure 3.2.27 showed that the total sugar substrate concentration did not change much over time. The substrate concentration for

each fermentor was increasing over time, which is not acceptable. Figure 3.2.30 showed that the total sugar substrate concentration did change over time. The substrate concentration for each fermentor was decreasing over time, which is expected.

The glucose media was made in accordance to Anderson et al. (1986) that used Bacto™ Peptone and Bacto™ Yeast Extract to make the media. Both of these ingredients were used by the cells as a carbon source with 10% of nitrogen, 80% of amino acids, and 4% of ashes. The Peptone and Yeast Extract contain protein and free amino acids that contribute to carbon quantification. The extra carbons from the Peptone and Yeast Extract affect the COD measurements, the biomass measurements, and possibly ethanol production. Therefore, the sugar measurements (using COD technique) would have higher soluble substrate concentrations than using the HPLC technique, because the COD technique accounts for all carbon sources in the glucose media (Appendix C tables: C.1 and C.2).

3.2.2.1.3 Product Quantification Using GC Method

The overall conversion of glucose to ethanol by yeast cells can be represented stoichiometrically as: $C_6H_{12}O_6 \rightarrow 2C_2H_5OH + 2CO_2$

MW	180	92	88
----	-----	----	----

From this equation, a theoretical yield of 51.1 g of ethanol can be obtained from the fermentation of 100 g of glucose (Jones et al. 1981).

Microbial products can be classified in three major categories: growth-associated product, nongrowth-associated product, and mixed-growth-associated product formation. Growth-associated products are produced simultaneously to microbial exponential growth. The specific rate of product formation is proportional to the specific rate of

growth (Shuler & Kargi, 1992). Ethanol production is an example of product directly associated with the generation of energy in the cell, where ethanol is synthesized in pathways that produce ATP. Ethanol and glycerol were then produced until glucose was depleted. The product was only determined for the fourth experiment with 5,000, 7,500, and 15,000 mg/L glucose concentrations. The product (ethanol) was determined using gas chromatography (GC) from 0.45µm filtered, and undiluted, frozen samples. Figure 3.2.31 shows the product formation over time for the three reactors.

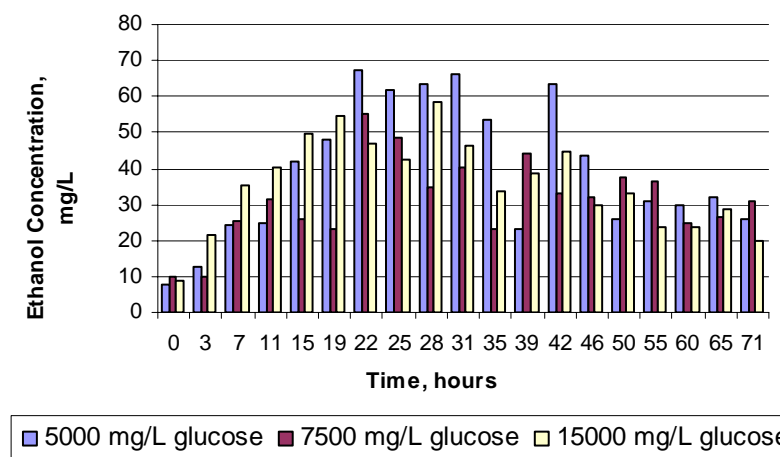


Figure 3.2.31 Ethanol concentration for the anaerobic experiment.

Figure 3.2.31 showed that the ethanol concentration was the highest for 5,000 mg/L initial substrate concentration fermentor achieving a maximum ethanol production of 70 mg/L from 21 to 42 hours. The reactor with 15,000 mg/L glucose also showed the next best ethanol production increasing continuously from 0 hour until 28 hours, and then we can see a slow decrease over time, when it achieved a maximum ethanol production of 60 mg/L. The reactor with 7,500 mg/L glucose did not show a very consistent ethanol production over time, but it did reach a maximum of ethanol production of 55 mg/L. While too early to be definitive as more replications would be desirable, the 5,000 mg/L

reactor had the highest ethanol production over time, even though the biomass yield was only 0.0031 (mg/L TSS biomass / mg/L COD substrate). The biomass yield of the 7,500 mg/L reactor was 0.0057 (mg/L TSS biomass / mg/L COD substrate) and the biomass yield of the 15,000 mg/L reactor was 0.0263 (mg/L TSS biomass / mg/L COD substrate). The biomass yield was calculated using the “time frame” already mentioned in section 3.2.1.2.2, and the Figures are found in Appendix G, part G2.

3.3 Conclusions

The preliminary experiments were investigated under aerobic environment using the orbital shaker bed which showed us that the tap water could be used in future experiments, even though we experienced a low specific growth rate of 0.0183/hr. Our interest in this part was to verify that this microbe would grow well in 1,000 mg/L using the orbital shaker bed, but it did not appear to be the case, because the 500 mg/L glucose concentration showed a higher specific growth rate of 0.438/hr than for 1,000 mg/L glucose concentration with a specific growth rate of 0.0183/hr. The next important experiments were to investigate this yeast growth in the two-liter Bioflo[®] 2000 fermentors (New Brunswick Scientific).

From Table 3.2.4 the 1,000 mg/L glucose media had the highest specific growth rate of 0.1076/hr under the aerobic environment, which was not expected to be so low, compared to Banat et al (1995). They found that *Kluyveromyces marxianus* had a specific growth rate ranging from 0.58 to 0.63 (hr⁻¹) for 10,000 mg/L glucose media at 45°C, under aerobic conditions. The other specific growth rates from Table 3.2.4 were expected to have lower values than the 1,000 mg/L glucose concentration. From Table 3.2.5 the μ_{\max} for the Hanes plot was 0.159 (hr⁻¹) which was higher than the Lineweaver-

Burk plot, which was expected because when $\left(\frac{1}{\mu}\right)$ and $\left(\frac{1}{S}\right)$ was plotted for the Lineweaver-Burk method, the small substrate concentration was further on the regression axis affecting the slope. A higher μ_{\max} estimate was still expected for this yeast under aerobic conditions, such as 0.93 hr^{-1} from Fleming et al. (1993) research. Further research should examine kinetic parameters studies with different substrate concentration range and temperature range, such as 35°C , 40°C and 50°C under aerobic conditions. Even though Banat et al. (1992) studied this yeast under anaerobic conditions, they also still showed higher specific growth rates from 0.49 to $0.53 \text{ (hr}^{-1}\text{)}$ at 48°C . According to Doran (1997), another problem may have been oxygen limitations where dissolved-oxygen (DO) concentrations at every point in the fermenter would need to be above the critical oxygen concentration, because glucose is generally consumed more rapidly than other sugars or carbon-containing substrates and the rates of oxygen demand are higher when glucose is used. The nonlinear method fit the Lee equation (1992), which was not a success because the data set measured from the laboratory experiments had many errors. Thus, further work was done to learn how well these nonlinear and linear methods could fit and give reasonable kinetic parameter results from a generated data set. This problem was investigated and discussed in Chapter 4.

Under anaerobic conditions the yeast strain showed lower specific growth rate results than for the aerobic conditions, which were expected. From Table 3.2.7 the highest specific growth rate value of 0.149 hr^{-1} was for the 200 mg/L glucose concentration, and the lowest value of 0.0022 hr^{-1} was for the $7,500 \text{ mg/L}$ glucose concentration, which did not reach a specific growth rate of 0.09 to 0.14 hr^{-1} using $10,000 \text{ mg/L}$ initial substrate concentration at 45°C , according to Banat et al. (1995) research.

Higher specific growth rates for higher initial substrate concentrations were expected but these experiments showed the opposite. The best R^2 coefficient was 0.97 for 15,000 mg/L initial substrate concentration with a specific growth rate of 0.005 hr^{-1} . The regression coefficient for the four experiments ranged from 0.77 to 0.97 which represent a reasonable and acceptable regression fitting of the data sets. The R^2 for the 7,500 mg/L initial substrate concentration was 0.95 showing a very reasonable regression fit of the data set with the lowest specific growth rate of 0.0022 hr^{-1} . Something was truly happening with either the media or the environment affecting the microbial growth under anaerobic conditions.

For the first three experiments our yeast strain was not capable of sustain growth under anaerobic conditions for more than 20 hours (Figures 3.2.18, 3.2.20, and 3.2.22), and for the fourth experiment the growth started after 40 hours and continued until 100 hours (Figure 3.2.24). When the overall conversion of glucose to ethanol stoichiometric equation was applied, the theoretical yield of ethanol for 5,000 mg/L was 2,556 mg/L, for 7,500mg/L was 3,833 mg/L, and for 15,000 mg/L was 7,665 mg/L. Unfortunately this yeast strain showed a low ethanol tolerance during growth (Figure 3.2.34).

The use of the thermotolerant yeast strain *Kluyveromyces marxianus* has been proposed as a method of improving the efficiency of fuel ethanol production from biomass, with the ability to operate at elevated temperatures (Hack et al. 1998). Even though this yeast strain had low biomass formation and small maximum specific growth rates ethanol was still formed under anaerobic conditions. According to Hack et al. (1998), batch fermentation was not viable for an industrial process using the *K. marxianus* strain because the initial substrate concentration would be limited by the

osmotolerance and the low ethanol tolerance by the yeast strain. According to Qureshi and Manderson (1994), they proved that using a simple continuous process with *K. marxianus* strain was also rejected due to the incapacity of the strain to sustain growth under anaerobic conditions. Therefore, future studies using this yeast strain should be applied to a continuous process, where the biomass could be retained in the fermenter by either recycling the biomass or immobilizing the biomass which would result in a higher cell concentration and improve ethanol productivity (Hack et al. 1998). This yeast strain could also be applied to a two-stage fermenters in series with first an aerobic condition allowing a continuous generation of biomass, and subsequently, expose the cells to an anaerobic fermentative condition to maximize ethanol production. According to Banat et al. (1996), they achieved a high biomass concentration of 10 g/L with ethanol levels up to 4.3% (v/v) using the two fermenters in a series (aerobic-anaerobic) with 150 g/L initial substrate concentration at 40°C.

In conclusion, many opportunities exist for improvement of the ethanol fermentation process for the industry and also to create new, innovative, and efficient technologies to advance research for any fermentation process.

3.4 References

1. Abdel-Fattah W.R., Fadil M., Nigam P., Banat I.M. 2000. Isolation of thermotolerant ethanologenic yeasts and use of selected strains in industrial scale fermentation in an Egyptian distillery. *Biotechnology and Bioengineering* 68: 531-535.
2. Aiba S., Shoda M., Nagatani M. 1968. Kinetics of product inhibition in alcohol fermentation. *Biotechnology and Bioengineering* 10: 845-864.
3. Anderson P. J., McNeil K., Watson K. 1986. High – Efficiency Carbohydrate Fermentation to Ethanol at Temperatures above 40C by *Kluyveromyces*

- marxianus* var. *marxianus* Isolated from Sugar Mills. Applied and Environmental Microbiology 51: 1314-1320.
4. APHA. 1995. Standard Methods for the Examination of Water and Wastewater, 19th Ed. American Public Health Association, Washington, D.C.
 5. Ballesteros I., Ballesteros M., Cabanas A., Carrasco J., Martin C., Negro M.J., Saez F., Saez R. 1991. Selection of thermotolerant yeasts for simultaneous saccharification and fermentation (SSF) of cellulose to ethanol. Applied Biochemistry and Biotechnology 28/29: 307-315.
 6. Banat, Singh I. M., Marchant D., R. 1996. The use of a thermotolerant fermentative *Kluyveromyces marxianus* IMB3 yeast strain for ethanol production. Acta Biotechnology 16: 215-223.
 7. Banat, Singh I. M., Marchant D., R. 1995. Characterization and potential industrial applications of five novel, thermotolerant fermentative yeast strains. World Journal of Microbiology and Biotechnology 11: 304-306.
 8. Banat I.M., Nigam P., Marchant R. 1992. Isolation of thermotolerant, fermentative yeasts growing at 52C and producing ethanol at 45C and 50C. World Journal of Microbiology and Biotechnology 8: 259-263.
 9. Barron N., Marchant R., McHale L., McHale A.P. 1995. Studies on the use of a thermotolerant strain of *Kluyveromyces marxianus* in simultaneous saccharification and ethanol formation from cellulose. Applied Microbiology and Biotechnology 43: 518-520.
 10. Drapcho C. 2000. Biological Engineering Reactor Design Class. BE-4341, Agricultural & Biological Engineering Department, Louisiana State University.
 11. Doran M. P. 1997. Bioprocess Engineering Principles. Academic Press, San Diego, CA.
 12. Hack C. J., Marchant R. 1998. Characterisation of a novel thermotolerant yeast, *Kluyveromyces marxianus* var *marxianus*: development of an ethanol fermentation process. Journal of Industrial Microbiology and Biotechnology 20: 323-327.
 13. Hacking A.J., Taylor I.W.F., Hanas C.M. 1984. Selection of yeast able to produce ethanol from glucose at 40°C. Applied Microbiology and Biotechnology 19: 361-363.
 14. Hughes D.B., Tudroszen N.J., Moye C.J. 1984. The effect of temperature on the kinetics of ethanol production by a thermotolerant strain of *Kluyveromyces marxianus*. Biotechnology letters 6: 1-6.

15. Hurst W. J., Martin Jr R. A., Zoumas B. L. 1979. Application of HPLC to characterization of individual carbohydrates in foods. *Journal of Food Science* 44: 892 – 895.
16. Jones R.P., Pamment N., Greenfield P.F. 1981. Alcohol fermentation by yeasts – the effect of environmental and other variables. *Process Biochemistry* 16: 42-49.
17. Kida K., Kume K., Morimura S., Sonoda Y. 1992. Repeated-batch fermentation process using a thermotolerant flocculating yeast constructed by protoplast fusion. *Journal of Fermentation and Bioengineering* 74: 169-173.
18. Liu, S. (2003) Personal communication, June.
19. Liu S. 2002. Fecal Coliform decay and regrowth kinetics in an anaerobic dairy wastewater environment. MS thesis. Biological Engineering Department, Louisiana State University, LA 1-76.
20. Madsen, L. (2003) Personal communication, February.
21. Morimura S., Ling Z.Ya., Kida K. 1997. Ethanol production by repeated-batch fermentation at high temperature in a molasses medium containing a high concentration of total sugar by a thermotolerant flocculating yeast with improved salt-tolerance. *Journal of Fermentation and Bioengineering* 83: 271-274.
22. Nagodawithana T.W., Castellano C., Steinkraus K.H. 1974. Effect of dissolved oxygen, temperature, initial cell count, and sugar concentration on the viability of *Saccharomyces cerevisiae* in rapid fermentations. *Applied Microbiology* 28: 383-391.
23. Peres M.F.S., Lallue C. 1998. Ethanol tolerance of thermotolerant yeasts cultivated on mixtures of sucrose and ethanol. *Journal of Fermentation and Bioengineering* 85: 388-397.
24. Reece N. N. 2003. Optimizing aconitate removal during clarification. MS thesis. Biological Engineering Department, Louisiana State University, LA 1-113.
25. Riordan C., Love G., Barron N., Nigam P., Marchant R., McHale L., McHale A.P. 1996. Production of ethanol from sucrose at 45C by alginate-immobilized preparations of the thermotolerant yeast strain *Kluyveromyces marxianus* IMB3. *Bio-resource Technology* 55: 171-173.
26. Robinson J.A. 1985. Determining microbial kinetic parameters using nonlinear regression analysis. *Advances in Microbial Ecology*, edited by K. C. Marshall 8: 61-114. Plenum Press, New York.

27. Saigal D. 1994. Isolation and selection of thermotolerant yeasts for ethanol production. *Indian Journal of Microbiology* 34: 193-203.
28. SAS Institute. 2002. SAS/STAT Guide for Personal Computers Version 9.0, SAS Institute, Inc., Cary, North Carolina.
29. Saxena A., Garg S.K., Verma J. 1992. Simultaneous saccharification and fermentation of waste newspaper to ethanol. *Bio-resource Technology* 42: 13-15.
30. Shuler L. M., Kargi F. 1992. *Bioprocess Engineering: Basic Concepts*. Prentice Hall PTR.
31. Szczodrak J., Targonski Z. 1987. Selection of thermotolerant yeast strains for simultaneous saccharification and fermentation of cellulose. *Biotechnology and Bioengineering* 31: 300-303.
32. White, B. (2003) Personal communication, February.
33. Zhu H. (2004) Personal communication, January.
34. Zhu H. 2002. Utilization of rice bran by *Pythium Irregulare* for lipid production. MS thesis, Biological Engineering Department, Louisiana State University 1-70.

CHAPTER 4

BIOLOGICAL GROWTH KINETIC PARAMETER DETERMINATION ANALYSIS USING MONTE CARLO SIMULATIONS

4.1 Introduction

Biological engineers have been using the Monod model equation to design aerobic or anaerobic biological reactors/fermentors for environmental and biotechnological purposes. The Monod model equation is similar to the Langmuir-Hinshelwood and Hougen-Watson equations for traditional chemical kinetics. It is also similar the Michaelis-Menten kinetics equation for enzyme reactions that accounts for microbial growth in most environmental conditions.

$$\mu = \frac{(\mu_{\max} * S_t)}{(K_s + S_t)} \quad (4.1.1)$$

where:

μ = Specific growth rate, time^{-1} ;

μ_{\max} = Maximum specific growth rate when $S \gg K_s$;

S_t = Substrate, mg/L;

K_s = Saturation constant or half-velocity constant, mg/L.

Where $K_s = S$, when $\mu = (1/2) * (\mu_{\max})$.

In biological engineering, to perform a reactor design it is necessary to find the specific Monod model kinetic parameters for the microorganism of interest. These specific growth kinetic parameters for any microbe are found by performing a mass balance around the biological reactor with respect to biomass (X_b).

$$\left(\frac{dX_b}{dt}\right) = (\mu * X_b) - (b * X_b) \quad (4.1.2)$$

where:

μ = Specific growth rate, time⁻¹;

b = Decay constant, time⁻¹;

X_b = Biomass concentration, mg/L;

This equation (4.1.2) is only applied to the exponential growth phase or logarithmic growth phase, so the decay constant (b) is assumed to be negligible and the estimate is the maximum specific growth rate. The Monod model is substituted into the mass balance equation with respect to biomass, yielding:

$$\left(\frac{dX_b}{dt}\right) = \left(\left(\frac{\mu_{\max} * S_t}{K_s + S_t}\right) * X_b\right) \quad (4.1.3)$$

The biomass yield, by definition, is the rate of biomass formation over the rate of substrate utilization during the exponential growth phase of the microorganism, which is the cell mass yield as a function of the limiting nutrient.

$$Y_b = \left(\frac{(X_{bt} - X_{bo})}{(S_o - S_t)}\right) \quad (4.1.4)$$

where:

Y_b = (mg/L of X_b / mg/L of S).

Equation (4.1.3) is then integrated and the biomass yield equation (4.1.4) is substituted, yielding the Lee equation (Lee, 1992).

$$time = \left(\left(\left(\frac{K_S Y_B}{X_{B,0} + S_0 Y_B} + 1 \right) \ln \left(\frac{X_B}{X_{B,0}} \right) + \left(\frac{K_S Y_B}{X_{B,0} + S_0 Y_B} \right) \ln \left(\frac{S_0}{S} \right) \right) / \mu_{\max} \right) + t_0 \quad (4.1.5)$$

This equation (4.1.5) is also known as the logistic equation. It is a nonlinear equation that produces a sigmoidal-shaped batch curve during the exponential growth phase describing the change in biomass and substrate concentrations with respect to time. This equation is used by many biological engineers and biologists to determine the growth kinetic parameters (K_S and μ_{\max}) of a microbe.

A second nonlinear equation developed by Shuler and Kargi (1992), who used the same background as the Lee equation to elaborate the following sigmoidal-shaped batch growth curve. This curve gives an implicit solution for biomass concentration while the Lee equation gives an implicit solution for biomass and substrate concentrations.

$$time = \left(\left(\left(\frac{K_S * Y_b + S_o * Y_b + X_{bo}}{S_o * Y_b + X_{bo}} \right) * \left(\ln \left(\frac{X_{bt}}{X_{bo}} \right) - \left(\frac{K_S * Y_b}{S_o * Y_b + X_{bo}} \right) \right) * \left(\ln \left(\frac{Y_b * S_o + X_{bo} - X_{bt}}{Y_b * S_o} \right) \right) \right) / \mu_{\max} \right) + t_0 \quad (4.1.6)$$

A third nonlinear equation was developed by Robinson (1985), who used the following equation (4.1.7) that describes the rate at which substrate is consumed in a batch system.

$$\left(\frac{dS_{bt}}{dt} \right) = - \left(\frac{\mu_{\max} * S_{bt}}{K_s + S_{bt}} \right) * \left(\frac{X_{bt}}{Y_{xb}} \right) \quad (4.1.7)$$

The biomass concentration (X_{bt}) in this equation (4.1.7) is replaced by the biomass derived from the biomass yield equation (4.1.4). Following integration, the implicit nonlinear equation is obtained:

$$time = \left(\left(\left(\left(\frac{K_s * Y_b}{X_{bo} + S_{bo} * Y_b} \right) + 1 \right) * \ln \left(\left(\frac{Y_b * (S_{bo} - S_{bt}) + X_{bo}}{X_{bo}} \right) \right) + \left(\left(\frac{K_s * Y_b}{X_{bo} + S_{bo} * Y_b} \right) * \ln \left(\frac{S_{bo}}{S_{bt}} \right) \right) \right) / \mu_{\max} \right) + t_o \quad (4.1.8)$$

The Robinson equation (4.1.8) gives an implicit solution for substrate concentration change over time.

Although equations 4.1.5, 4.1.6, and 4.1.8 can all be used to estimate growth kinetic parameters, they do not always converge on reasonable estimates for non-perfect data sets from laboratory experiments. Further, it is not possible to know if good parameter estimates have been produced when the equations do converge.

In addition to the nonlinear methods, linear methods have been utilized to find the kinetic parameter estimates for many microbes. One linear method was developed by dividing the Monod model by one, yielding the Lineweaver-Burk model. A second linearized method was developed by multiplying the inverted Monod model by substrate concentration, yielding the Hanes model.

The following equation shows the Lineweaver-Burk model:

$$\left(\frac{1}{\mu} \right) = \left[\left(\frac{K_s}{\mu} \right) * \left(\frac{1}{S} \right) + \left(\frac{1}{\mu_{\max}} \right) \right] \quad (4.1.9)$$

The slope is $\left(\frac{K_s}{\mu_{\max}} \right)$ and the intercept is $\left(\frac{1}{\mu_{\max}} \right)$ from plotting $\left(\frac{1}{\mu} \right)$ versus $\left(\frac{1}{S} \right)$.

The next equation shows the Hanes model:

$$\left(\frac{S}{\mu} \right) = \left[\left(\frac{K_s}{\mu_{\max}} \right) + \left(\frac{1}{\mu_{\max}} \right) * S \right] \quad (4.1.10)$$

The slope is $\left(\frac{1}{\mu_{\max}} \right)$ and the intercept is $\left(\frac{K_s}{\mu_{\max}} \right)$ of the plot $\left(\frac{S}{\mu} \right)$ versus S.

Both linearized methods provide estimates for K_s and μ_{\max} , but it is uncertain how well these models perform in comparison to the nonlinear models. It is also uncertain how the nonlinear methods compare in relation to each other. The objective of this research is to investigate the performance of these models and to determine which of the models provides the more accurate and reliable estimates.

The “Markov Chain Monte Carlo” method, also known as “MCMC” is used extensively to simulate data and can be employed to test the fit of complex equations. It originated in physics where the desired integrals for hydrodynamics in complicated geometries with internal heating were not easily determined (<http://cscs.umich.edu/~crshalizi/notebooks/monte-carlo.html>). The well-recognized nonlinear and linear equations previously discussed were tested with the Monte Carlo method to determine which performed best.

4.2 Materials and Methods

The Monte Carlo method is a numerical method that can be described as a statistical simulation method. A statistical simulation is defined in general terms to be any method that utilizes sequences of random numbers to perform the simulation. It is a method where the properties of the distribution of the response variables are investigated through the use of simulated random numbers. Simulated numerical quantities that are difficult or impossible to compute by purely analytic means may be determined by using Monte Carlo simulation to quickly identify promising statistical methods (<http://csep1.phy.ornl.gov/mc/node1.html>).

The Monte Carlo simulation samples from differential equations, which necessitate a fast and effective way to generate normally-distributed random numbers, utilize random sampling techniques to arrive at a solution of the physical problem.

The basic approach of the Monte Carlo technique was to generate a data set from given initial conditions and to simulate the growth curve once the data set was generated. Then, the best fit of the nonlinear and linear equations was determined. The Monte Carlo technique is only as good as the simulation.

4.2.1 Data Generation

The SAS[®] (Statistical Analysis Software) program was used to perform these studies. The values of the parameter K_s was set equal to 50 mg/L, and the parameter μ_{\max} was set to 0.6 hr^{-1} . A normally distributed standard error of 10% was applied to both kinetic parameters (μ_{\max} and K_s) in each iteration. The K_s and μ_{\max} 10% standard errors were intended to represent the biological variability of the microorganism over time, and insure that no two growth curves were exactly alike.

The initial conditions to start the data generation were as follows: the initial biomass concentration (X_{bo}) was 0.5 mg/L and the biomass yield (Y_{xb}) was 0.5. Thirteen levels of substrates were generated, from 200 mg/L to 1000 mg/L by levels of 50 mg/L. The time frame generated was from 0 to 20 hours by 0.001 hours intervals. The generation of data stopped if either the change in biomass fell below zero or the substrate level fell to 1.0 mg/L. The total number of simulated microbial growth curves generated was 5,000 replicates of the 13 levels of substrate concentrations examined for total of 85,000.

A stochastic process is a sequence of states whose evolution is determined by random events. A Monte Carlo method is one that involves deliberate use of random

numbers in a calculation that has a stochastic structure (a stochastic model is the opposite of a deterministic model, where this deterministic model has all the mathematical relationships of fixed elements) (Despa, 1999). In addition to the two stochastic variables previously mentioned (the 10% normally distributed standard errors for K_s and μ_{\max}) this study included a third term to simulate stochastic variation in the sampling. The biological process was modeled at intervals of 0.001 hour, but the “sampled” data set was output at integer, hourly intervals. Although the time frame was simulated from 0 to 20 hours, the simulation was stopped when either the change in biomass reached zero or the substrate level was reduced to 1.0 mg/L.

An additional stochastic variation of 1% of the total biomass was added to these hourly sampling values. Due to the biomass yield definition which connects substrate and biomass, the standard error term given to biomass also affects the substrate.

Equations 4.1.11 and 4.1.12 show the equations used to create the stochastic variables with a normally distributed standard error. Where the function RAND is equal to a normally distributed random variate with mean 0 and variance 1, the equations are:

$$K_s = MEANk_s + RAND * (0.10 * MEANk_s) \quad (4.1.11)$$

$$\mu_{\max} = MEAN\mu_{\max} + RAND * (0.10 * MEAN\mu_{\max}) \quad (4.1.12)$$

4.2.2 Data Simulation

The goal was to simulate a microorganism’s growth behavior through a logistic growth pattern under aerobic conditions. To do so, the mass balance around the reactor with respect to biomass was used with the Monod model substituted into the equation. The change in substrate over the change in biomass equals the inverse of biomass yield.

The equations 4.1.13 and 4.1.14, given below were coded in SAS to simulate the data sets for biomass produced over time and substrate utilized over time.

$$dBiomassT = \left(\left(\frac{\mu_{\max} * SubstrateT}{K_s + SubstrateT} \right) * BiomassT \right) * dt \quad (4.1.13)$$

$$dSubstrateT = \left(\left(\frac{1}{Y_{xb}} \right) * dBiomassT \right) \quad (4.1.14)$$

The “hourly” output observations included the following variables: time, SubstrateT, BiomassT, Yxb, dBiomassT, dSubstrateT, rep, SubstrateINIT, ks, and umax. Plots of BiomassT versus time, SubstrateT versus time and BiomassT versus SubstrateT were developed from this data set.

4.2.3 Monte Carlo Fitting the Models

The nonlinear and linear models were fit to the hourly output data set. The objective was to determine how well these models could estimate the kinetic parameters K_s and μ_{\max} for an aerobic fermentor. The nonlinear simulations used the entire available time frame to estimate the kinetic parameters. In laboratory experiments frequently only the first four hours, the exponential growth phase, are employed for fitting the kinetic parameter estimates of the bacteria or yeast cells. Microorganisms often grow very rapidly and then quickly decay, causing a potential problem if the whole time frame is used to determine the kinetic parameters from a laboratory experiment. In order to consider this aspect of the model we fit varying time segments to the linear equations.

4.2.3.1 Nonlinear Method

The parameters of the Lee (4.1.5), Shuler & Kargi (4.1.6), and Robinson (4.1.8) equations were estimated using 'proc model' from SAS software. The Lee equation was coded in the SAS program for biomass and substrate changing over time. The Shuler & Kargi equation with biomass changing over time, and the Robinson equation with substrate changing over time, were both coded in the SAS program.

For each of the three nonlinear equations, two types of initial substrate and biomass conditions were studied. They were referred to as "fixed" and "fitted" values. The fixed condition occurs when the initial values of substrate and biomass (at time = 0) were set to a constant intercept value. The fixed values were the known initial substrate concentrations (200 to 1,000 mg/L by 50) and biomass equal to 0.5 mg/L. The use of fixed values assumes that the intercepts (initial substrate and biomass concentrations) are known. The alternative is to fit the intercepts. For the fitted option initial conditions were provided, but the values for initial substrate and biomass are reevaluated while the other parameters are estimated. The initial conditions provided were for the substrate concentration of 600 mg/L and biomass concentration of 0.5 mg/L.

When fitting nonlinear models the usual procedure is to provide starting values for the parameters being estimated. When reasonable starting values are available it is advisable to provide these values. If starting values are not known, SAS can provide starting values. Since in practice starting values for the kinetic parameters are often not known, the SAS models were fitted for both cases, starting values specified and starting values omitted. The parameters fitted were the two kinetic parameter values of primary interest (K_s and μ_{max}) and the two intercepts (initial substrate and initial biomass).

Table 4.2.1 shows the twelve combinations (three nonlinear models * two initial substrate and biomass conditions * two initial starting values (kinetic parameters) conditions) used for evaluation.

Table 4.2.1 The Twelve Combinations for the Nonlinear Method.

Lee Equation				Shuler & Kargi Equation				Robinson Equation			
Fitted		Fixed		Fitted		Fixed		Fitted		Fixed	
Starting values given	Starting values not given	Starting values given	Starting values not given	Starting values given	Starting values not given	Starting values given	Starting values not given	Starting values given	Starting values not given	Starting values given	Starting values not given

The Monte Carlo generated data was fitted to the nonlinear models. Information about the fit was written to a permanent output file. This file contained the following variables: case being studied (table 4.2.1), initial biomass (t=0), initial substrate (t=0), observations number (N), Convergence Status, ks estimate, mu estimate, and replicate number. The permanent output file was further subset into two files, one with information on successful nonlinear fits and one with fits classified as “errors”. Fits were classified with errors under the following conditions: the SAS reported convergence status was ‘3 error’, Ks estimated was less then zero, Ks was greater than 1,000, μ_{max} less than zero, the initial substrate estimate was less than zero, and the initial substrate estimate was greater than 10,000.

4.2.3.2 Linear Method

The two linear equations were fit using the ‘proc reg’ function from SAS software, the Hanes plot and the Lineweaver-Burk plot models.

In order to examine the necessity of fitting the exponential phase alone the time was divided into four ‘time frames’. These were “Whole” (from 0 hours to 20 hours),

“Exponential 1” (from 0 hours to 4 hours), “Exponential 2” (from 5 hours to 8 hours), and “Stationary” (from 8 hours to 20 hours).

The linear models are normally fit across various levels of substrate, in practice usually a wide range of substrates. To examine the effectiveness of this approach the substrate concentrations were divided into five categories. These were “Whole” (all available values from 200 to 1,000 by 50), “Selected” (five widely spaces values from 200 to 1,000 by 200), “High” (from 800 to 1,000 by 50), “Medium (from 500 to 700 by 50), and “Low (from 200 to 400 by 50). Table 4.2.2 shows the combinations elaborated for each linear equation. The first set had 10 combinations (two linear models * one time frame * five substrate concentrations), the second set had 12 combinations (two linear models * three time frames * two substrate concentrations).

Table 4.2.2 The Combinations for the Linear Methods.

Hanes Equation and Lineweaver-Burk Equation				
‘Time frame’: Whole (0-20 hrs)				
Substrate Concentration				
Whole	Selected	High	Medium	Low
‘Time frame’: Exponential 1 (0-4 hrs)				
Substrate Concentration				
Whole		Selected		
‘Time frame’: Exponential 2 (5-8 hrs)				
Substrate Concentration				
Whole		Selected		
‘Time frame’: Stationary (9-20 hrs)				
Substrate Concentration				
Whole		Selected		

There were a total of 22 cases examined for the linear models. For each case in the linear equations the substrate concentrations were averaged over each ‘time frame’ and the averaged substrates were used to calculate the specific growth rate. The Hanes and Lineweaver-Burk equations were output into one permanent file. The permanent file contained the variables data set (Hanes and Lineweaver-Burk) cases, and the estimated values for μ_{Max} and K_s . The SAS code for this entire research is available in Appendix I.

4.3 Results and Discussion

This preliminary analysis was run on 5,000 replicates.

4.3.1 Results from the Data Generation and Simulation

Figures 4.3.1, 4.3.2, and 4.3.4 represent the biomass formation versus time for each substrate respective category (High, Medium and Low), generated by the SAS software.

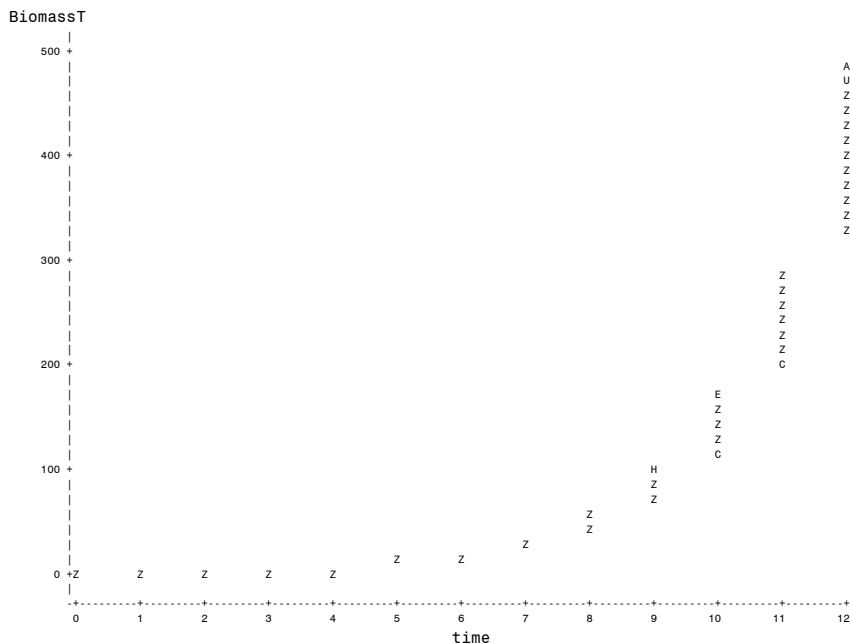


Figure 4.3.1 Biomass (mg/L) for the high substrate concentration versus time.

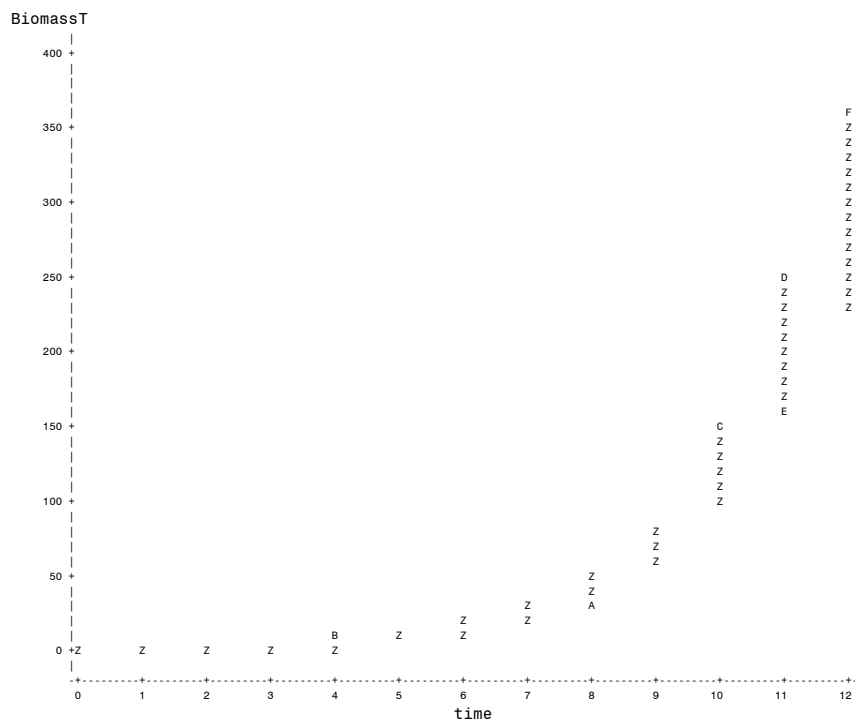


Figure 4.3.2 Biomass (mg/L) for the medium substrate concentration versus time.

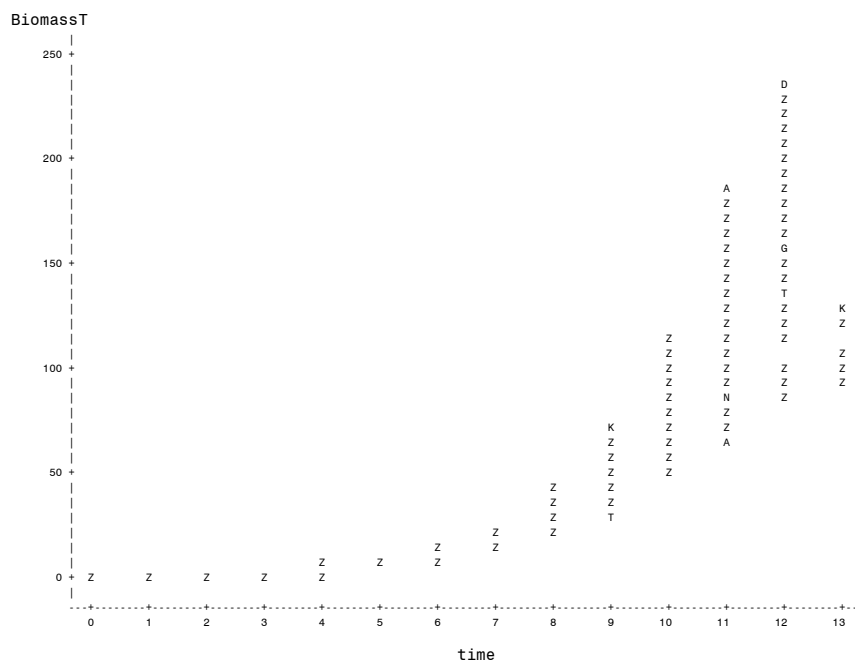


Figure 4.3.3 Biomass (mg/L) for the low substrate concentration versus time.

Figures 4.3.4, 4.3.5, and 4.3.6 represent the substrate concentrations (high, medium, and low) versus time, generated by the SAS software.

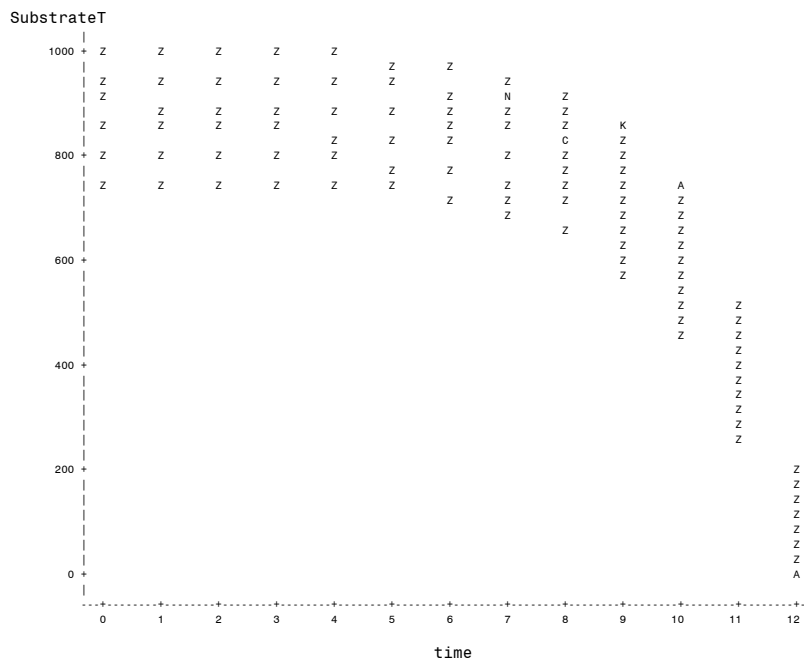


Figure 4.3.4 The high substrate concentration (mg/L) versus time.

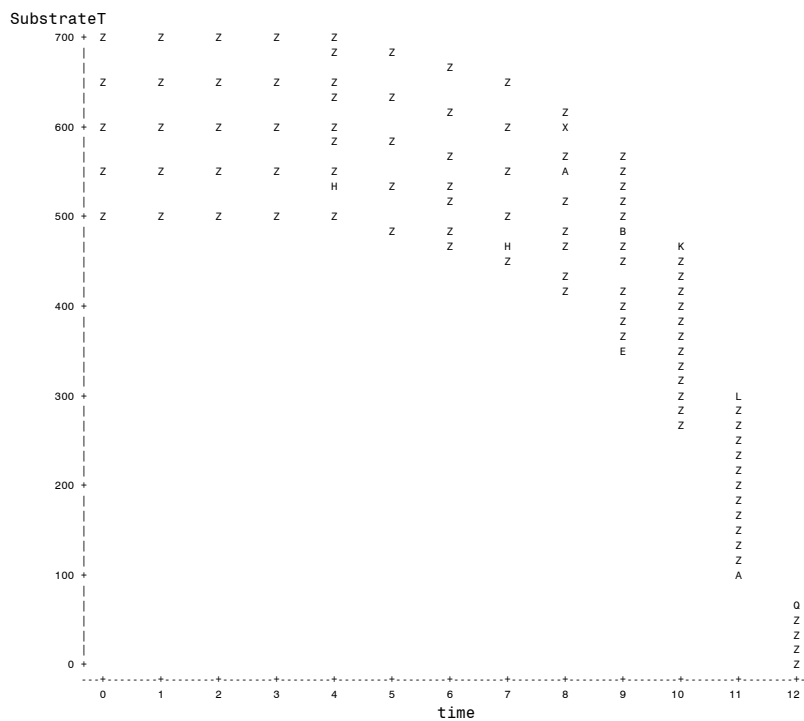


Figure 4.3.5 The medium substrate concentration (mg/L) versus time.

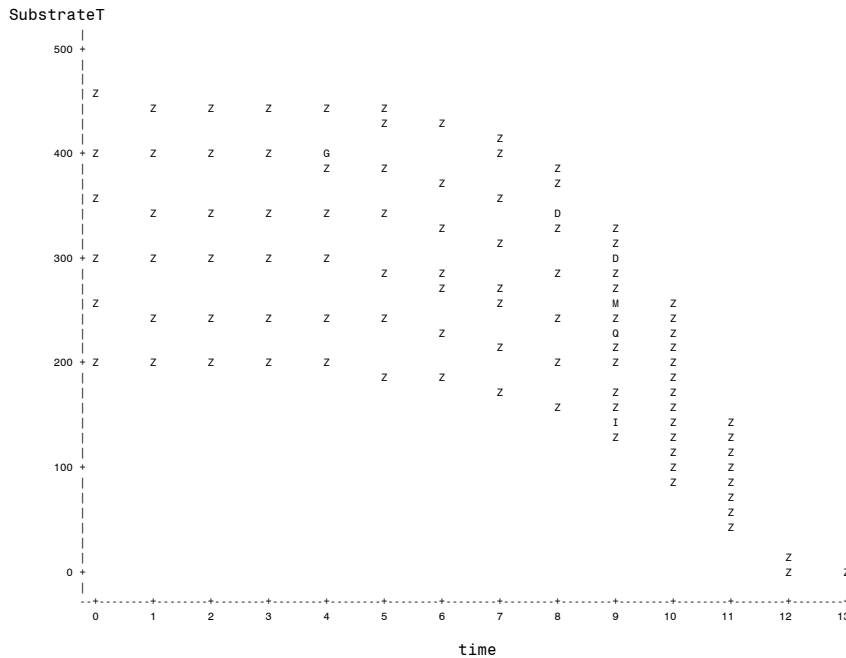


Figure 4.3.6 The low substrate concentration (mg/L) versus time.

The simulations for each substrate and biomass concentration were separated into a low group (200 to 450 mg/L), a medium group (500 to 700 mg/L), and a high group (750 to 1,000 mg/L). The figures showed that the biomass simulation was generated over time for each substrate group, and that the simulated substrate was utilized. Although the time period for the simulation was set to 20 hours, the simulation was stopped when the change in biomass reached zero or the substrate level was reduced to 1 mg/L. As a result the biomass was generally generated and the substrate was nearly fully utilized within 13 hours. The substrate concentrations were limiting the cell growth after 12 hours. These figures showed that the microorganism was growing quickly until the substrate concentrations became depleted. According to the Banat et. al. (1996), *Kluyveromyces marxianus* yeast strain grows exponentially under anaerobic conditions for 10 hours. Therefore, under aerobic conditions the time period simulated of 12 hours was expected.

4.3.2 Results for the Nonlinear Models

The nonlinear models were fit to 5,000 replicates of each of seventeen different substrate concentrations. This produced 85,000 generated growth curves which were then fitted with each model.

Table 4.3.1 shows the means of the estimated for growth kinetic parameters for each of the twelve combinations with errors excluded from this output (exclusion criteria given in 4.2.3.1). The percentage differences were calculated for each mean of K_s and μ_{\max} .

The % Difference for Mean K_s

$$\left(\frac{(MeanK_s - 50)}{50} \right) * 100\% \quad (4.1.15)$$

The % Difference for Mean μ

$$\left(\frac{(Mean\mu - 0.6)}{0.6} \right) * 100\% \quad (4.1.16)$$

Table 4.3.1 The Nonlinear Models Outputs for K_s and μ_{\max} without errors.

Dataset	Substrate Category	Frequency	Mean K_s	% Difference for Mean K_s	Mean μ	% Difference for Mean μ
Shuler-fitted-starting value not given	Integer (200 - 1,000 by 50)	8140	35.8548	-28.2904	0.58548	-2.42
Shuler-fitted-starting value given	Integer (200 - 1,000 by 50)	62917	56.6051	13.2102	0.60012	0.02
Shuler-fixed-starting value not given	Integer (200 - 1,000 by 50)	84987	50.1083	0.2166	0.60034	0.056667
Shuler-fixed-given	Integer (200 - 1,000 by 50)	84987	50.1079	0.2158	0.60034	0.056667
Lee-fitted-starting value given	Integer (200 - 1,000 by 50)	84999	49.449	-1.102	0.59925	-0.125
Lee-fitted-starting value not given	Integer (200 - 1,000 by 50)	84999	49.4486	-1.1028	0.59925	-0.125
Lee-fixed-starting value given	Integer (200 - 1,000 by 50)	84993	49.4576	-1.0848	0.59929	-0.11833
Lee-fixed-starting value not given	Integer (200 - 1,000 by 50)	84993	49.4576	-1.0848	0.59929	-0.11833
Robinson-fitted-starting value given	Integer (200 - 1,000 by 50)	5000	49.5424	-0.9152	0.59906	-0.15667
Robinson-fitted-starting value not given	Integer (200 - 1,000 by 50)	35018	49.6632	-0.6736	0.59938	-0.10333
Robinson-fixed-starting value given	Integer (200 - 1,000 by 50)	85000	49.7809	-0.4382	0.59957	-0.07167
Robinson-fixed-starting value not given	Integer (200 - 1,000 by 50)	85000	49.7809	-0.4382	0.59957	-0.07167

Table 4.3.2 shows the means of the growth kinetic parameters which were output to the error file. This output was determined by setting a large range of unacceptable values calculated from the nonlinear models. The percentage difference for each mean was calculated using the equations 4.1.15 and 4.1.16.

Table 4.3.2 The Nonlinear Models Output for Ks and μ_{\max} with errors.

Dataset	Substrate Category	Frequency	Mean Ks	% Difference for Mean Ks	Mean Mu	% Difference for Mean Mu
Shuler-fitted-starting value not given	Integer (200 - 1,000 by 50)	76860	6.86E+72	1.37158E+73	-5.94E+28	-9.9E+30
Shuler- fitted-starting value given	Integer (200 - 1,000 by 50)	22083	418117788.6	836235477.2	32326.03	5387572
Shuler-fixed-starting value not given	Integer (200 - 1,000 by 50)	13	-5.86	-111.72	0.55	-8.33333
Shuler-fixed-starting value given	Integer (200 - 1,000 by 50)	13	-5.87	-111.74	0.55	-8.33333
Lee- fitted-starting value given	Integer (200 - 1,000 by 50)	1	-0.77	-101.54	0.56	-6.66667
Lee- fitted-starting value not given	Integer (200 - 1,000 by 50)	1	-0.23	-100.46	0.56	-6.66667
Lee-fixed-starting value given	Integer (200 - 1,000 by 50)	7	-3.06	-106.12	0.56	-6.66667
Lee-fixed-starting value not given	Integer (200 - 1,000 by 50)	7	-3.06	-106.12	0.56	-6.66667
Robinson-fitted-starting value given	Integer (200 - 1,000 by 50)	20000	-101.12	-302.24	0	-100

From Table 4.3.1 the percent (%) difference column shows that the worst values acquired for Ks and μ_{\max} were obtained from the Shuler & Kargi equation with fitted initial conditions and the kinetic parameters not given. The next worse results were obtained by the Robinson equation with fitted initial conditions and the kinetic parameters given. The ‘Shuler-fitted-starting value not given’ combination had only 8,140 converged values that were not placed in the error output file. The ‘Robinson-fitted-starting value given’ combination had only 5,000 converged values that were not placed in the error output file. The two best combinations with 85,000 convergences and with the least % difference were the Robinson model with both fixed initial conditions and with either given or not-given kinetic parameters. By looking at the % difference

columns for the means of K_s , we could express a rank from the largest percentage difference to the smallest (descending order) for the datasets as follows: the Shuler equation with fitted initial conditions and not given the kinetic parameters, the Shuler equation with fitted initial conditions and given the kinetic parameters, the Robinson equation with fitted initial conditions and given the kinetic parameters, and the Lee equation with fitted initial conditions and not given the kinetic parameters. The fifth best result was Lee equation with fitted initial conditions and given the kinetic parameters, then both Lee equations with fixed initial conditions and either given or not given the kinetic parameters. The seventh best results was the Robinson equation with fitted initial conditions and not given the kinetic parameters, then both the Robinson equations with fixed initial conditions and either given or not given the kinetic parameters. The last best results were the Shuler & Kargi equations with fixed initial conditions and either given or not given the kinetic parameters. The best values for K_s and μ_{\max} determined using the nonlinear models were, in first place, the ‘Shuler & Kargi-fixed-starting value not given’ and the ‘Shuler & Kargi-fixed-starting value given’ with 50.1079 mg/L for K_s and 0.60034 hr^{-1} for μ_{\max} ; and in second place were ‘Robinson-fixed-starting value not given’ and the ‘Robinson-fixed-starting value given with 49.7809 mg/L for K_s and 0.59957 hr^{-1} μ_{\max} ; and in third place was ‘Robinson-fitted-starting value not given’ with 49.6632 mg/L for K_s and 0.59938 hr^{-1} for μ_{\max} . Table 4.3.2 showed that the Shuler equation with fitted initial conditions and not given the kinetic parameters had the highest % difference for the kinetic parameters, with $1.3715\text{E}+73$ mg/L for K_s and $-9.9\text{E}+30 \text{ hr}^{-1}$ for μ_{\max} , and also had 76,860 unconverged replicates. The Robinson equation with fitted initial conditions and given kinetic parameters had 20,000 unconverged replicates

with -302.24 mg/L for the percentage difference of mean K_s and -100 hr^{-1} for the percentage difference of mean μ_{\max} , and the third worse case was the Shuler equation with fitted initial conditions and given kinetic parameters with 22,083 unconverged replicates.

Figures 4.3.7 to 4.3.18 show the results as a histogram for the midpoints of the K_s parameter, for each of the nonlinear combinations. The K_s parameters were more sensitive than the μ_{\max} parameters, because each μ_{\max} result did not show as large a range as the K_s , which were quite reasonable. The majority of the μ_{\max} parameters ranged from 0.5 to 0.8 (hr^{-1}) for the nonlinear models. The μ_{\max} midpoints histograms are available in Appendix J. Figures 4.3.7 to 4.3.14 have their x-axis range from 0 to 110 by 5, Figures 4.3.15 and 4.3.16 have their x-axis range from 0 to 130 mg/L by 5 mg/L, Figure 4.3.17 has the x-axis range from 0 to 950 mg/L by 50 mg/L, and Figure 4.3.18 has the x-axis range from 0 to 280 mg/L by 20 mg/L. The y-axis for all the figures is the frequency of the replications. Most of the figures were centered at the midpoint of K_s (50 mg/L) and they were normally distributed.

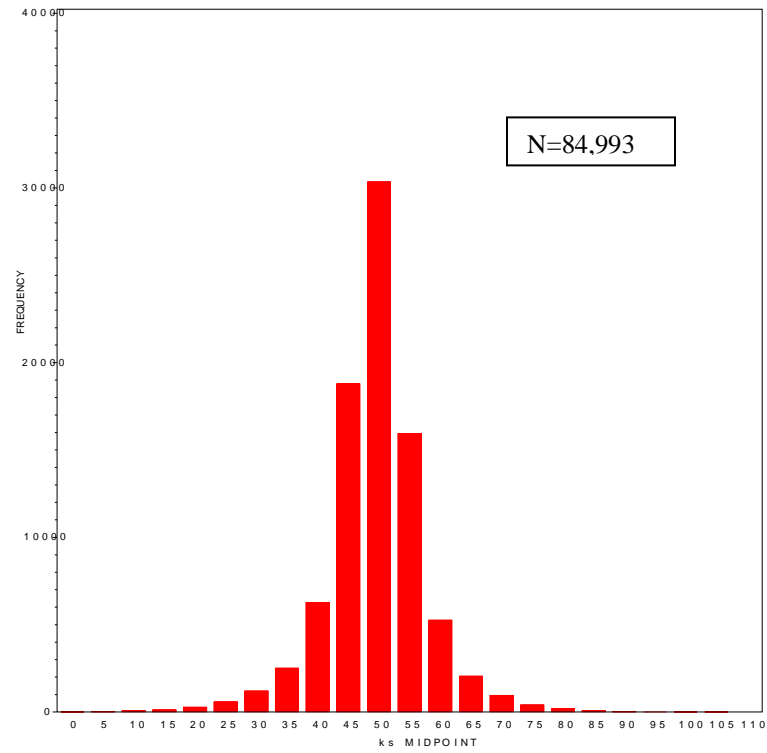


Figure 4.3.7 Lee Equation-Fixed-Starting Value Given

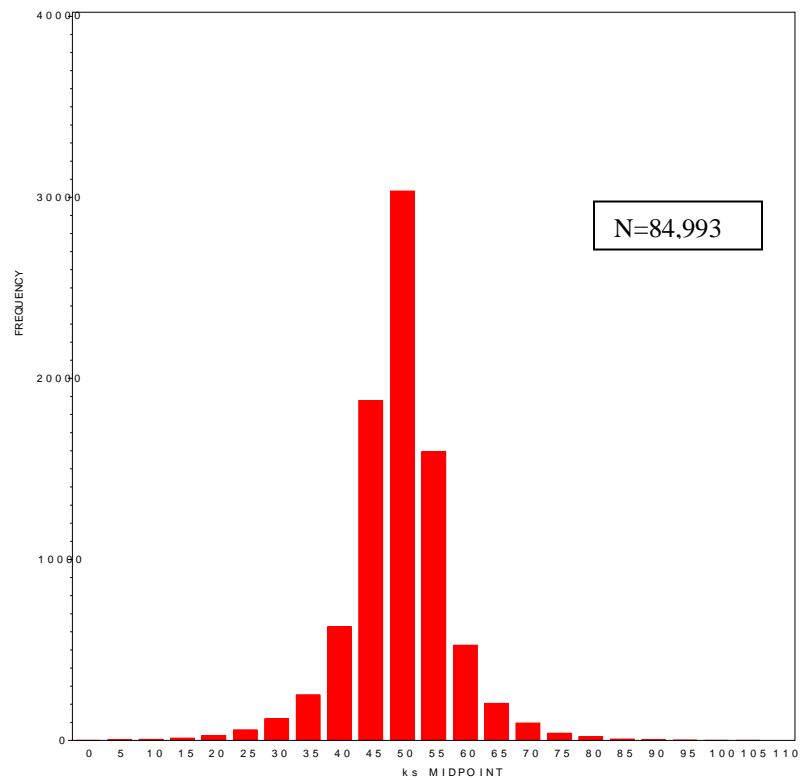


Figure 4.3.8 Lee Equation-Fixed-Starting Value Not Given

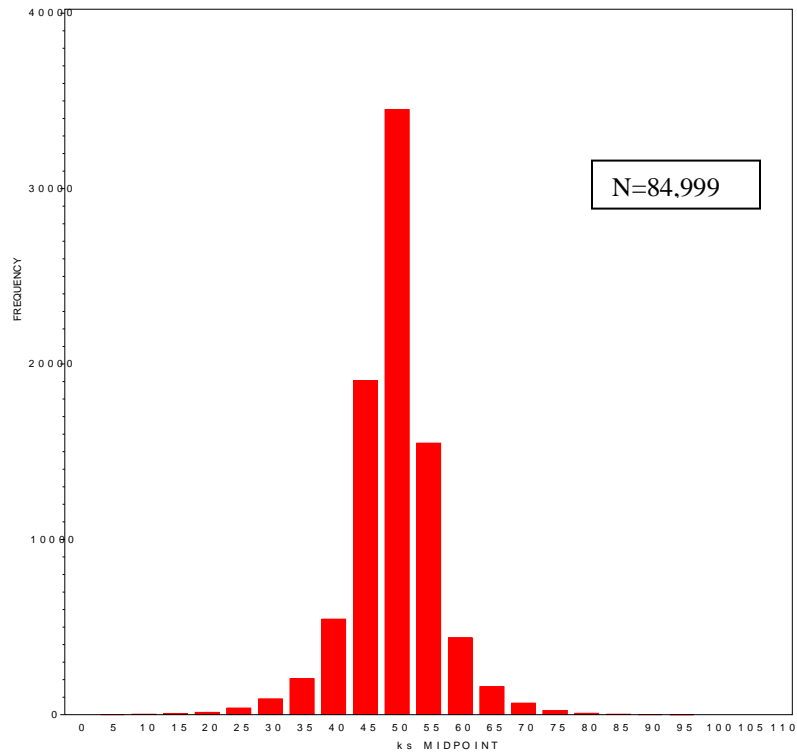


Figure 4.3.9 Lee Equation-Fitted-Starting Value Given

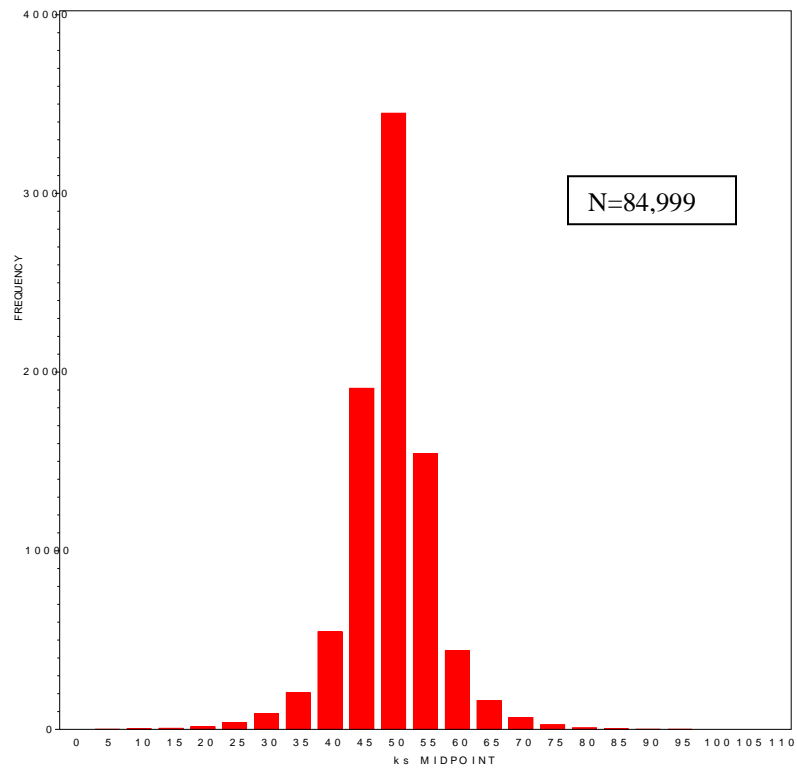


Figure 4.3.10 Lee Equation-Fitted-Starting Value Not Given

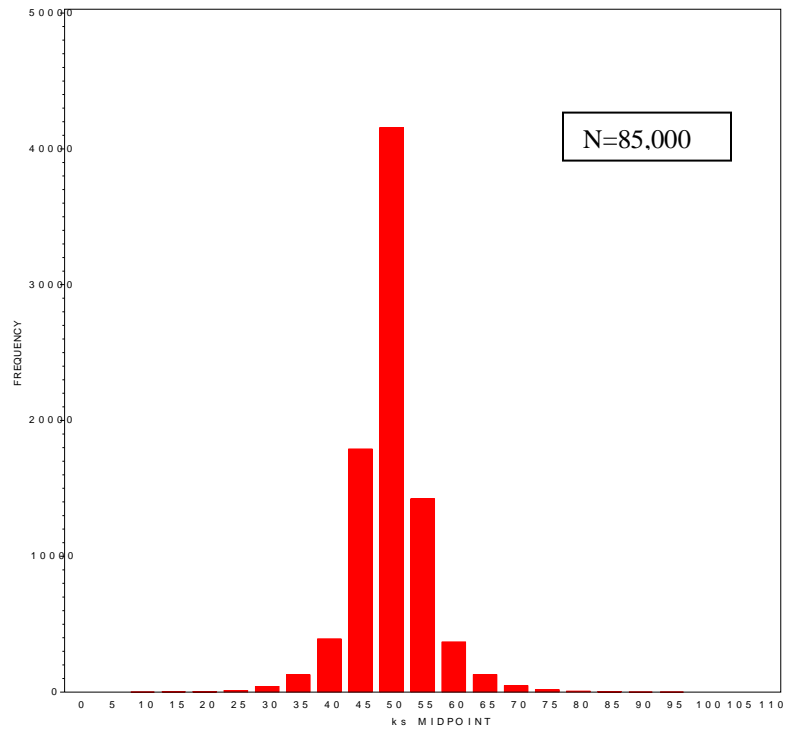


Figure 4.3.11 Robinson Equation-Fixed-Starting Value Given

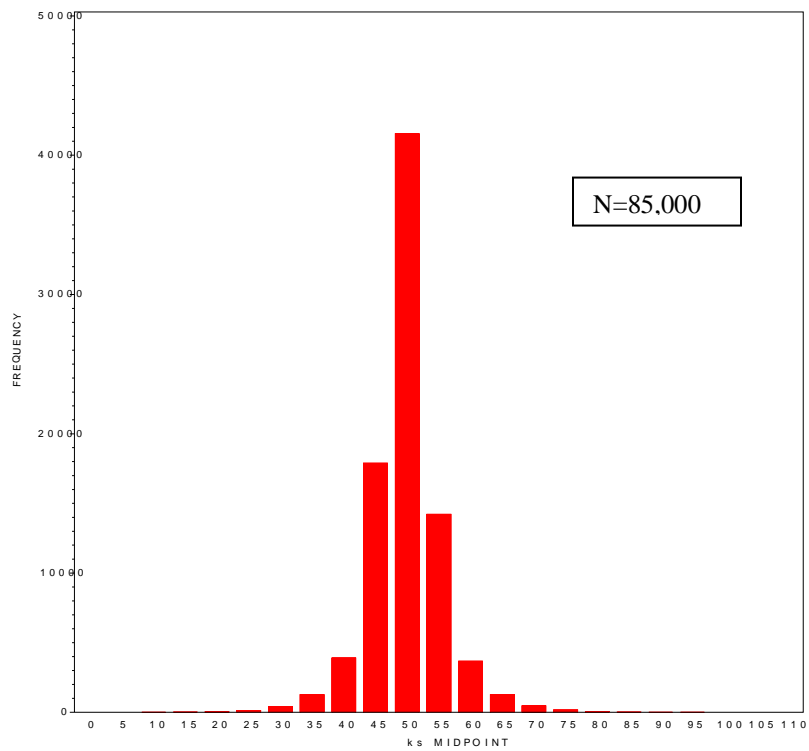


Figure 4.3.12 Robinson Equation-Fixed-Starting Value Not Given

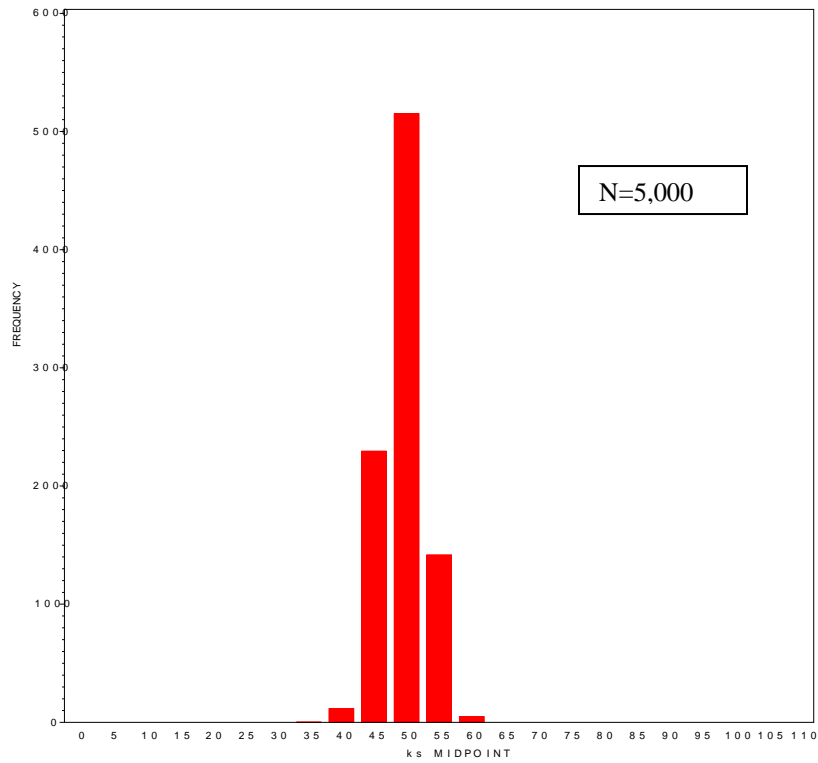


Figure 4.3.13 Robinson Equation-Fitted-Starting Value Given

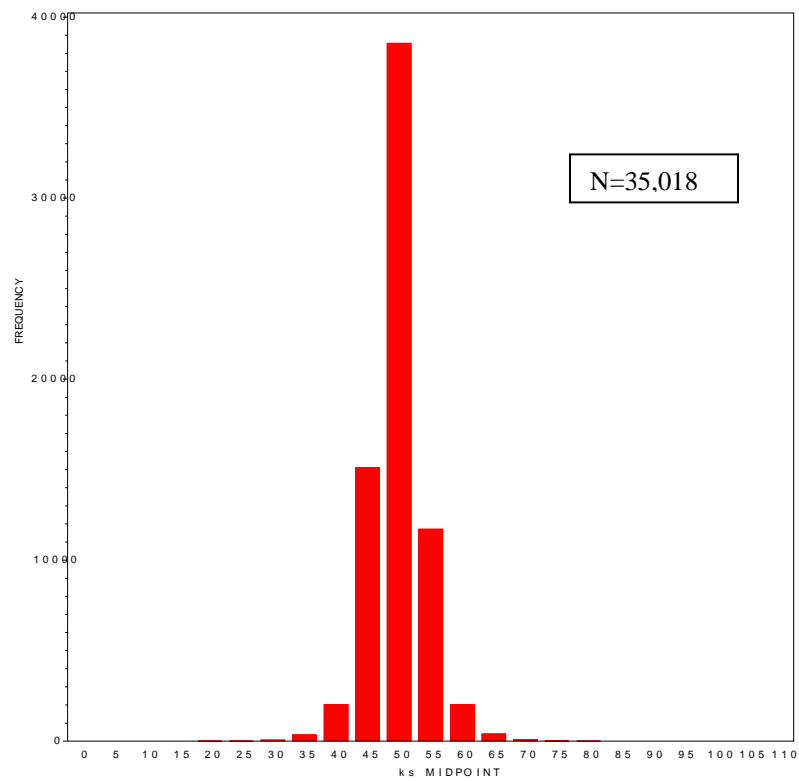


Figure 4.3.14 Robinson Equation-Fitted-Starting Value Not Given

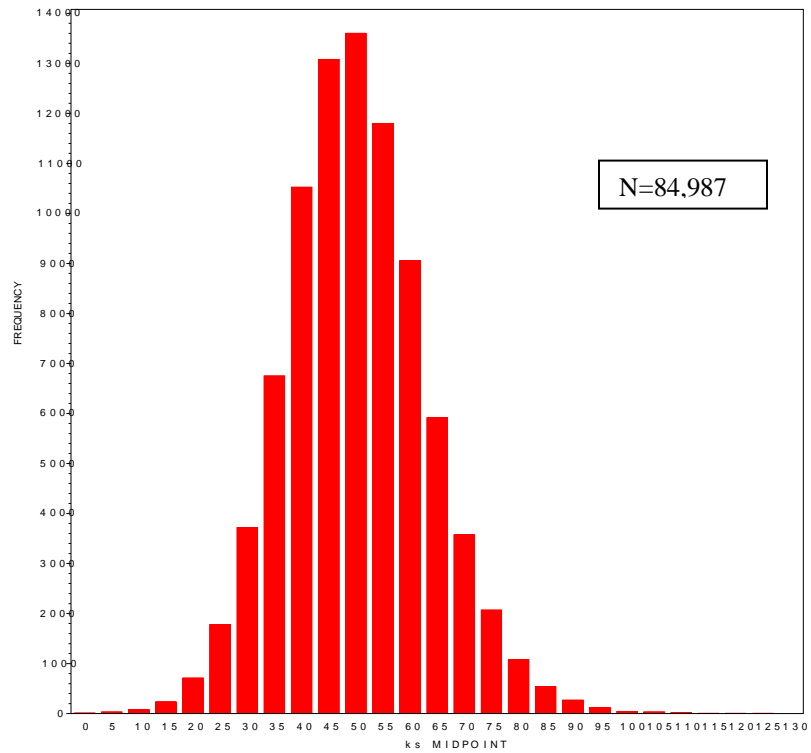


Figure 4.3.15 Shuler & Kargi Equation-Fixed-Starting Value Given

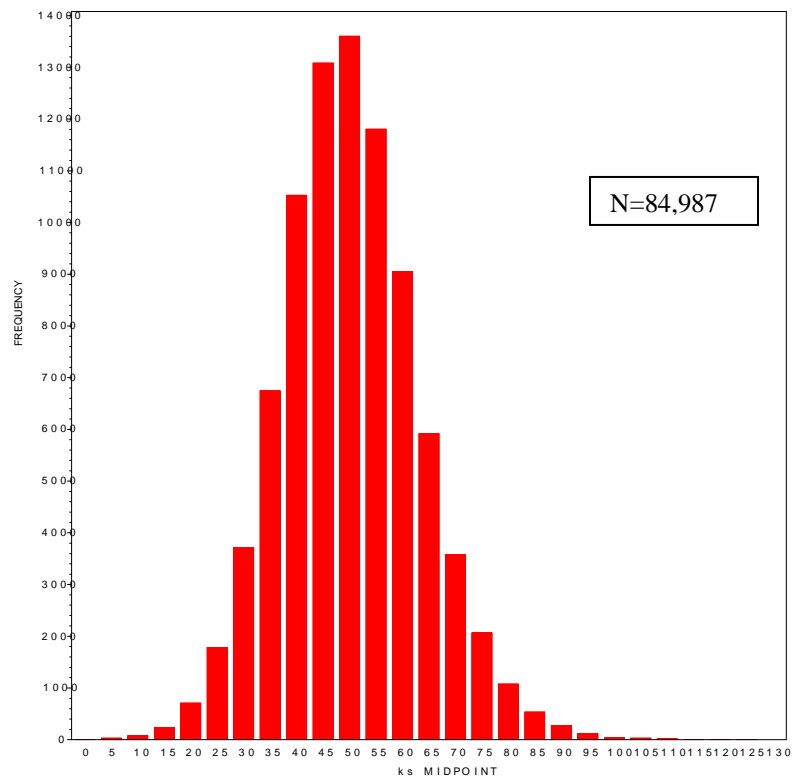


Figure 4.3.16 Shuler & Kargi Equation-Fixed-Starting Value Not Given

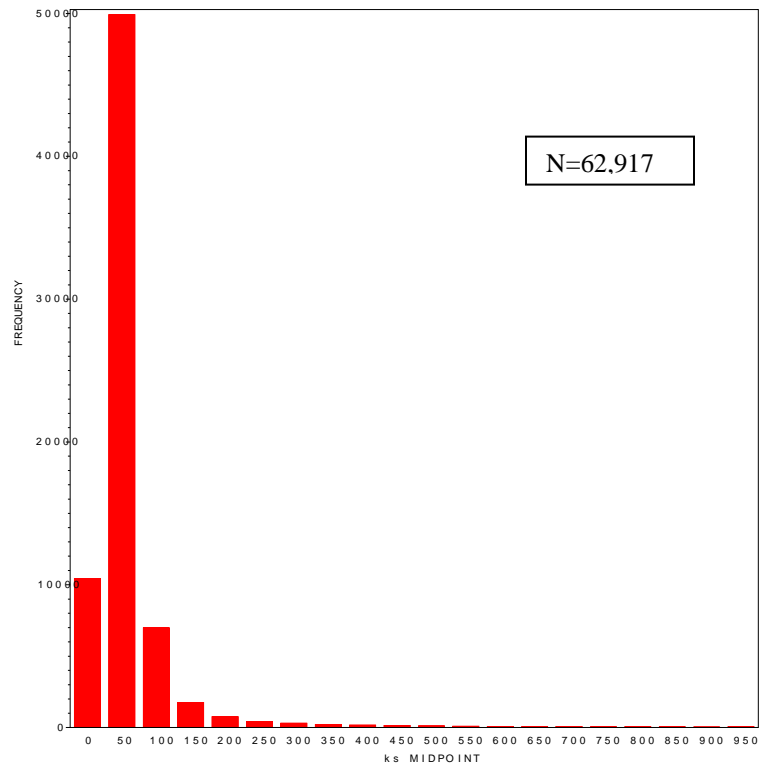


Figure 4.3.17 Shuler & Kargi Equation-Fitted-Starting Value Given

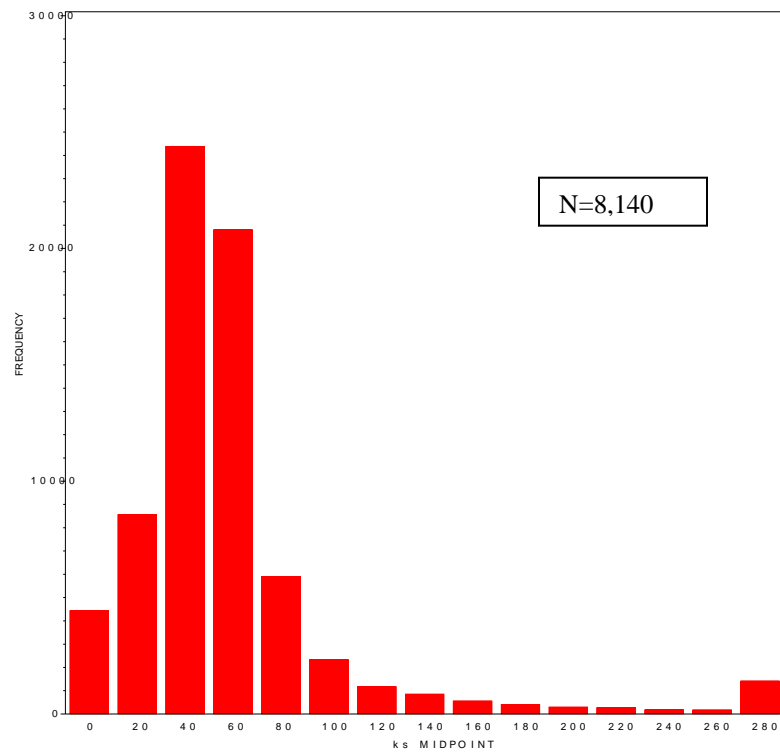


Figure 4.3.18 Shuler & Kargi Equation-Fitted-Starting Value Not Given

Figures 4.3.7 and 4.3.8 show results for the Lee equation with fixed initial conditions and with either given or not given kinetic parameters. These histograms generally show a normal bell shaped curve with 30,000 frequencies occurring at 50 mg/L, with a 19,000 occurring at 45 mg/L and with a 16,000 occurring at 55 mg/L for K_s . Figures 4.3.9 and 4.3.10 show results for the Lee equation with fitted initial conditions and with either given or not given kinetic parameters. These also have a normal bell shaped curve with 35,000 frequencies occurring at 50 mg/L, with a 19,000 mg/L occurring at 45 mg/L and with a 16,000 mg/L occurring at 55 mg/L for K_s . Figures 4.3.11 and 4.3.12 show results for the Robinson equation with fixed initial conditions and with either given or not given kinetic parameters. Here the results indicate a narrower normal bell shaped curve with 41,000 frequencies occurring at 50 mg/L, with an 18,000 mg/L occurring at 45 mg/L and with 14,000 occurring at 55 mg/L for K_s . Figure 3.4.13 showed results for the Robinson equation with a narrower normal bell shaped curve with only 5,100 frequencies occurring at 50 mg/L, with a 2,200 frequencies occurring at 45 mg/L and with a 1,400 frequencies occurring at 55 mg/L for K_s . Figure 4.3.14 showed results for the Robinson equation with a narrow normal bell shaped curve with a 38,000 frequencies occurring at 50 mg/L, with a 15,000 frequencies occurring at 45 mg/L and with an 11,000 frequencies occurring at 55 mg/L for K_s . Figures 4.3.15 and 4.3.16 showed results for the Shuler and Kargi equation with fixed initial conditions and with either given or not given kinetic parameters with the broadest normal bell shaped curve with a 13,500 frequencies for K_s occurring at 50 mg/L, with a 13,000 frequencies occurring at 45mg/L and the rest of the frequencies were evenly distributed from the center for the K_s . Figures 4.3.17 and 4.3.18 showed results for the Shuler and Kargi equation with fitted initial conditions and with

either given or not given kinetic parameters with a positive skewedness where the mode was larger than the median and the median was larger than the mean (mode<median<mean) for the K_s values. Figure 4.3.16 showed 50,000 frequencies of K_s occurring at 50 mg/L and 10,000 frequencies occurring between 0 and 45 mg/L and the rest of the values were skewed to the right reaching 750 mg/L. Figure 4.3.18 showed 25,000 frequencies of K_s occurring at 40 mg/L, and 21,000 frequencies of K_s occurring at 60 mg/L, and the rest of the values drifted slowly to the right reaching 280 mg/L. The means of K_s for the Shuler & Kargi equation-fitted-starting value given and not given, and for the Robinson equation-fitted-starting value given and not given had the highest unconverged values due to large outliers. The K_s values were estimated to be outside the acceptable range pre-determined for K_s .

4.3.3 Results for the Linear Models

Table 4.3.3 shows the average growth kinetic parameters K_s and μ_{\max} for the Hanes equation for each time frame and substrate concentrations. The percentage differences were calculated for each mean of the kinetic parameters using the equations 4.1.15 and 4.1.16.

Table 4.3.3 The Hanes equation output for each time frame and substrate categories.

Dataset	Time Frame	Substrate Categories	Mean Ks	% Difference for Mean Ks	Mean Mu	% Difference for Mean Mu
Hanes Plot	Whole (0-20 hrs)	Whole	54.9496	9.8992	0.60346	0.576667
Hanes Plot	Exponential-1 (0-4 hrs)	Whole -EarlyTime	49.7636	-0.4728	0.59960	-0.06667
Hanes Plot	Exponential-2 (5-8 hrs)	Whole -MiddleTime	49.8129	-0.3742	0.59969	-0.05167
Hanes Plot	Stationary (9-20 hrs)	Whole -LateTime	72.7130	45.426	0.61498	2.496667
Hanes Plot	Whole (0-20 hrs)	High Substrate	54.8509	9.7018	0.60358	0.596667
Hanes Plot	Whole (0-20 hrs)	Medium Substrate	56.6322	13.2644	0.60483	0.805
Hanes Plot	Whole (0-20 hrs)	Low Substrate	55.4965	10.993	0.60534	0.89
Hanes Plot	Whole (0-20 hrs)	Selected	56.3800	12.76	0.60466	0.776667
Hanes Plot	Exponential-1 (0-4 hrs)	Selected-Exponential1	49.6994	-0.6012	0.59957	-0.07167
Hanes Plot	Exponential-2 (5-8 hrs)	Selected-Exponential2	49.8239	-0.3522	0.59970	-0.05
Hanes Plot	Stationary (9-20 hrs)	Selected-Stationary	75.5466	51.0932	0.61830	3.05

Table 4.3.4 shows the averaged growth kinetic parameters K_s and μ_{\max} for the Lineweaver-Burk equation with each time frame and substrate concentrations. The percentage differences were calculated for each mean of the kinetic parameters using the equations 4.1.15 and 4.1.16.

Table 4.3.4 The Lineweaver-Burk equation output for each time frame and substrate categories.

Dataset	Time Frame	Substrate Categories	Mean Ks	% Difference for Mean Ks	Mean Mu	% Difference for Mean Mu
Lineweaver-Burk Plot	Whole (0-20 hrs)	Whole	55.2161	10.4322	0.60385	0.641667
Lineweaver-Burk Plot	Exponential-1 (0-4 hrs)	Whole - EarlyTime	49.7231	-0.5538	0.59956	-0.07333
Lineweaver-Burk Plot	Exponential-2 (5-8 hrs)	Whole - MiddleTime	49.7229	-0.5542	0.59959	-0.06833
Lineweaver-Burk Plot	Stationary (9-20 hrs)	Whole -LateTime	70.9740	41.948	0.61219	2.031667
Lineweaver-Burk Plot	Whole (0-20 hrs)	High Substrate	54.9880	9.976	0.60368	0.613333
Lineweaver-Burk Plot	Whole (0-20 hrs)	Medium Substrate	56.5257	13.0514	0.60471	0.785
Lineweaver-Burk Plot	Whole (0-20 hrs)	Low Substrate	57.8664	15.7328	0.61055	1.758333
Lineweaver-Burk Plot	Whole (0-20 hrs)	Selected	56.8966	13.7932	0.60534	0.89
Lineweaver-Burk Plot	Exponential-1 (0-4 hrs)	Selected-Exponential1	49.6890	-0.622	0.59956	-0.07333
Lineweaver-Burk Plot	Exponential-2 (5-8 hrs)	Selected-Exponential2	49.7509	-0.4982	0.59962	-0.06333
Lineweaver-Burk Plot	Stationary (9-20 hrs)	Selected-Stationary	74.3277	48.6554	0.61610	2.683333

Tables 4.3.3 and 4.3.4 have shown that some of the % difference values of K_s and μ_{\max} were negative because the parameters were underestimated by Hanes and Lineweaver-Burk plots, with either whole or selected substrate concentrations for the exponential-1 and exponential-2 time frames. Tables 4.3.3 and 4.3.4 showed the other values of K_s and μ_{\max} were overestimated by Hanes and Lineweaver-Burk plots. For either the Hanes or the Lineweaver-Burk equations, the highest percentage difference was for the selected substrate concentration during the stationary time frame (9 – 20 hours); with 48 – 51 % larger for K_s and 2.68 – 3.05 % larger for μ_{\max} .

The two best kinetic estimations for K_s parameter with the smallest % difference for the means were the selected substrate concentrations (from 200 to 1,000 by 200) during the exponential-2 time period (from 5 to 8 hours) for either the Hanes or the Lineweaver-Burk plots, and the whole substrate concentrations (from 200 to 1,000 by 50) during exponential-2 time period (from 5 to 8 hours) for the Hanes plot, and the whole substrate

concentrations (from 200 to 1,000 by 50) during exponential-1 time period (from 0 to 4 hours) for the Lineweaver-Burk plot.

The two best kinetic estimations for μ_{\max} parameter with the smallest % difference for the means were the selected substrate concentrations (from 200 to 1,000 by 200) during exponential-2 time period (from 5 to 8 hours) for either the Hanes or the Lineweaver-Burk plots, and the whole substrate concentrations (from 200 to 1,000 by 50) during exponential-2 time period (from 5 to 8 hours) for either the Hanes or the Lineweaver-Burk plots.

Therefore, the Hanes equation estimated the best μ_{\max} of 0.5997 hr^{-1} and K_s of 49.8239 mg/L with selected substrate concentration from 5 to 8 hours and the Lineweaver-Burk equation estimated the best μ_{\max} of 0.59962 hr^{-1} and K_s of 49.7509 mg/L with selected substrate concentration from 5 to 8 hours.

There were slightly differences between both linearization methods, but the Hanes plot still gave smaller % differences for the kinetic parameter means than the Lineweaver-Burk plot.

4.3.4 Comparison between Nonlinear and Linear Models

Tables 4.3.1, 4.3.3 and 4.3.4 show the nonlinear models and the linear models results, respectively. For each kinetic parameter the means and the percentage differences of the means from the known values are given.

One of the more interesting and useful aspects of the Monte Carlo approach is the ability to compare the performance of nonlinear and the linear models. Table 4.3.1 shows the nonlinear output with most of the K_s results from 50.1 to 49.4 mg/L (considering 35.5 and 61.3 mg/L as outliers) and μ_{\max} results from 0.604 to 0.591 hr^{-1} .

Table 4.3.3 shows the linear output for the Hanes equation which varied from 56.6 to 49.6 mg/L for K_s (considering 72.7 and 75.5 mg/L as outliers) and from 0.618 to 0.599 for μ_{\max} . Table 4.3.4 shows the Lineweaver-Burk equation output that varied from 57.8 to 49.6 mg/L for K_s (considering 70.9 and 74.3 mg/L as outliers) and from 0.616 to 0.599 hr^{-1} for μ_{\max} . The overall performance of nonlinear models seemed to either estimate correctly estimate or to underestimate the K_s values, while the linear models seemed to either estimate almost correctly or overestimate the K_s values. In general for either method, the μ_{\max} were estimated with more accuracy than K_s estimations, but the nonlinear models showed a higher accuracy and smaller overestimation of μ_{\max} than the linear models. Even though, for the linear and nonlinear models time frames were not similar, the nonlinear models still performed with more accuracy and consistent results.

4.4 Conclusions

“Biological Engineers” encounter serious problems trying to design biological reactors since their design is dependent on growth kinetic parameters are determined for an observed microbial process. However, important design parameters depend on how well the models used to determine the corresponding kinetic parameters perform. The main reason for this study was to determine which nonlinear and linear models gave the best solutions to this very important aspect of reactor design.

The determination of growth kinetic parameter estimates can cause research problems when data from real laboratory experiments are used to determine those kinetic parameters. Due to random variability, sampling errors and microbial growth variations, reasonable kinetic parameter values were not always estimated accurately using either nonlinear or linear models. Mathematical modeling from Monte Carlo simulations

provides the ability to evaluate the current modeling methodologies used to determine the growth kinetic parameters.

All simulations were done in SAS software using differential equations to generate data sets with simulated substrate values from 200 to 1,000 mg/L and a simulated biomass of 0 to 500 mg/L. The time frame was generated from 0 up to 20 hours, though the program output time frame from 0 to 12 hours for biomass formation and substrate utilization.

Under these conditions, literature has shown that microorganisms grow rapidly (mainly bacteria and yeast cells) between 0 to 8 hours achieving exponential growth phase, and by 10 hours the microorganisms would have achieved stationary phase (Banat et. al. 1996). According to Saigal (1994), several yeast cells were evaluated growing exponentially between 0 to 9 hours, and also according to Hack et al. (1998), the yeast cells grew exponentially from 0 to 7 hours. Thus, the time frame from 0 to 12 hours appears to be a reasonable time period to assume that the simulated microorganisms were growing exponentially. The best nonlinear models results, which used the 'whole' substrate concentrations without failures, were the Robinson equations with fixed initial conditions and with either the starting value given or not-given. The next-best nonlinear models results, with one failure, were the Lee equations with fitted initial conditions and with either the starting value given or not-given. The most contradictory were the Shuler & Kargi equations with fixed initial conditions and with either the starting value given or not-given. Even with thirteen failures, it had the smallest percentage difference for either kinetic parameter means (0.215% for K_s and 0.056% for μ_{\max}), the best estimations of K_s and μ_{\max} . However, this was interesting because the Shuler & Kargi equation gives an implicit solution for biomass concentration, and in real laboratory experiments, the

biomass concentrations are the hardest measurement to determine with accuracy and precision, as was noted with *Pythium Irregulare* (Zhu 2002).

The ‘fixed’ condition, where the initial substrate and biomass concentrations were set to known values, had the fewest failures and the best estimates, presumably because the models were not required to estimate the initial conditions for substrate. The ‘fixed’ condition differed from the ‘fitted’ condition in that it gave better parameter estimations for all the models. In most cases it made little difference whether the initial kinetic parameters were provided to initialize the simulation or not. The simulation was generally accurate with either choice. However, the Shuler & Kargi and Robinson equations gave good estimates for K_s and μ_{\max} only with fixed initial conditions. Overall, the Lee equation gave the best estimates of K_s and μ_{\max} with the most reliable results with any of the four combinations.

The ‘best estimations’ for the linear models, as judged by the percent differences, were obtained by the Hanes equation at the ‘exponential 2’ time frame (from 5 to 8 hours), with selected substrate (from 200 to 1,000 by 200 mg/L) and with the whole substrate concentrations (from 200 to 1,000 by 50 mg/L). The Lineweaver-Burk equation had the best estimations at ‘exponential 2’ time frame, with selected substrate concentrations, and at the ‘exponential 1’ time frame (from 0 to 4 hours) with the whole substrate concentrations (from 200 to 1,000 by 50 mg/L). Among the linear models Hanes equation produced the best kinetic parameter estimations with the least percentage difference for both kinetic parameters (0.352% for K_s and 0.05% for μ_{\max}). The Hanes equation was expected to yield a better estimate than the Lineweaver-Burk equation because the Lineweaver-Burk equation uses the smallest substrate concentration to

determine the slope $\left(\frac{K_s}{\mu_{\max}}\right)$ and the largest substrate concentration to determine the

intercept $\left(\frac{1}{\mu_{\max}}\right)$. This affects the slope determination greatly due to the fact that it is

hardest to measure biomass concentrations at the smaller substrate concentration.

According to Robinson (1985), the Lineweaver-Burk expression should simply be abandoned and the Hanes equation should be adopted.

The linear models are based on the nonlinear models; therefore the linearized forms should be relied on for instructive purposes and to provide initial parameter estimates for the nonlinear models. The linear versions are not as statistically reliable as their nonlinear forms.

4.5 Future Recommendations

- (1) Larger standard errors for K_s and μ_{\max} should be investigated with greater percentages of the coefficients, such as 20% or even 25%.
- (2) The standard errors for biomass and substrate should be investigated with different percentage coefficients, such as 2%, 3% or even 5%.
- (3) The microorganism decay constant could be incorporated to the nonlinear models and investigated.
- (4) Investigation is needed of different substrate ranges, higher than those examined here.
- (5) Investigation is needed of alternate exclusion terms and ranges for the errors calculated from those used for the nonlinear models.

(6) Investigation is needed of the replicates that failed to converge or that were excluded as failures for other reasons. This study examined only the failure rate and not the reasons for failure.

In conclusion, the Monte Carlo technique shows much promise for evaluation of the important linear and nonlinear tools used by engineers. Further studies and analyses relating to fitting nonlinear and linearized models to determine the growth kinetic parameters should be conducted.

4.6 References

1. Banat, Singh I. M., Marchant D., R. 1996. The use of a thermotolerant fermentative *Kluyveromyces marxianus* IMB3 yeast strain for ethanol production. *Acta Biotechnology* 16: 215-223.
2. Despa S. 1999. Small sample comparison of tests for homogeneity of variances by Monte Carlo simulation using SAS. Special problem series no. SP-99-214, Applied and Experimental Statistics Department, Louisiana State University, 1-18.
3. Franz W., Goggelmann K., Schellhorn M., Winker P. 2000. Quasi-Monte Carlo methods in stochastic simulations: An application to policy simulations using a disequilibrium model of the West German economy 1960-1994. *Empirical Economics* 25: 247-259.
4. Hack C. J., Marchant R. 1998. Characterisation of a novel thermotolerant yeast, *Kluyveromyces marxianus* var *marxianus*: development of an ethanol fermentation process. *Journal of Industrial Microbiology and Biotechnology* 20: 323-327.
5. Hui Z. 2002. Utilization of rice bran by *Pythium Irregulare* for lipid production. MS thesis, Biological Engineering Department, Louisiana State University 1-70.
6. Mizuseki H., Jin Y., Kawazoe Y., Wille L.T. 2001. Cluster growth processes by direct simulation monte carlo method. *Applied Physics A* 73, 731-735.
7. Prokopakis G. J., Liu L.C. 1997. Monte Carlo simulation of the enzymatic lysis of yeast. *Biotechnology and Bioengineering* 53: 290-295.

8. Robinson J.A. 1985. Determining microbial kinetic parameters using nonlinear regression analysis. *Advances in Microbial Ecology*, edited by K. C. Marshall 8: 61-114. Plenum Press, New York.
9. Saigal D. 1994. Isolation and selection of thermotolerant yeasts for ethanol production. *Indian Journal of Microbiology* 34: 193-203.
10. SAS Institute. 2002. SAS/STAT Guide for Personal Computers Version 9.0, SAS Institute, Inc., Cary, North Carolina.
11. Shuler L. M., Kargi F. 1992. *Bioprocess Engineering: Basic Concepts*. Prentice Hall PTR.
12. Sobol, Llya M. 1994. *A primer for the Monte Carlo Methods*, CRC press LLC.
13. Zhu H. 2002. Utilization of rice bran by *Pythium Irregulare* for lipid production. MS thesis, Biological Engineering Department, Louisiana State University 1-70.
14. <http://www.cscs.umich.edu/~crshalizi/notebooks/monte-carlo.html>, 2/31/2003
15. <http://www.csepl.phy.ornl.gov/mc/node1.html>, 12/31/2003
16. http://www.puc-rio.br/marco.ind/sim_stoc_proc.html, 12/31/2003

CHAPTER 5

SUMMARY AND CONCLUSIONS

Since 1972, with the increase of the cost of oil and the possibility of shortages in oil supplies, extensive evaluations of alternative technologies have been pursued for production of liquid fuels such as bio-ethanol. The main objectives of this research were to determine the growth kinetic parameters (K_s and μ_{\max}) of a thermotolerant yeast strain called *Kluyveromyces marxianus* under aerobic and anaerobic conditions, using different concentrations of glucose medium (Anderson et al. 1986), and at optimum temperature of 45°C; to quantify the ethanol production under anaerobic condition from a batch process; and to fit and evaluate the nonlinear and linear models used in the biological growth kinetic parameter determination analysis using Monte Carlo simulation method.

A maximum ethanol production of 70 mg/L from 5,000 mg/L glucose fermenter was achieved with a maximum specific growth rate of 0.0051 (hr^{-1}). Even though *Kluyveromyces marxianus* did not show much growth throughout the fermentation trails ethanol was formed and recovered. There are many articles that have researched ethanol production from this thermotolerant yeast strain, which have shown high ethanol production at high temperature (45°C) and high substrate concentrations (150 g/L). Further studies are recommended using this yeast strain in other processes besides batch process, such as in continuous saccharification and fermentation processes.

The nonlinear and linear equations used to calculate the growth kinetic parameters were unable to give realistic results from the experimental data set due to unreliability and inconsistency often associated with biological data. Therefore, the model equations

were investigated for convergence properties from a realistic data set using the Monte Carlo simulation method. The Monte Carlo simulation method was used to generate a realistic data set and simulate the data set using four combinations for three nonlinear models, and using eleven combinations for two linear models. The nonlinear models had the better estimation values for K_s and μ_{\max} than did the linear models. The nonlinear models required initial estimates of the parameters and was an iterative or recursive technique in which the initial parameter estimates were sequentially improved until the “best” estimates (for example, those that minimize differences between the observed and predicted values of the dependent variable) were calculated (Robinson 1985). But the linear models have several limitations because they transform data sets and fit them into a linearized version of a nonlinear model; therefore, linear models tend to transform the magnitudes or types of measurement errors associated with the data sets, and the assumption of normally distributed measurement errors may be violated when the data sets are transformed and fitted to a linearized model of a nonlinear model (Robinson 1985).

The most interesting discoveries were that our time frame was generated from 0 and stopped around 12 hours to form biomass while substrate was being used; that the Shuler & Kargi equation with fixed initial conditions and with either given or not-given kinetic parameters estimated the best values for K_s and μ_{\max} with the lowest percentage difference, such as 0.00215% for K_s mean and 0.000567% for μ_{\max} mean. The “best” kinetic parameter estimations were expected from the Lee equation. Another interesting discovery was to see that the Robinson equation with fixed initial conditions and with either given or not-given kinetic parameters did not generate any failures, even though

this equation is a permutation of the Lee equation, with only the substrate changing. As the Robinson equation has an implicit solution for the substrate concentration, eliminating the effects of biomass measurement errors, it can have a smooth-fitting result without failures.

The main conclusion is that this research has opened the door for further studies and investigations by other researchers interested in fermentation and model evaluations. Many more investigations should be conducted with respect to the nonlinear models, such as to add the decay constant for the microorganism, to evaluate the error terms at smaller ranges for failure, and to investigate a larger replication size.

As a final recommendation, future studies should focus on the *Kluyveromyces marxianus* yeast strain with different substrate concentrations and different biological processes, such as in continuous two-stage fermentation processes. Also, ethanol production may be improved for this yeast strain by minimizing the ethanol inhibition present during its exponential growth phase.

REFERENCES

1. **Abdel-Fattah W.R., Fadil M., Nigam P., Banat I.M.** 2000. Isolation of thermotolerant ethanologenic yeasts and use of selected strains in industrial scale fermentation in an Egyptian distillery. *Biotechnology and Bioengineering* 68: 531-535.
2. **Ahluwalia A., Gupta J.K., Vadehra D.V., Sharma P.** 1988. Production of beta-glucosidase by *Cladosporium resinae*. *Mircen Journal* 5: 205-215.
3. **Aiba S., Shoda M., Nagatani M.** 1968. Kinetics of product inhibition in alcohol fermentation. *Biotechnology and bioengineering* 10: 845-864.
4. **Amoa-Awua W.K., Frisvad J.C., Sefa-Dedeh S., Jakobsen M.** 1997. The contribution of moulds and yeasts to the fermentation of 'agbelima' cassava dough. *Journal of Applied Microbiology* 83: 288-296.
5. **Anderson P. J., K. McNeil, K. Watson.** 1986. High – Efficiency Carbohydrate Fermentation to Ethanol at Temperatures above 40C by *Kluyveromyces marxianus* var. *marxianus* Isolated from Sugar Mills. *Applied and Environment Microbiology* 51: 1314-1320.
6. **APHA.** 1995. Standard Methods for the Examination of Water and Wastewater, 19th Ed. American Public Health Association, Washington, D.C.
7. **Awafo V.A., Chahal D.S., Simpson B.K.** 1998. Optimization of ethanol production by *Saccharomyces cerevisiae* (ATCC 60868) and *Pichia stipitis* Y-7124: a response surface model for simultaneous hydrolysis and fermentation of wheat straw. *Journal of food biochemistry* 22: 489-509.
8. **Ballesteros I., Ballesteros M., Cabanas A., Carrasco J., Martin C., Negro M.J., Saez F., Saez R.** 1991. Selection of thermotolerant yeasts for simultaneous saccharification and fermentation (SSF) of cellulose to ethanol. *App. Biochemistry and Biotechnology* 28/29: 307-315.
9. **Banat, Singh I. M., Marchant D., R.** 1996. The use of a thermotolerant fermentative *Kluyveromyces marxianus* IMB3 yeast strain for ethanol production. *Acta Biotechnology* 16: 215-223.
10. **Banat, Singh I. M., Marchant D., R.** 1995. Characterization and potential industrial applications of five novel, thermotolerant fermentative yeast strains. *World Journal of Microbiology and Biotechnology* 11: 304-306.
11. **Banat I.M., Nigam P., Marchant R.** 1992. Isolation of thermotolerant, fermentative yeasts growing at 52C and producing ethanol at 45C and 50C. *World Journal of Microbiology and Biotechnology* 8: 259-263.

12. **Barron N., Marchant R., McHale L., McHale A.P.** 1995. Studies on the use of a thermotolerant strain of *Kluyveromyces marxianus* in simultaneous saccharification and ethanol formation from cellulose. *Appl. Microbiol Biotechnol* 43: 518-520.
13. **Cabeca-Silva C., Madeira-Lopes A.** 1984. Temperature relations of yield, growth and thermal death in the yeast *Hansenula polymorpha*. *Z. Allg.Mikrobiol.* 24: 129-132.
14. **Chang L.A., Hammett L.K., Pharr D.M.** 1983. Carbon dioxide effects on ethanol production, pyruvate decarboxylase, and alcohol dehydrogenase activities in anaerobic sweet potato roots. *Plant Physiology* 71: 59-62.
15. **Despa S.** 1999. Small sample comparison of tests for homogeneity of variances by Monte Carlo simulation using SAS. Special problem series no. SP-99-214, Applied and Experimental Statistics Department, Louisiana State University, 1-18.
16. **Diwany A.I.El., Selim M.H., Elshafei A.M., Nada Abd-Alla M.A.** 1991. Partial acid an enzymatic hydrolysis of cellulose prior to beta-glucosidase production by *Debaryomyces sp.* *Egypt J. Microbiology* 26: 27-35.
17. **Drapcho C.** 2000. Biological Engineering Reactor Design Class. BE-4341, Agricultural & Biological Engineering Department, Louisiana State University.
18. **Doran J.B., Cripe J., Sutton M., Foster B.** 2000. Fermentations of pectin-rich biomass with recombinant bacteria to produce fuel ethanol. *Applied biochemistry and biotechnology* 84-86: 141-152.
19. **Doran M.** Pauline. 1997. *Bioprocess Engineering Principles*. Academic Press, San Diego, CA.
20. **Franz W., Goggelmann K., Schellhorn M., Winker P.** 2000. Quasi-Monte Carlo methods is stochastic simulations: An application to policy simulations using a disequilibrium model of the West German economy 1960-1994. *Empirical Economics* 25: 247-259.
21. **Garg S.K., Neelakantan S.** 1982. Production of SCP and cellulase by *Aspergillus terreus* from bagasse substrate. *Biotechnology and Bioengineering* 24: 2407-2417.
22. **Golias H., Dumsday G.J., Stanley G.A., Pamment N.B.** 2000. Characteristics of cellulase preparations affecting the simultaneous saccharification and fermentation of cellulose to ethanol. *Biotechnology Letters* 22: 617-621.

23. **Gokahale D.V., Patil S.G., Bastawde K.B.** 1998. Potential application of yeast cellulase-free xylanase in agrowaste material treatment to remove hemicellulose fractions. *Bioresource Technology* 63: 187-191.
24. **Hack C. J., Marchant R.** 1998. Characterisation of a novel thermotolerant yeast, *Kluyveromyces marxianus* var *marxianus*: development of an ethanol fermentation process. *Journal of Industrial Microbiology and Biotechnology* 20: 323-327.
25. **Hacking A.J., Taylor I.W.F., Hanas C.M.** 1984. Selection of yeast able to produce ethanol from glucose at 40C. *Appl. Microbiol. and Biotechnology* 19: 361-363.
26. **Hoda, El-Masry G., Alian, Hagwa A.M., El-Shimi M., Fadel M.A.** 1990. Enzymatic hydrolysis of some cellulosic wastes for fodder yeast production 1. Transformation of wastes to fermentable sugars. *Annals Agric. Sci.* 35: 143-155.
27. **Hughes D.B., Tudroszen N.J., Moye C.J.** 1984. The effect of temperature on the kinetics of ethanol production by a thermotolerant strain of *Kluyveromyces marxianus*. *Biotechnology letters* 6: 1-6.
28. **Hurst W. J., Martin Jr R. A., Zoumas B. L.** 1979. Application of HPLC to characterization of individual carbohydrates in foods. *Journal of Food Science* 44: 892 – 895.
29. **Jimenez M., Gonzalez A.E., Martinez M.J., Martinez A.T.** 1991. Screening of yeasts isolated from decayed wood for lignocellulose-degrading enzyme activities. *Mycol. Res.* 95: 1299-1302.
30. **Jones A., Hamilton M.G., Dukes P.D.** 1983. Sweet potato cultivars for ethanol production. 3rd Annual solar and biomass workshop, April: 26-28.
31. **Jones R.P., Pamment N., Greenfield P.F.** 1981. Alcohol fermentation by yeasts – the effect of environmental and other variables. *Process biochemistry* 16: 42-49.
32. **Kadam K.L., Shmidt S.L.** 1997. Evaluation of *Candida acidothermophilum* in ethanol production from lignocellulosic biomass. *Appl Microbiol Biotechnol* 48: 709-713.
33. **Kadam K.L., Schmidt S.L.** 1997. Evaluation of *Candida acidothermophilum* in ethanol production from lignocellulosic biomass. *Appl. Microbiol. and Biotechnology* 48: 709-713.
34. **Kida K., Kume K., Morimura S., Sonoda Y.** 1992. Repeated-batch fermentation process using a thermotolerant flocculating yeast constructed by protoplast fusion. *Journal of fermentation and bioengineering* 74: 169-173.

35. **Kim K., Hamdy M.K.** 1985. Acid hydrolysis of sweet potato for ethanol production. *Biotechnology and Bioengineering* 27: 316-320.
36. **Lee Ki-Young, Lee Sung-Taik.** 1996. Continuous process for yeast biomass production from sugar beet stillage by a novel strain of *Candida rugosa* and protein profile of the yeast. *J. Chem. Tech. Biotechnol.* 66: 349-354.
37. **Liu, S.** (2003) Personal communication, June.
38. **Liu S.** 2002. Fecal Coliform decay and regrowth kinetics in an anaerobic dairy wastewater environment. MS thesis. Biological Engineering Department, Louisiana State University, LA 1-76.
39. **Mandels M, Andreotti R, Roche C.** 1976. Measurement of saccharifying cellulase. *Biotechnology and Bioengineering Symposium.* 6: 21-23.
40. **Madsen, L.** (2003) Personal communication, February.
41. **Mizuseki H., Jin Y., Kawazoe Y., Wille L.T.** 2001. Cluster growth processes by direct simulation monte carlo method. *Appl. Phys. A* 73, 731-735.
42. **Mohagheghi A., Tucker M., Grohmann K., Wyman C.** 1991. High solids simultaneous saccharification and fermentation of pretreated wheat straw to ethanol. *App. Biochem. and Biotechnol.* 33: 67-81.
43. **Morimura S., Ling Z.Ya., Kida K.** 1997. Ethanol production by repeated-batch fermentation at high temperature in a molasses medium containing a high concentration of total sugar by a thermotolerant flocculating yeast with improved salt-tolerance. *Journal of fermentation and bioengineering* 83: 271-274.
44. **Nagodawithana T.W., Castellano C., Steinkraus K.H.** 1974. Effect of dissolved oxygen, temperature, initial cell count, and sugar concentration on the viability of *Saccharomyces cerevisiae* in rapid fermentations. *Applied Microbiology* 28: 383-391.
45. **O'Connor-Cox E.S.C., Paik J., Ingledew W.M.** 1991. Improved ethanol yields through supplementation with excess assimilable nitrogen. *Journal of Industrial Microbiology* 8: 45-52.
46. **Odumeru J.A., D'Amore T., Russell I., Stewart G.G.** 1992. Changes in protein composition of *Saccharomyces* brewing strains in response to heat shock and ethanol stress. *Journal of Industrial Microbiology* 9: 229-234.
47. **Paranjpe M.S., Chen P.K.** 1979. Morphogenesis of *Agaricus bisporus*: changes in proteins and enzyme activity. *Mycologia* 71: 233-467.

48. **Parekh S.R., Parekh R.S., Wayman M.** 1983. Fermentation of xylose and cellobiose by *Pichia stipitis* and *Brettanomyces clausenii*. Applied Biochemistry and Biotechnology 18: 321-329.
49. **Peres M.F.S., Lalue C.** 1998. Ethanol tolerance of thermotolerant yeasts cultivated on mixtures of sucrose and ethanol. Journal of fermentation and bioengineering 85: 388-397.
50. **Prokopakis G. J., Liu L.C.** 1997. Monte Carlo simulation of the enzymatic lysis of yeast. Biotechnology and Bioengineering 53: 290-295.
51. **Rauramaa A., Setälä J., Moisio T., Sivela S.** 1987. The effect of inoculants and cellulase on the fermentation and microbiological composition of grass silage. II microbiological changes in the silages. Journal of Agr Sci in Finland 59: 371-377.
52. **Reece N. N.** 2003. Optimizing aconitate removal during clarification. MS thesis. Biological Engineering Department, Louisiana State University, LA 1-113.
53. **Riordan C., Love G., Barron N., Nigam P., Marchant R., McHale L., McHale A.P.** 1996. Production of ethanol from sucrose at 45C by alginate-immobilized preparations of the thermotolerant yeast strain *Kluyveromyces marxianus* IMB3. Bioresource technology 55: 171-173.
54. **Robinson J.A.** 1985. Determining microbial kinetic parameters using nonlinear regression analysis. Advances in Microbial Ecology, edited by K. C. Marshall 8: 61-114. Plenum Press, New York.
55. **Roychoudhury P.K., Ghose T.K., Ghosh P.** 1992. Operational strategies in vacuum-coupled SSF for conversion of lignocellulose to ethanol. Enzyme Microb Technol 14: 518-585.
56. **Saigal D.** 1994. Isolation and selection of thermotolerant yeasts for ethanol production. Indian Journal of Microbiology 34: 193-203.
57. **SAS Institute.** 2002. SAS/STAT Guide for Personal Computers Version 9.0, SAS Institute, Inc., Cary, North Carolina.
58. **Saxena A., Garg S.K., Verma J.** 1992. Simultaneous saccharification and fermentation of waste newspaper to ethanol. Bioresource Technology 42: 13-15.
59. **Selmer-Olsen I., Henderson A.R., Robertson S., McGinn R.** 1993. Cell wall degrading enzymes for silage. 2. Aerobic stability of enzyme-treated laboratory silages. Grass Forage Science 48: 55-63.

60. **Seki T., Myoga S., Limtong S., Uedono S.** 1983. Genetic construction of yeast strains for high ethanol production. *Biotechnology letters* 5: 351-356.
61. **Shuler L. M., Kargi F.** 1992. *Bioprocess Engineering: Basic Concepts*. Prentice Hall PTR.
62. **Sobol, Llya M.** 1994. *A primer for the Monte Carlo Methods*, CRC press LLC.
63. **Spindler D.D., Wyman C.E., Grohmann K., Mohagheghi A.** 1989. Simultaneous saccharification and fermentation of pretread wheat straw to ethanol with selected yeast strains and beta-glucosidase supplementation. *Applied Biochemistry and Biotechnology* 20-21: 529-540.
64. **Strauss M.L.A., Jolly N.P., Lambrechts M.G., van Rensburg P.** 2001. Screening for the production of extracellular hydrolytic enzymes by non-*Saccharomyces* wine yeasts. *Journal of Applied Microbiology* 91: 182-190.
65. **Spoelstra S.F., van Wikselaar P.G.** 1992. The effects of ensiling whole crop maize with a multi-enzyme preparation on the chemical composition of the resulting silages. *Journal of Sci Food Agric.* 60: 223-228.
66. **Szczodrak J., Targonski Z.** 1987. Selection of thermotolerant yeast strains for simultaneous saccharification and fermentation of cellulose. *Biotechnology and Bioengineering* 31: 300-303.
67. **Tan T.K., Leong W.F.** 1986. Screening for extracellular enzymes of fungi from manufacturing wastes. *Mircen Journal* 2: 445-452.
68. **Watson K.** 1982. Unsaturated fatty acid but not ergosterol is essential for high ethanol production in *Saccharomyces*. *Biotechnology letters* 4: 397-402.
69. **Watson K., Cavicchioli R.** 1983. Acquisition of ethanol tolerance in yeast cells by heat shock. *Biotechnology letters* 5: 683-688.
70. **White, B.** (2003) Personal communication, February.
71. **Yu B., Zhang F., Zheng Y., Wang P.** 1996. Alcohol fermentation from the mash of dried sweet potato with its dregs using immobilized yeast. *Process biochemistry* 31: 1-6.
72. **Zhu H.** (2004) Personal communication, January.
73. **Zhu H.** 2002. Utilization of rice bran by *Pythium Irregulare* for lipid production. MS thesis, Biological Engineering Department, Louisiana State University 1-70.
74. <http://www.cscs.umich.edu/~crshalizi/notebooks/monte-carlo.html>, 2/31/2003

75. <http://www.csep1.phy.ornl.gov/mc/node1.html>, 12/31/2003
76. http://www.puc-rio.br/marco.ind/sim_stoc_proc.html, 12/31/2003

APPENDIX A

SWEET POTATO WASTE PRELIMINARY EXPERIMENT

The determination of biomass and substrate concentrations using Sweet Potato Waste media for the *Kluyveromyces marxianus* yeast strain under anaerobic condition using the three Two-Liter Bioflo[®] 2000 Fermentors (New Brunswick Scientific).

A.1 Introduction

Fermentation is the oxidation/reduction of organic compounds that takes place in the absence of external electron acceptors. In fermentation, internally balanced oxidation reactions occur, in which the oxidation of the original compound is coupled to the reduction of an organic compound produced in catabolism. We have used a high temperature tolerant yeast strain called *Kluyveromyces marxianus*.

The overall reaction for fermentation of organic compounds by yeast is as follows;



A.2 Procedure

- a. Moisture content was determined: $M_w = 100 * (M_w / M_t) = 20\%$ dry basis.
- b. 3 L glass beakers were used as reactors with hot plates and stir motors during 10 hours to allow the sweet potato hydrolyze.
- c. Sweet Potato was blended (500g/L dry basis) was heated up to 35-40°C for 3 hours and cellulase enzymes were added to speed up the hydrolysis process. Then, the sweet potato was heated up to 65-70°C during 4 hours and amylase enzymes were added to speed up the starch hydrolysis. The enzymes were added to convert the complex sugars (cellulose and starches) into simple sugars (glucose) in a short time period.

- d. The particulate substrates were filtered through a long process to achieve a soluble substrate (S.P.Media). The first filtration step was to separate the largest particles through straining the media and then using cottons fibers into a funnel to separate smaller particles. The second step was to pass the left media through a 0.2 um filtration apparatus. The process was long and time consuming because many different particles sizes were going through the same 0.2 um filter.
- e. The Total reducing sugars of sweet potato media starting with is 18 g/L.
- f. Three Two-Liter Bioflo® 2000 Fermentors were autoclaved making a sterile environment for the media and yeast.
- g. Three Two-Liter Bioflo® 2000 Fermentors were filled with the non-sterile Sweet Potato Media.
- h. The reactors will be set as follows: Reactor #1 at 40°C, Reactor #2 at 45°C, and Reactor #3 at 50°C.
- i. Yeast has been prepared using aseptic technique, and the pre-culture yeast has been growing in four 250 mL flasks with 100 mL glucose media (Marchant et al.).
- j. Each four (250mL) flasks were placed in the “Orbital Shaker Bed” at 35C, 120rpm for 24 hours.

A.3 Materials and Methods

The entire procedure used to make the sweet potato media is found in Chapter 3 at the ‘Materials and Methods’ part. The following analytical techniques were conducted such as TSS, OD, soluble and total COD, and TRS.

A.4 Results

Total Reducing Sugars were carried out for all the 3 reactors using the “Available Carbohydrates Procedure”. The principal of the available carbohydrates procedure is to monitor how much reducing sugar was liberated, after the carbohydrates in foods were hydrolyzed by sulfuric acid, to react with DNS (3,5-dinitrosalicylic acid) reagent to form a red-brown reaction product, which was monitored by reading the optical density at 540 nm in the Spectrophotometer (Carpenter 1995).

Total reducing sugars standard curve made for sweet potato laboratory.

Table A.1: Total reducing sugar standard dilutions data

Sample ID (g/L)	Mean Absorbance (540 nm)
0	0
1	0.2275
2	0.5185
3	0.8135
4	1.0175

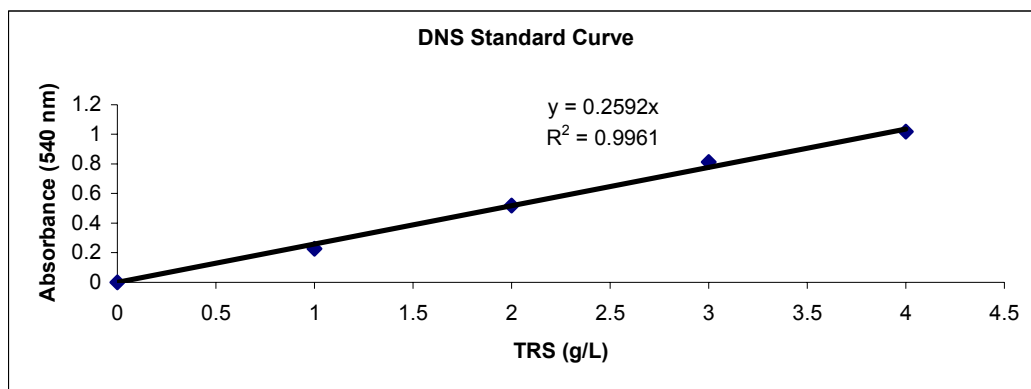


Figure A.1: Total reducing sugars standard curve

The Standard curve was created by diluting the glucose stock solution to: 0, 1.0, 2.0, 3.0, and 4.0 g/L (Table 1). The regression equation of the standard TRS was, $y =$

0.2592x with $R^2 = 0.9961$ (Figure 1). The slope of the standard curve is used to divide the yeast mean absorbance readings to find how much sugar was available in the yeast concentration media.

The TSS and OD calibration curve for yeast concentrations from laboratory #2 was used to calculate the predicted TSS for this laboratory. The following table is the data collected for the calibration curve.

Table A.2 The TSS and OD readings for yeast #1 culture at 0%, 20%, 50%, 60%, 80% and 100% concentrations.

Sample ID	Tin#	1 st Weighing dried sample + filter (g)	2nd Weighing dried sample + filter (g)	Clean Filter (g)	Volume Filtered (L)	Blank Weight gain/loss (g)	TSS (mg/L)	OD reading
Blank #1	1	1.0738	1.0741	1.0738	0.025	0.00015	0	0
Blank #2	2	1.0996	1.0998	1.0994	0.025	0.0003	0	0
20%yeast	3	1.0919	1.0921	1.0875	0.025	-	171	0.2653
40%yeast	4	1.1002	1.1004	1.0916	0.025	-	339	0.5055
60%yeast	5	1.1002	1.1127	1.1014	0.025	-	393	0.695
80%yeast	8	1.1174	1.1175	1.1038	0.025	-	537	0.8375
100%yeast	7	1.1122	1.1128	1.09	0.025	-	891	0.975

The optical density (OD) readings for the yeast increased as the concentration of the culture solution increased because higher concentration meant higher density, which also meant that it had more biomass. When there is more biomass, the solution absorbs more light, thus giving an increased value for absorption as the concentration increases (Table A.2).

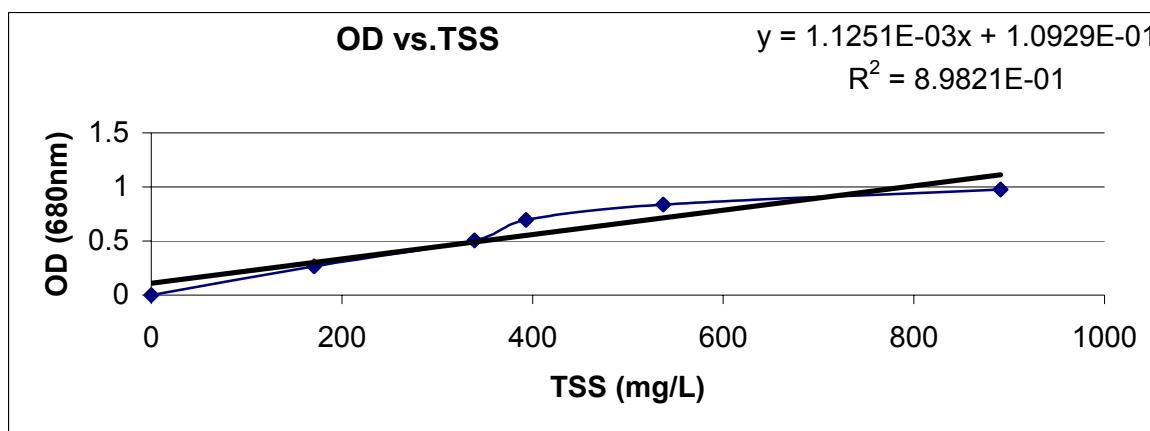


Figure A.2 Calibration curve (TSS vs. OD) for yeast.

Generally, the concentration of TSS increased as the concentration of yeast culture increased from 0% to 20%, 50%, 60%, and 100% (Table 2).

The optical density (OD) readings also increased as the concentrations of the yeast culture increased (Figure 2).

The regression equation for the calibration curve (TSS vs. OD) of the yeast was, $y = 1.1251 \times 10^{-3}x + 1.0929 \times 10^{-1}$ with $R^2 = 8.9821 \times 10^{-1}$, which equation was used to readjust the TSS values obtained from the sweet potato media.

The TSS concentration values can be obtained based on an OD reading for a similar culture. The OD values will be substituted as y in the regression equation and the equation will be solved for x , which represents the TSS concentration (Figure 2).

Data Analysis for Reactor at 50°C

The fermentation was carried out at 50°C for a period of approximately 24 hours. The following table shows the observed data which was collected during laboratory

experiment, and the predicted data which was the calculated using the calibration curve equation (figure 2).

Table A.3 Fermentation data at Temperature of 50C during 24 hours of experiment.

Time (hours)	Absorbance, OD (680 nm)	Predicted Biomass Produced, TSS (mg/L)	Substrate concentration, Glucose (g/L)	Observed Biomass Produced, TSS (mg/L)	Observed biomass yield (Yb, mg/L/mg/L)	Predicted biomass yield (Yb mg/L/mg/L)
0	0.66	489.4765	16.97673	0		
1.166667	0.802	615.6875	15.25764	2130		-0.07342
2.75	1.025	813.8921	8.89064	1840	0.045547	-0.03113
4.166667	1.19	960.5457	5.363322	1935	-0.02693	-0.04158
5.716667	1.205	973.8779	3.006147	1840	0.040302	-0.00566
7.166667	1.275	1036.095	1.790862	1845	-0.00411	-0.0512
8.783333	1.275	1036.095	2.179249	2300	1.171512	0
10.16667	1.275	1036.095	2.121946	4288	-34.6928	0
11.66667	1.275	1036.095	1.826517	2005	7.72775	0
23.41667	1.275	1036.095	1.727192	2160	-1.56053	0

The observed data are the collected data from the experiment, therefore is the real data that each group collect using TSS, and TRS techniques. The predicted biomass produced was calculated using the calibration curve equation (figure 2). OD absorbance was read at 680 nm and TRS absorbance was read at 540 nm.

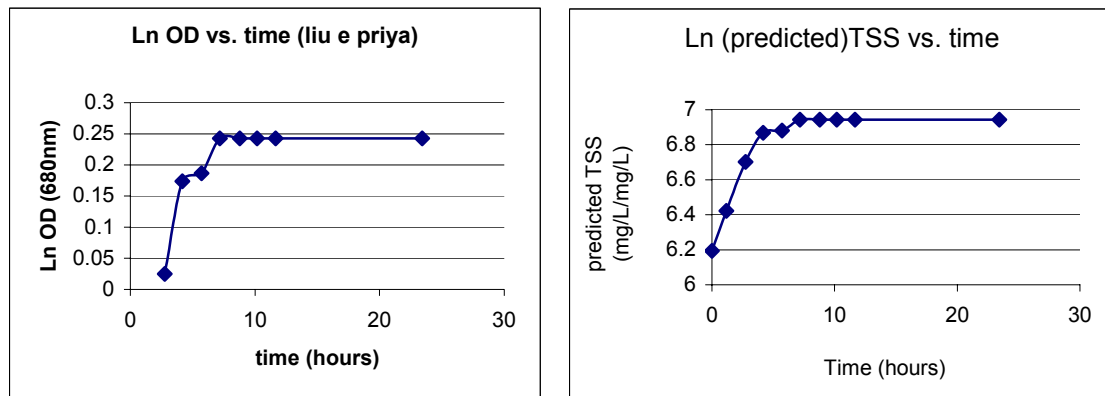


Figure A.4 The natural log of the biomass growth versus time.

The slope of the Ln OD versus time curve during exponential growth of the yeast is the specific growth rate, μ , for the microorganism at the substrate concentration present in the reactor.

$$\mu = \ln(OD_t) - \ln(OD_0) / t - t_0$$

$$\mu = 0.0389 \text{ hr}^{-1}$$

The predicted Ln TSS versus time plot was calculated with the calibration curve of the different yeast percentages from laboratory #2 (figure 2).

The biomass yield was calculated from the predicted TSS, which values used came from the data collected during the lab.

The following graph shows the growth curve of biomass while substrate is being utilized during 24 hours of experiment.

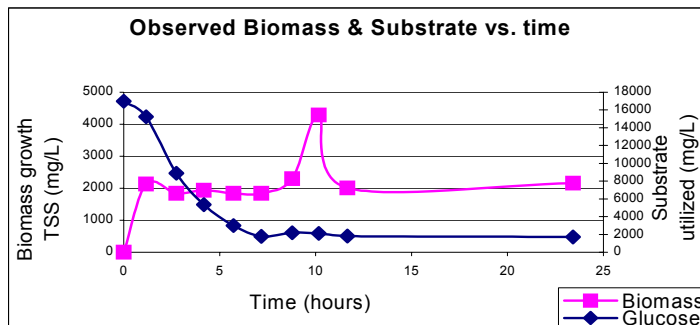


Figure A.5 The real TSS collected and TRS analysis over time

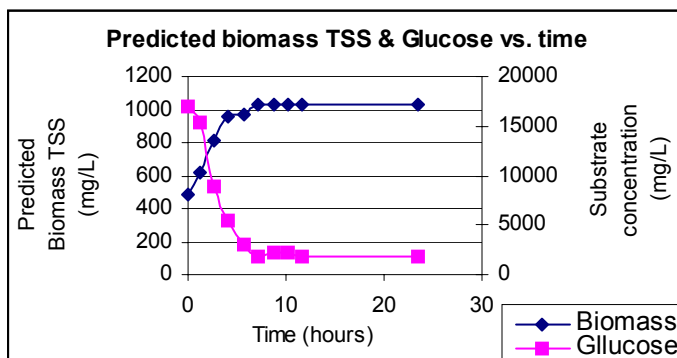


Figure A.6 Predicted TSS data and TRS data over time.

The following tables show the calculations for biomass rate of formation and substrate rate of utilization for the observed data. The rate of biomass formation is $R_{Xb} = (u \cdot X_b - b \cdot X_b)$ and the rate of substrate utilization is $R_{su} = ((u \cdot X_b)/Y_b)$.

Table A.4 The observed data used to find the rates during 8 hours.

Time (hours)	Growth rate, u (hr^{-1})	Decay constant, b (hr^{-1})	Observed biomass formed, TSS	Observed, biomass yield (Y_b , mg/L/mg/L)	Rate of biomass formation, mg/Lhr	Rate of Substrate utilization, mg/Lhr
0	0.0389	0.005	0		0	
1.166667	0.0389	0.005	2130		72.207	
2.75	0.0389	0.005	1840	0.045547	62.376	1571.463
4.166667	0.0389	0.005	1935	0.045547	65.5965	1652.599
5.716667	0.0389	0.005	1840	0.045547	62.376	1571.463
7.166667	0.0389	0.005	1845	0.045547	62.5455	1575.734
8.783333	0.0389	0.005	2300	0.045547	77.97	1964.329
10.16667	0.0389	0.005	4288	0.045547	145.3632	3662.193
11.66667	0.0389	0.005	2005	0.045547	67.9695	1712.383
23.41667	0.0389	0.005	2160	0.045547	73.224	1844.761

Table A.5 The predicted data used to find the rates during 8 hours.

Growth rate, u (hr^{-1})	Decay constant, b (hr^{-1})	Predicted Biomass Produced, TSS (mg/L)	Predicted, biomass yield (Y_b mg/L/mg/L)	Rate of biomass formation, mg/Lhr	Rate of Substrate utilization, mg/Lhr
0.0389	0.005	489.4765		16.59325	
0.0389	0.005	615.6875	0.045547	20.87181	
0.0389	0.005	813.8921	0.045547	27.59094	695.1096
0.0389	0.005	960.5457	0.045547	32.5625	820.36
0.0389	0.005	973.8779	0.045547	33.01446	831.7464
0.0389	0.005	1036.095	0.045547	35.12361	884.883
0.0389	0.005	1036.095	0	35.12361	
0.0389	0.005	1036.095	0	35.12361	
0.0389	0.005	1036.095	0	35.12361	
0.0389	0.005	1036.095	0	35.12361	

The following graph was plotted to compare the rates of formation and utilization for the data collected in the lab and the predicted data calculated.

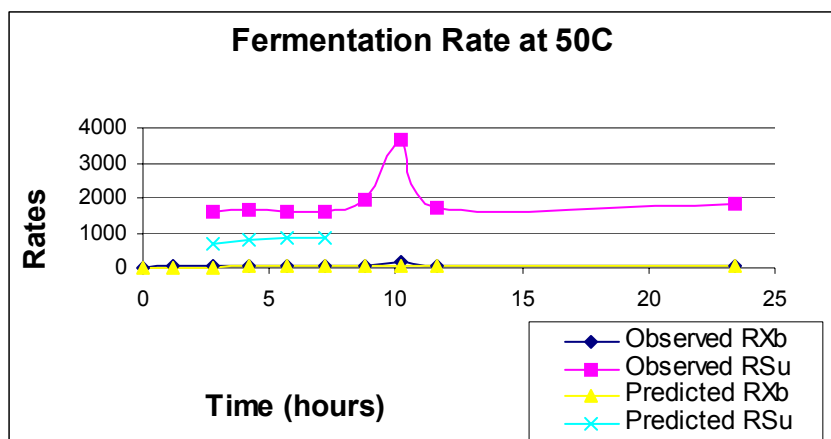


Figure A.7 The rates of formation and utilization at temperature 50C.

Data Analysis for Reactor at 45°C

This fermentation was conducted at 45C. The following table shows the observed data collected during the laboratory experiment, which was the real data. The predicted data was calculated using the calibration regression equation $y = 1.1251e^{-3x} + 1.0929e^{-1}$, where y = OD observed data and x = TSS predicted data.

Table A.5 Fermentation data at temperature of 45C during six hours.

Time (hours)	Observed Biomass Average Produced TSS (mg/L)	Substrate Concentration utilized TRS (mg/L)	Absorbance, produced OD (680 nm)	Predicted Biomass produced TSS (mg/L)	Predicted Biomass yield, Yb (mg/L/mg/L)	Observed Biomass yield, Yb (mg/L/mg/L)
0		0	0	0		
1.2	1680	2788	0.875	460.5263		
2	1380	2183	0.88	463.1579	-0.00435	0.495868
3	1800	2008	0.962	506.3158	-0.24662	-2.4
4	1510	1873	0.935	492.1053	0.105263	2.148148
5	1750	1120	0.937	493.1579	-0.0014	-0.31873
6	1560	503	0.935	492.1053	0.001706	0.307942

The predicted biomass produced was calculated using the calibration equation curve for the yeast (figure 2). The OD absorbance read at 680 nm was used as the x variable in the calibration equation.

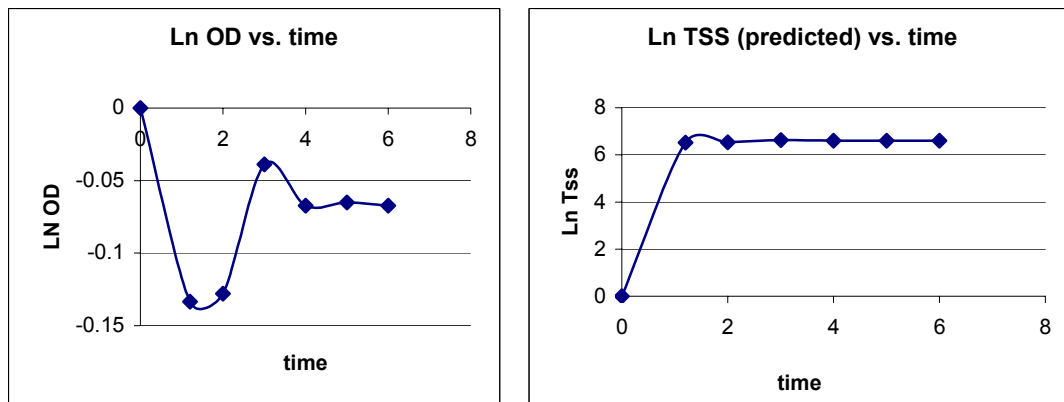


Figure A.8 Ln of biomass formed versus time for the data collected (LnOD) and for the calculated TSS values.

The slope of the Ln OD versus time curve during exponential growth of the yeast is the specific growth rate, μ for the microorganism at the substrate concentration present in the reactor.

$$\mu = \ln(\text{OD}_t) - \ln(\text{OD}_0) / t - t_0$$

$$\mu = 0.05261 \text{ hr}^{-1}$$

The predicted Ln TSS versus time plot was calculated with the calibration curve of the different yeast percentages from laboratory #2 (figure 2).

The biomass yield was calculated from the predicted TSS, which values used came from the collected data during the laboratory experiment.

The following graph shows the observed biomass formed and substrate utilized during 8 hours of experiment.

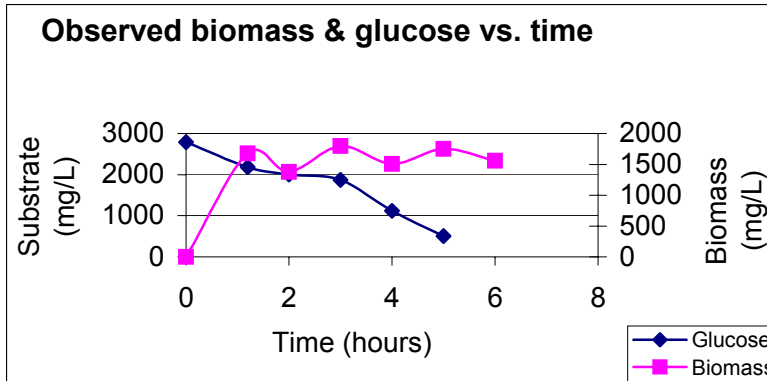


Figure A.9 Biomass formed (TSS) and substrate analyzed (TRS) during 8 hours of data collecting.

The following graph is the predicted biomass formed and substrate utilized calculated from the calibration regression equation (Figure A.2).

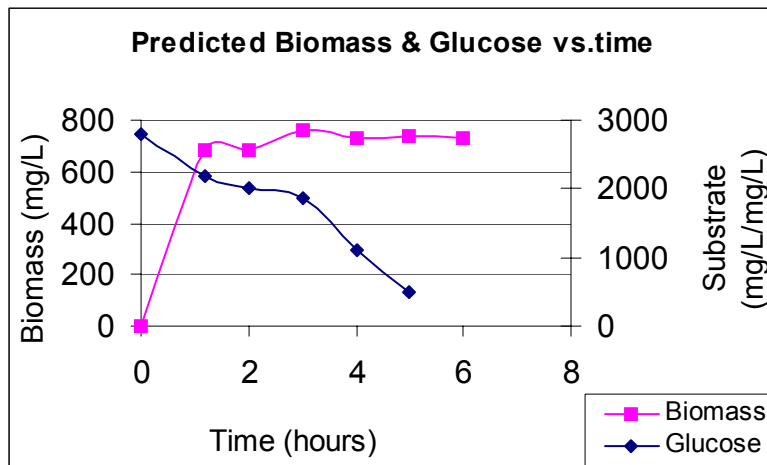


Figure 10: Calculated biomass formed and substrate used versus time.

The following tables show the calculations for biomass rate of formation and substrate rate of utilization for the observed data and predicted data. The rate of biomass formation is $R_{Xb} = (u \cdot X_b - b \cdot X_b)$ and the rate of substrate utilization is $R_{su} = ((u \cdot X_b)/Y_b)$.

Table A.6 Predicted rates during 6 hours of fermentation.

Time (hours)	Growth rate, μ (hr ⁻¹)	Decay constant, b (hr ⁻¹)	Predicted Biomass Produced, TSS (mg/L)	Predicted, biomass yield (Y _b , mg/L/mg/L)	Rate of biomass formation, mg/Lhr	Rate of Substrate utilization, mg/Lhr
0	0.05261	0.005	0		0	
1.2	0.05261	0.005	460.5263		21.92566	
2	0.05261	0.005	463.1579	0.10526	22.05095	231.4909
3	0.05261	0.005	506.3158	0.10526	24.10569	253.0617
4	0.05261	0.005	492.1053	0.10526	23.42913	245.9591
5	0.05261	0.005	493.1579	0.10526	23.47925	246.4852
6	0.05261	0.005	492.1053	0.10526	23.42913	245.9591

Table A.7: Observed rates during 6 hours of fermentation.

Time (hours)	Growth rate, μ (hr ⁻¹)	Decay constant, b (hr ⁻¹)	Observed biomass formed, TSS	Observed, biomass yield (Y _b , mg/L/mg/L)	Rate of biomass formation, mg/Lhr	Rate of Substrate utilization, mg/Lhr
0	0.05261	0.005			0	
1.2	0.05261	0.005	1680		79.9848	
2	0.05261	0.005	1380	0.495868	65.7018	146.4136
3	0.05261	0.005	1800	0.495868	85.698	190.9743
4	0.05261	0.005	1510	0.495868	71.8911	160.2062
5	0.05261	0.005	1750	0.495868	83.3175	185.6695
6	0.05261	0.005	1560	0.495868	74.2716	165.5111

The following graph was plotted to compare the rates of formation and utilization for the data collected in the lab and the predicted data.

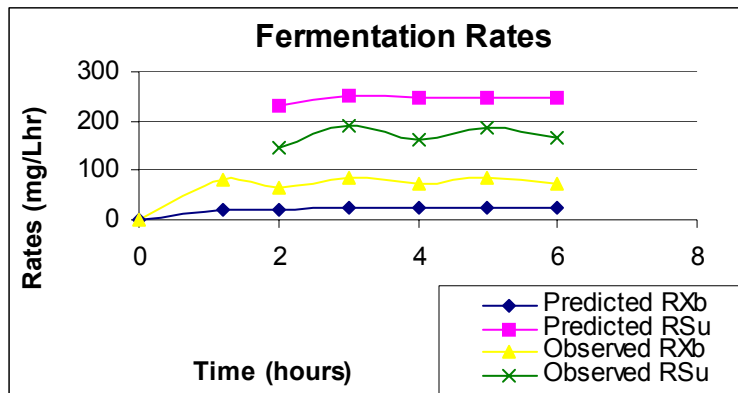


Figure A.11 The predicted and observed rates of biomass formation and substrate utilization.

Data Analysis for Reactor at 40°C

Fermentation at a temperature of 40C was carried during 24 hours. The following table shows the data collected during the laboratory experiment, which is the real data, and the predicted biomass formed and biomass yield, which were calculated using the calibration regression equation $y = 1.1251e^{-3x} + 1.0929e^{-1}$ (Figure A.2).

Table A.8 Experiment and calculated fermentation data for 40C.

Time (hrs)	Absorbance, OD (680 nm)	Substrate concentration, glucose TRS (mg/L)	Observed biomass produced, TSS (mg/L)	Observed biomass yield, Yb (mg/L/mg/L)	Predicted biomass produced, TSS mg/L	Predicted biomass yield, Yb (mg/L/mg/L)
0	0.658	8217.71			487.6989	
1.5	0.562	13450	887.5		402.3731	-0.01631
3	0.755	5912	765	0.016251	573.9134	-0.02276
5	1.05	2290.7	1385	-0.17121	836.1123	-0.0724
7	1.24	3233.1	885	-0.53056	1004.986	0.179196
24	1.365	3004.28	1945	-4.63246	1116.087	-0.48554

The predicted biomass produced was calculated using the calibration equation curve for the yeast on figure 2. The OD absorbance was read at 680 nm.

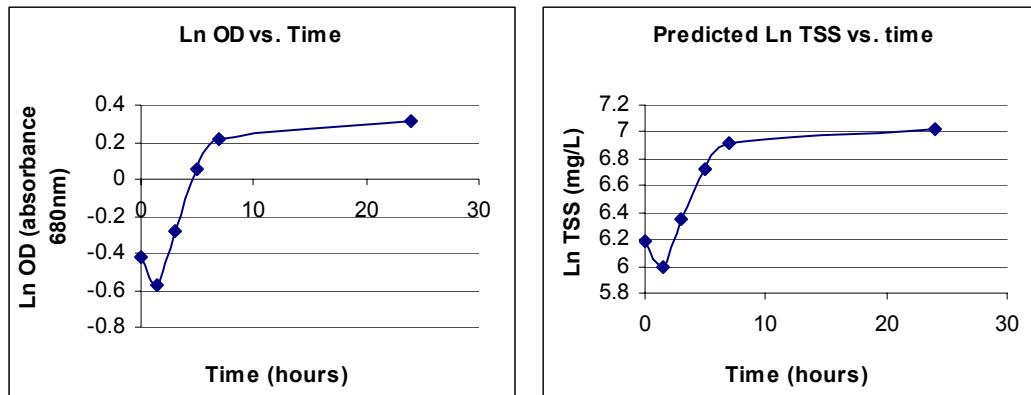


Figure 12: Biomass formed during a period of 24 hours.

The slope of the Ln OD versus time curve during exponential growth of the yeast is the specific growth rate, μ for the microorganism at the substrate concentration present in the reactor.

$$\mu = \ln(OD_t) - \ln(OD_0) / t - t_0$$

$$\mu = 0.18818 \text{ hr}^{-1}$$

The predicted Ln TSS versus time plot was calculated with the calibration curve of the different yeast percentages (figure 2).

The biomass yield was calculated from the predicted TSS, which values used came from the collected data during the lab.

The following graph shows the observed biomass growth and substrate utilized during 24 hours of experiment.

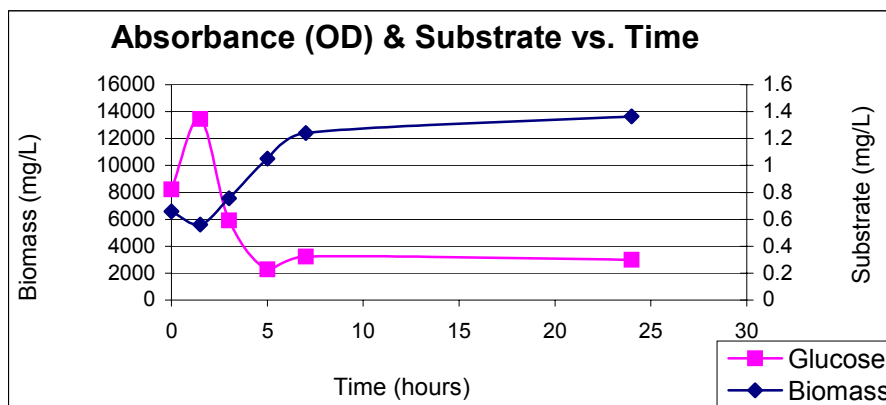


Figure A.13 Biomass growth and substrate utilization during 24 hours of data analysis.

The following graph shows the predicted biomass formed and substrate utilized during 24 hours.

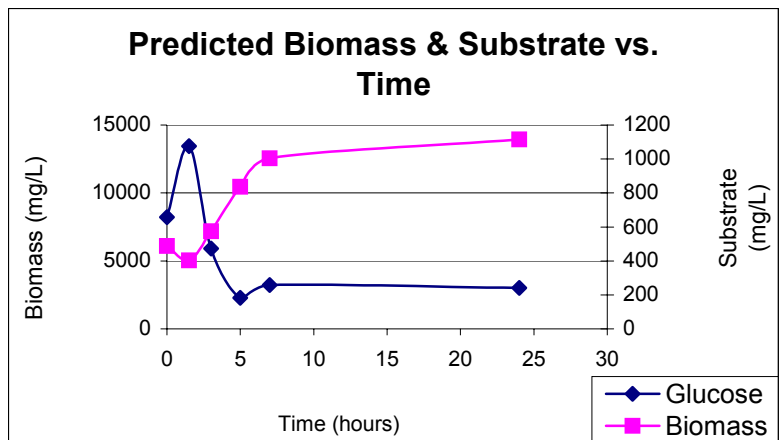


Figure A.14 Predicted biomass formed and substrate used for 24 hours.

The following tables show the calculations of biomass rate of formation and substrate rate of utilization for the observed and predicted data. The rate of biomass formation is $R_{Xb} = (u \cdot X_b - b \cdot X_b)$ and the rate of substrate utilization is $R_{su} = ((u \cdot X_b) / Y_b)$.

Table A.9 The rate of biomass formed and substrate utilized for the collected data during 7 hours.

Time(hrs)	Growth rate, u (hr^{-1})	Decay constant, b (hr^{-1})	Observed biomass formed, TSS	Observed, biomass yield (Y_b , mg/L/mg/L)	Rate of biomass formation, mg/Lhr	Rate of Substrate utilization, mg/Lhr
0	0.18818	0.005	887.5		162.5723	
1.5	0.18818	0.005	765	0.016251	140.1327	8858.393
3	0.18818	0.005	1385	0.016251	253.7043	16037.74
5	0.18818	0.005	885	0.016251	162.1143	10247.94
7	0.18818	0.005	1945	0.016251	356.2851	22522.32

Table A.10 The rate of biomass formed and substrate utilized for the calculated data during 24 hours.

Time(hrs)	Growth rate, u (hr^{-1})	Decay constant, b (hr^{-1})	Predicted biomass formed, TSS	Predicted biomass yield (Y_b , mg/L/mg/L)	Net rate of biomass formation, mg/Lhr	Rate of Substrate utilization, mg/Lhr
0	0.18818	0.005	487.6989		89.33668	
1.5	0.18818	0.005	402.3731	0.179196	73.70671	422.5472
3	0.18818	0.005	573.9134	0.179196	105.1295	602.6882
5	0.18818	0.005	836.1123	0.179196	153.1591	878.0331
7	0.18818	0.005	1004.986	0.179196	184.0934	1055.374
24	0.18818	0.005	1116.087	0.179196	204.4449	1172.046

The following graph was plotted to compare the rates of formation and utilization for the data collected in the lab and the predicted data calculated.

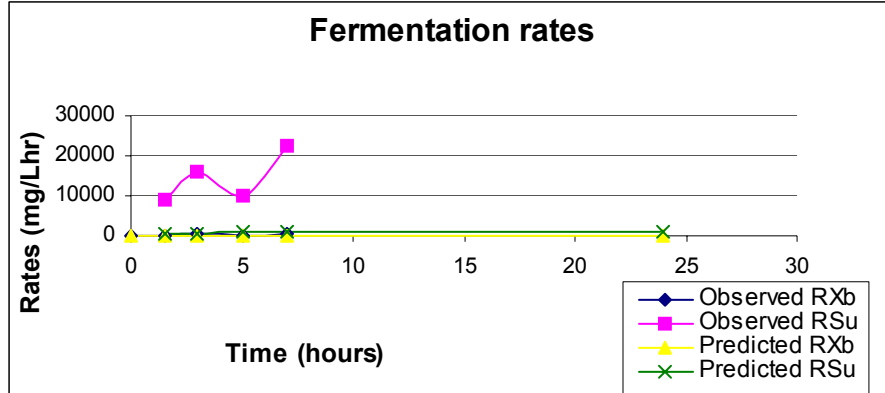


Figure A.16 The predicted and observed rates of biomass formation and substrate utilization.

Arrhenius Equation Calculations

The temperature dependent fermentations were used to calculate arrhenius constant and to plot the natural log of specific growth rate versus 1/temperature (K) for 50C, 45C, and 40C.

Table A.11 The arrhenius calculations for the 3 fermentors.

Growth rate	Temperature C	Temperature (K)	1/ Temperature(K)	Assume maximum growth rate	rate, day-1	Ln Rate	Ln max growth rate	(Ln max growth rate)*(-1)	1/A (Arrhenius constant)	A (Arrhenius constant)
0.0389	50	323.15	0.003095	0.0389	0.9336	-0.06871	-3.24676	3.246761	1.42702E-33	7.0076E+32
0.05261	45	318.15	0.003143	0.05261	1.26264	0.233205	-2.94485	2.944849	3.05461E-34	3.2737E+33
0.18818	40	313.15	0.003193	0.18818	4.51632	1.507698	-1.67036	1.670356	2.37631E-35	4.2082E+34

The Arrhenius equation is used to caculate a reaction rate constant as a function of temperature. This equation is $u_{max} = A \cdot e^{(-E_a/RT)}$.

The maximum growth rate (u_{max}) was assumed to be equal to specific growth rate (u) to calculate the equation values.

$$u_{max}=u=\text{growth coefficient, hr}^{-1}$$

A=arrhenius constant, hr^{-1}

Ea=Activation energy, kJ/mol

R=gas constant, 0.008314 kJ/molK

T=absolute temperature, K

In order to determine Ea for this specific fermentation it is necessary to plot $\ln(u)$ versus $1/(\text{Temperature, K})$. The slope of line is $-Ea/R$.

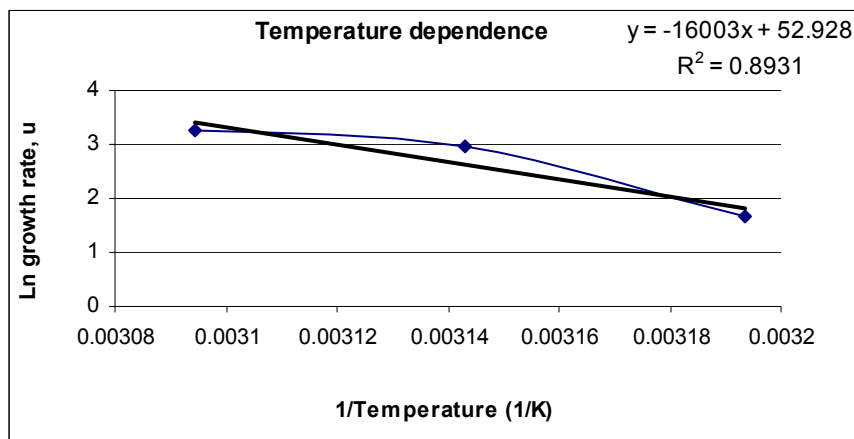


Figure A.17 The plot of $\ln(u)$ versus $1/\text{Temperature}$ for the three temperatures.

The regression equation of the line is $y = -16003x + 52.928$, and the $R^2 = 0.8931$. The $Ea/R = \text{slope} = -16003$, then $Ea = 133.048 \text{ kJ/mol}$.

APPENDIX B

B.1 DIONEX DX-600 HPLC (HIGH PERFORMANCE LIQUID CHROMATOGRAPHY) METHOD

Dionex Peaknet software version 6.0: Carbohydrates Method Procedure

```
-2.000 Pressure.LowerLimit =      70
      Pressure.UpperLimit =     4000
      %A.Equate = "WATER"
      %B.Equate = "200 mM NaOH"
      %C.Equate = "%C"
      %D.Equate = "%D"
      LoadPosition
      Mode =      IntAmp
      Pump_Relay_1.Closed      Duration=1.00
      IntAmp.Cell =      On
      ECD.Data_Collection_Rate =      1.0
      IntAmp.Electrode = AgCl
      pH.LowerLimit =      10.0
      pH.UpperLimit =      13.0
      Waveform Time = 0.00, Potential = 0.05
      Waveform Time = 0.20, Potential = 0.05, Integration = Begin
      Waveform Time = 0.40, Potential = 0.05, Integration = End
      Waveform Time = 0.41, Potential = 0.75
      Waveform Time = 0.60, Potential = 0.75
      Waveform Time = 0.61, Potential = -0.15
      Waveform Time = 1.00, Potential = -0.15
0.000 ECD.Autozero
      InjectPosition Duration=30.00
      Flow = 1.00
      %B = 22.0
      %C = 0.0
      %D = 0.0
      Curve =      5
0.100 IntAmp_1.AcqOn

0.100 Flow = 1.00
      %B = 22.0
      %C = 0.0
      %D = 0.0
      Curve =      5
1.250 Flow = 1.00
      %B = 22.0
      %C = 0.0
```

```

%D = 0.0
Curve =      5
5.000 Flow = 1.00
      %B = 22.0
      %C = 0.0
      %D = 0.0
      Curve =      5
6.500 Flow = 1.00
      %B = 44.8
      %C = 0.0
      %D = 0.0
      Curve =      5
7.500 Flow = 1.00
      %B = 60.0
      %C = 0.0
      %D = 0.0
      Curve =      5
8.000 Flow = 1.00
      %B = 100.0
      %C = 0.0
      %D = 0.0
      Curve =      5
8.500 Flow = 1.00
      %B = 100.0
      %C = 0.0
      %D = 0.0
      Curve =      5
9.000 Flow = 1.00
      %B = 100.0
      %C = 0.0
      %D = 0.0
      Curve =      5
9.500 Flow = 1.00
      %B = 100.0
      %C = 0.0
      %D = 0.0
      Curve =      5
10.000 Flow = 1.00
      %B = 100.0
      %C = 0.0
      %D = 0.0
      Curve =      5
12.000 Flow = 1.00
      %B = 100.0
      %C = 0.0
      %D = 0.0

```

```
Curve =      5
13.000 Flow = 1.00
  %B = 22.0
  %C = 0.0
  %D = 0.0
Curve =      5
17.000 Flow = 1.00
  %B = 22.0
  %C = 0.0
  %D = 0.0
Curve =      5

17.000 IntAmp_1.AcqOff

End
```


APPENDIX C

GLUCOSE BROTH MEDIA AND SWEET POTATO ANALYSIS

Table C.1 The Ingredients of Glucose Broth Media from Anderson et al. (1986).

The Original Glucose Media	
Glucose	100g/L
Bacto™ Yeast Extract	10g/L (10% of glucose)
Bacto™ Peptone	5g/L (5% of glucose)
(NH ₄) ₂ SO ₄	3g/L (3% of glucose)
KH ₂ PO ₄	3g/L (3% of glucose)
CaCl ₂ *H ₂ O	0.025g/L (0.025% of glucose)
MgSO ₄ *7H ₂ O	0.025g/L (0.025% of glucose)

Table C.2 The typical component analysis of Bacto™ Peptone and Bacto™ Yeast Extract (10%nitrogen, 80% amino acids (materials with carbon in it, used as protein which has about 4 calories per gram), 4% ash and the rest).

Typical Analyses- Peptones and Hydrolysates	Bacto Peptone	Bacto Yeast Extract
Total Nitrogen (%)	15.4	10.9
Amino Nitrogen (%)	3.5	6
ANTN	0.2	0.55
Ash (%)	3.8	11.2
Loss on Drying (%)	2.7	3.1
NaCl (%)	1.7	0.1
pH (2% solution)	7.1	6.7
Calcium (ug/g)	18	130
Magnesium (ug/g)	1	750
Potassium (ug/g)	2542	31950
Sodium (ug/g)	18440	14900
Chloride (%)	0.9	0.38
Sulfate (%)	0.32	0.09
Phosphate (%)	0.4	3.27
Alanine (% free)	1.2	4.4
Alanine (% total)	9.2	5.6
Arginine (%free)	2.8	1.4
Arginine (% total)	5.8	2.6
Asparagine (% free)	0.3	1
Aspartic Acid (% free)	0.3	1.6
Aspartic Acid (%)	5	5.3

total)		
Cystine (% free)	*	0.2
Glutamic Acid (% free)	0.7	6.6
Glutamic Acid (% total)	8.1	9.4
Glutamine (% free)	*	0.2
Glycine (% free)	0.7	1
Glycine (% total)	15.9	3
Histidine (% free)	0.2	0.4
Histidine (% total)	0.8	1.3
Isoleucine (% free)	0.6	1.8
Isoleucine (% total)	2.1	3
Leucine (% free)	1.6	3
Leucine (% total)	3.8	4.1
Lysine (% free)	2.2	1.9
Lysine (% total)	3.4	4.6
Methionine (% free)	0.3	0.6
Methionine (% total)	0.7	0.8
Phenylalanine (% free)	1.4	2
Phenylalanine (% total)	2.8	2.6
Proline (% free)	0.3	0.8
Proline (% total)	8.8	2
Serine (% free)	0.4	1.3
Serine (% total)	1.5	1.6
Theonine (% free)	0.3	1.1
Theonine (% total)	1.1	1.6
Tryprophene (% free)	0.3	0.5
Tyrogine (% free)	0.5	0.8
Tyrogine (% total)	0.6	1.2
Valine (% free)	0.7	2.2
Valine (% total)	2.8	3.5

Table C.3 The detailed analysis of sweet potato, raw, unprepared (Scientific Name: Ipomoea Batatas (Sweet Potatoes)).

Nutrient	Units	Value per 100 grams of edible portion	Sample Count	Std. Error
Proximate				
Water	G	79.78	4	1.125
Energy	Kcal	76	0	
Energy	Kj	317	0	
Protein	G	1.57	4	0.145
Total lipid (fat)	G	0.05	4	0.033
Ash	G	0.99	4	0.056
Carbohydrate, by difference	G	17.61	0	
Fiber, total dietary	G	3.0	0	
Sugars, total	G	3.89	0	
Sucrose	G	2.17	4	0.180
Glucose (dextrose)	G	1.01	4	0.332
Fructose	G	0.71	4	0.190
Lactose	G	0.00	4	0.000
Maltose	G	0.00	4	0.000
Galactose	G	0.00	0	
Minerals				
Calcium, Ca	Mg	30	3	4.632
Iron, Fe	Mg	0.61	3	0.070
Magnesium, Mg	Mg	25	3	3.180
Phosphorus, P	Mg	47	3	7.413
Potassium, K	Mg	337	3	27.552
Sodium, Na	Mg	13	9	1.300
Zinc, Zn	Mg	0.30	3	0.033
Copper, Cu	Mg	0.151	3	0.015
Manganese, Mn	Mg	0.258	3	0.052
Selenium, Se	Mcg	0.6	1	
Vitamins				
Vitamin C, total ascorbic acid	Mg	22.7	12	2.577
Thiamin	Mg	0.078	4	0.007
Riboflavin	Mg	0.061	4	0.005
Niacin	Mg	0.557	4	0.076
Pantothenic acid	Mg	0.800	4	0.152
Vitamin B-6	Mg	0.209	4	0.014
Folate, total	Mcg	14	9	1.710

Folic acid	Mcg	0	0	
Folate, food	Mcg	14	9	1.710
Folate, DFE	Mcg_DFE	14	0	
Vitamin B-12	Mcg	0.00	0	
Vitamin A, IU	IU	14545	0	
Vitamin A, RAE	Mcg_RAE	727	0	
Retinol	Mcg	0	0	
Vitamin E (alpha-tocopherol)	Mg	0.26	2	
Tocopherol, beta	Mg	0.01	2	
Tocopherol, gamma	Mg	0.00	2	
Tocopherol, delta	Mg	0.00	2	
Vitamin K (phylloquinone)	Mcg	1.8	2	
Lipids				
Fatty acids, total saturated	G	0.018	0	
4:0	G	0.000	0	
6:0	G	0.000	0	
8:0	G	0.000	2	
10:0	G	0.000	2	
12:0	G	0.000	2	
14:0	G	0.000	2	
15:0	G	0.000	2	
16:0	G	0.018	2	
17:0	G	0.000	2	
18:0	G	0.001	2	
20:0	G	0.000	2	
22:0	G	0.000	2	
24:0	G	0.000	2	
Fatty acids, total monounsaturated	G	0.001	0	
14:1	G	0.000	2	
15:1	G	0.000	2	
16:1 undifferentiated	G	0.000	2	
17:1	G	0.000	2	
18:1 undifferentiated	G	0.001	2	
20:1	G	0.000	2	
22:1 undifferentiated	G	0.000	2	
Fatty acids, total polyunsaturated	G	0.014	0	
18:2 undifferentiated	G	0.013	2	
18:3 undifferentiated	G	0.001	2	
18:4	G	0.000	2	
20:2 n-6 c,c	G	0.000	2	

20:3 undifferentiated	G	0.000	2	
20:4 undifferentiated	G	0.000	2	
20:5 n-3	G	0.000	2	
22:5 n-3	G	0.000	2	
22:6 n-3	G	0.000	2	
Cholesterol	Mg	0	0	
Phytosterols	Mg	12	0	
Amino acids				
Tryptophan	G	0.020	8	
Threonine	G	0.082	14	
Isoleucine	G	0.082	14	
Leucine	G	0.121	14	
Lysine	G	0.081	14	
Methionine	G	0.041	14	
Cystine	G	0.013	7	
Phenylalanine	G	0.099	14	
Tyrosine	G	0.068	14	
Valine	G	0.108	14	
Arginine	G	0.077	14	
Histidine	G	0.031	14	
Alanine	G	0.090	14	
Aspartic acid	G	0.282	14	
Glutamic acid	G	0.161	14	
Glycine	G	0.074	14	
Proline	G	0.072	14	
Serine	G	0.085	14	
Other				
Alcohol, ethyl	G	0.0	0	
Caffeine	Mg	0	0	
Theobromine	Mg	0	0	
Carotene, beta	Mcg	8727	41	235.058
Carotene, alpha	Mcg	0	37	
Cryptoxanthin, beta	Mcg	0	34	
Lycopene	Mcg	0	1	
Lutein + zeaxanthin	Mcg	0	1	

USDA National Nutrient Database for Standard Reference, Release 16 (July 2003)

APPENDIX D

D.1 SHIMADZU GC 17-A GAS CHROMATOGRAPHY, CLASS VP CHROMATOGRAPHY DATA SYSTEM

The following figures D.1, D.2, and D.3 are the alcohol method setup parameters.

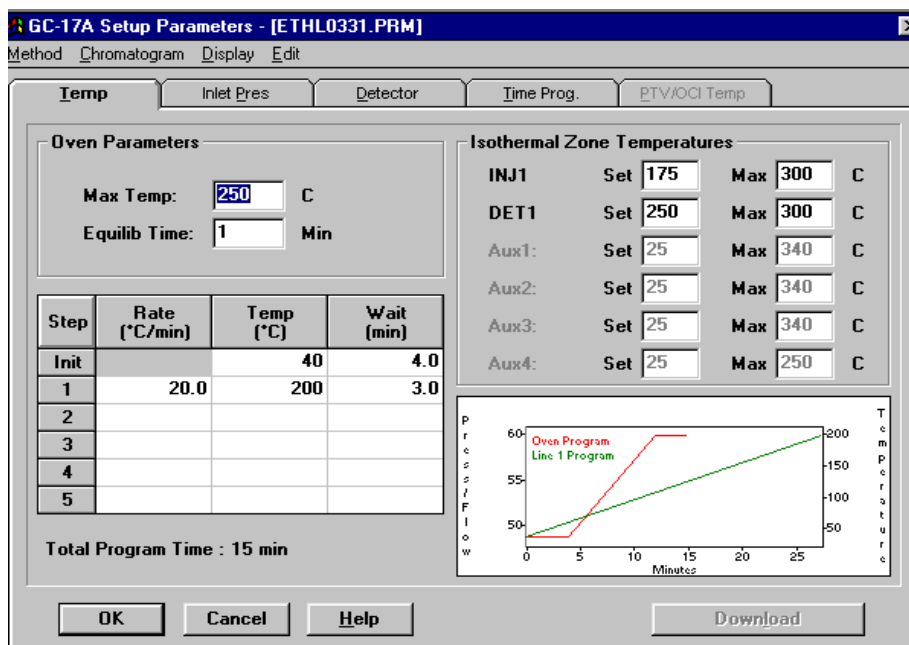


Figure D.1 The temperature setup.

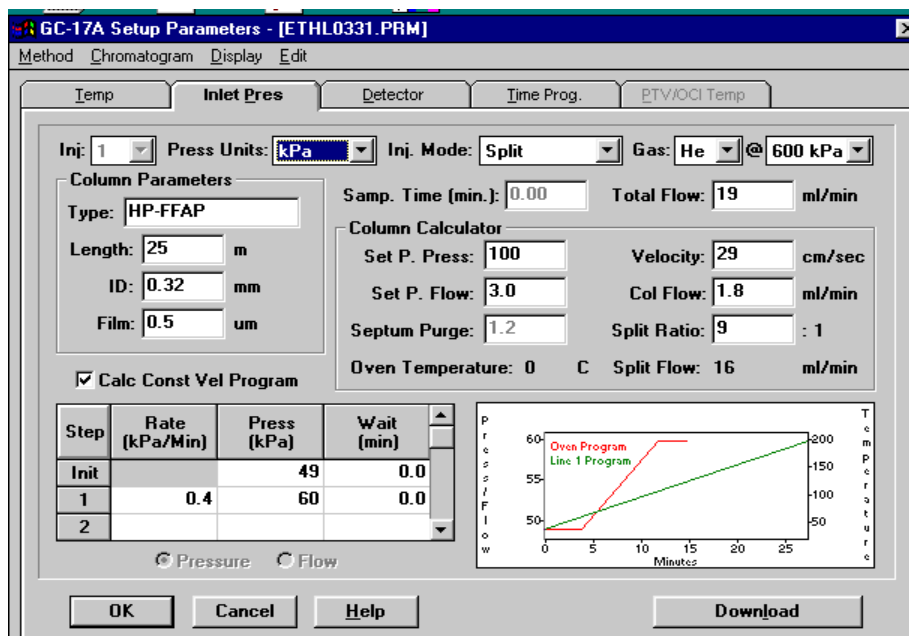


Figure D.2 The inlet pressure setup.

GC-17A Setup Parameters - [ETHL0331.PRM]

Method Chromatogram Display Edit

Temp Inlet Pres **Detector** Time Prog. PTV/OCI Temp

	On	Range	Polarity	Current	H2 Flow ml/min	Air Flow ml/min	Make Up Gas Flow
FID	<input checked="" type="checkbox"/>	1	2	0	40	400	30
None	<input checked="" type="checkbox"/>	0	2	0	0	0	0
None	<input checked="" type="checkbox"/>	0	2	0	0	0	0
None	<input checked="" type="checkbox"/>	0	2	0	0	0	0

OK Cancel Help Download

Figure D.3 The detector setup.

D.2 The RRf determination for ethanol concentration calculations.

The following Table D.1 shows the RRf calculation for ethanol concentration determination.

Table D.1 External Standard of Ethanol and n-Propanol areas used to calculate RRf.

External Standard					
	Methanol	Ethanol	n-Propanol	Butanol	RRf (etoh)
Concentration mg/L	10	10	10	10	
AREA	590	837	1114	1347	1.330943847
			4230		.
Concentration mg/L	25	25	25	25	
AREA			10116		
			14096		
Concentration mg/L	41.66	41.66	41.66	41.66	
AREA	2332	3046	4165	4528	1.367367039

Concentration mg/L	50	50	50	50	
AREA	12225	14379	23138	24909	1.609152236
AREA	8110	11486	19512	16028	
AREA	2996	3947	5590	6119	
AVERAGE AREA	7777	9937.33333	16080	15685.3333	1.618140346
Concentration mg/L	83.33	83.33	83.33	83.33	
AREA	4682	6088	8747	9411	1.436760841
Concentration mg/L	100	100	100	100	
AREA			41124		
Concentration mg/L	166.66	166.66	166.66	166.66	
AREA	9447	12438	17686	18758	1.330944
Concentration mg/L	250	250	250	250	
AREA	15383	18581	28603	29668	1.330944
Concentration mg/L	500	500	500	500	
AREA	82140	118600	232596	165287	1.330944
AREA	30961	40243	54787	60026	
AVERAGE AREA	56550.5	79421.5	143691.5	112656.5	
AVERAGE CONC ppm	157.3785714	157.378571	136.2944444	157.378571	1.419399539
AVERAGE AREA	13823.07143	18621.2619	30147.38889	27436.2619	

APPENDIX E

E.1 THE PICTURES OF THE *KLUYVEROMYCES MARXIANUS* YEAST STRAIN

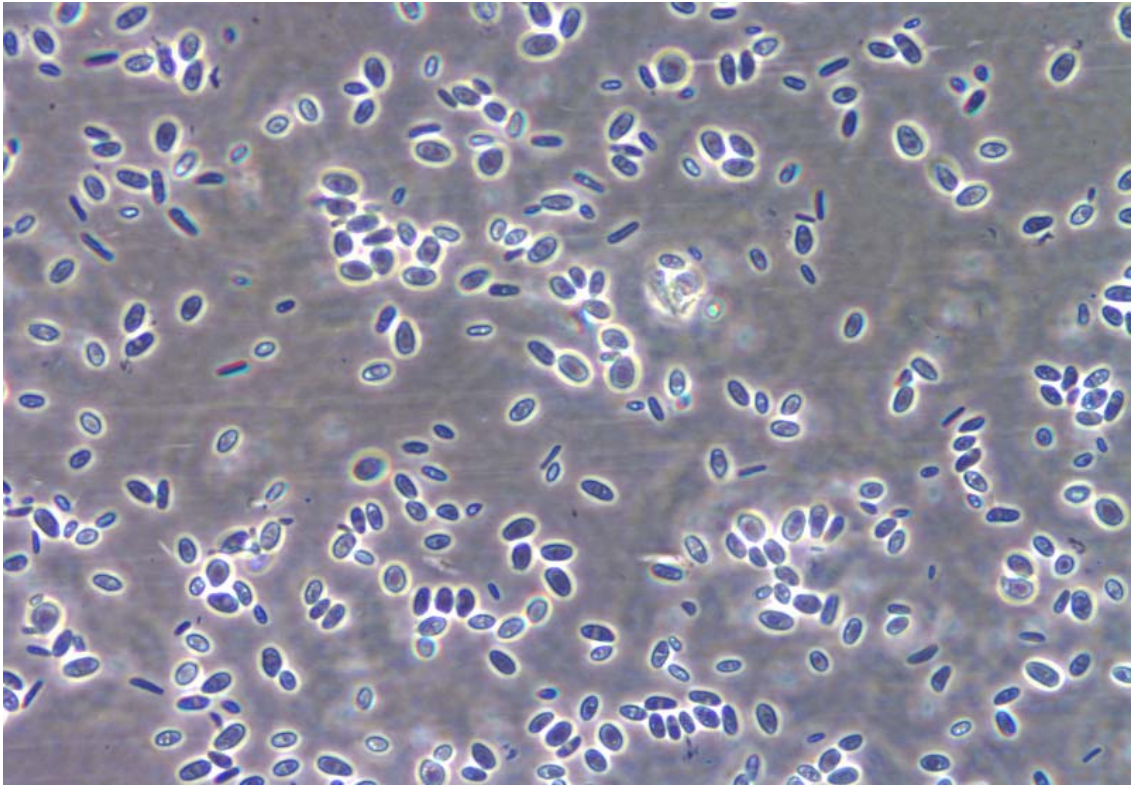


Figure E.1 *Kluyveromyces marxianus* cells from the sterile agar petri dish.

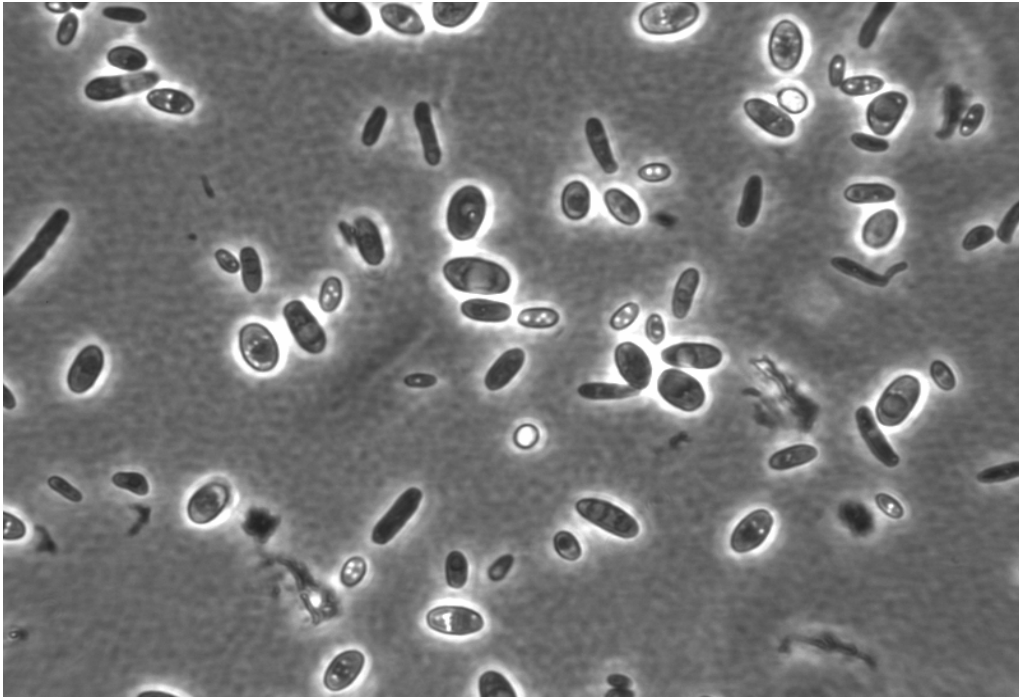


Figure E.2 *Kluveromyces marxianus* cells from glucose media the aerobic Orbital Shaker bed.

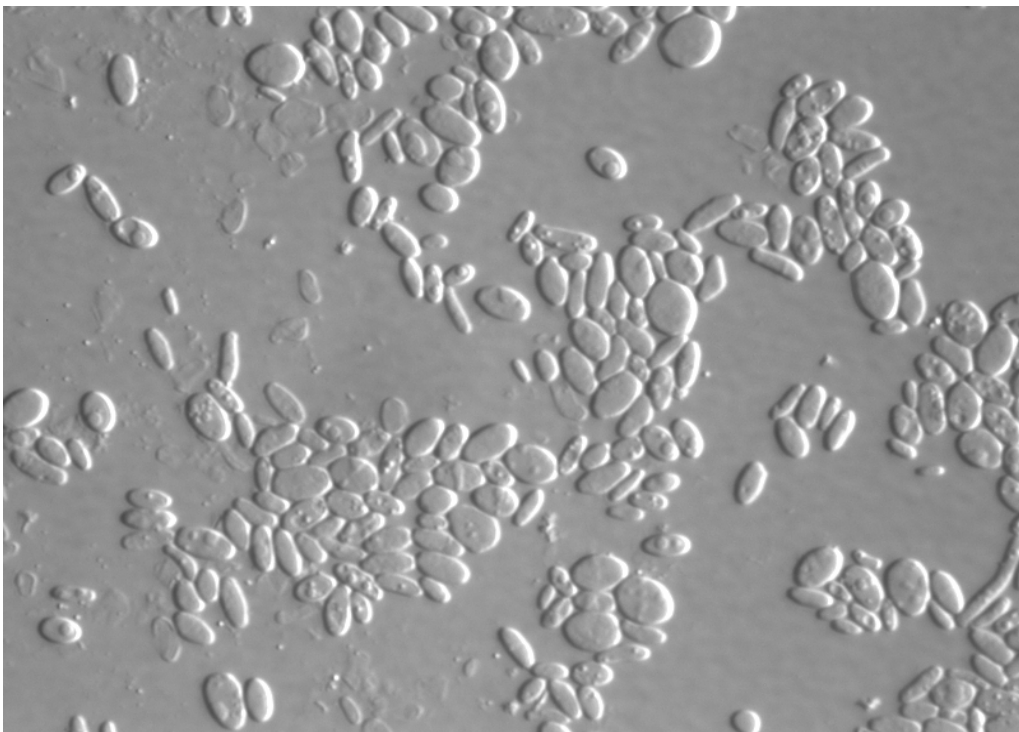


Figure E.3 *Kluveromyces marxianus* cells from the glucose media anaerobic Bioflo® 2000 fermentor.

APPENDIX F

THE CALIBRATION CURVES FOR *KLUYVEROMYCES MARXIANUS*

The calibration curves for *Kluyveromyces marxianus* used for the anaerobic experiments which used the Two-Liter Bioflo® 2000 Fermentors. Figure F.1 shows the calibration curve for 1,000 mg/L glucose media which was used by the lower substrates until 3,000 mg/L glucose media substrate used in the experiments.

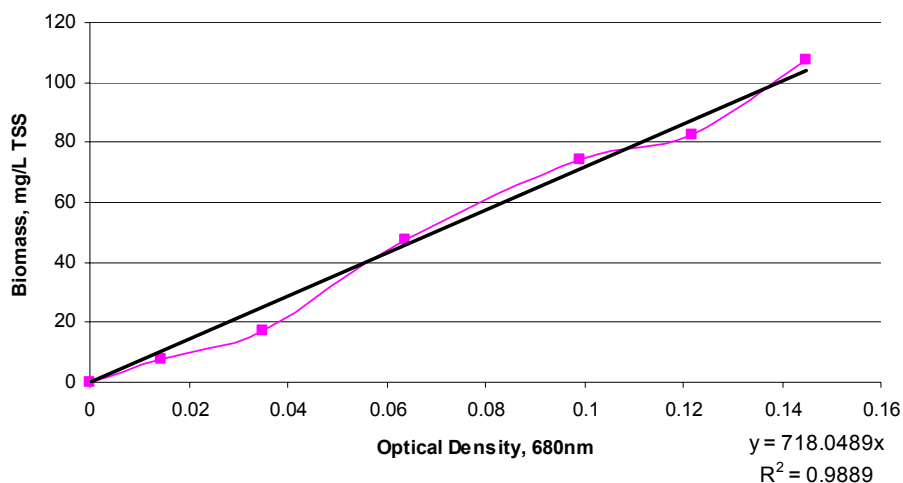


Figure F.1 The calibration curve for 1,000 mg/L glucose media yeast strain.

The Figure F.2 shows the calibration curve for 100 g/L glucose media which was used by the substrates from 5,000 mg/L glucose concentration until 80,000 mg/L glucose concentration for the experiments.

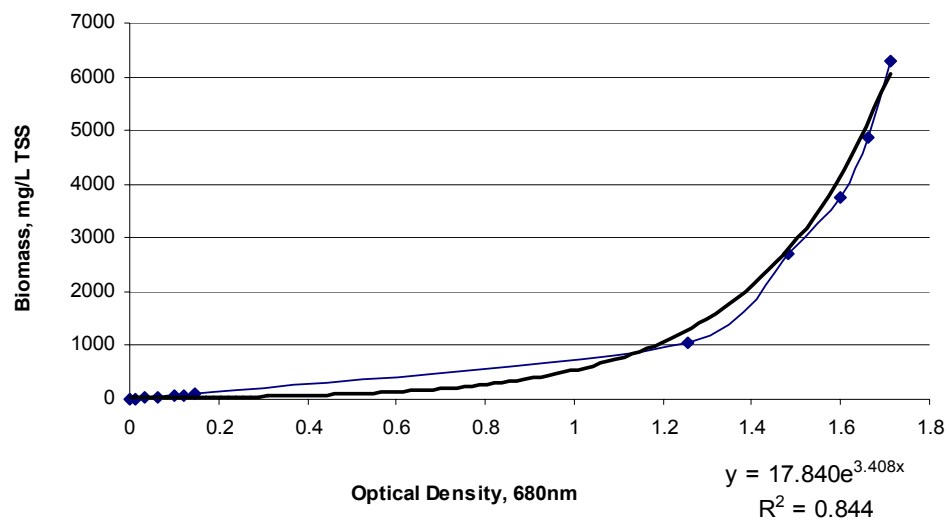


Figure F.2 The calibration curve for 100 g/L glucose media yeast strain.

APPENDIX G

G.1 AEROBIC CONDITIONS USING THE TWO-LITER BIOFLO[®] 2000 FERMENTORS

The following Figures G.1, G.2, and G.3 are from the first run which shows the line trend for the soluble substrate measured using COD, and the biomass predicted from the OD data set using the calibration curve already mentioned. These figures were used to calculate the biomass yield by breaking the time into five parts or five “time frames” averaging the biomass (mg/L TSS) and the substrate (mg/L COD) over each five time frames.

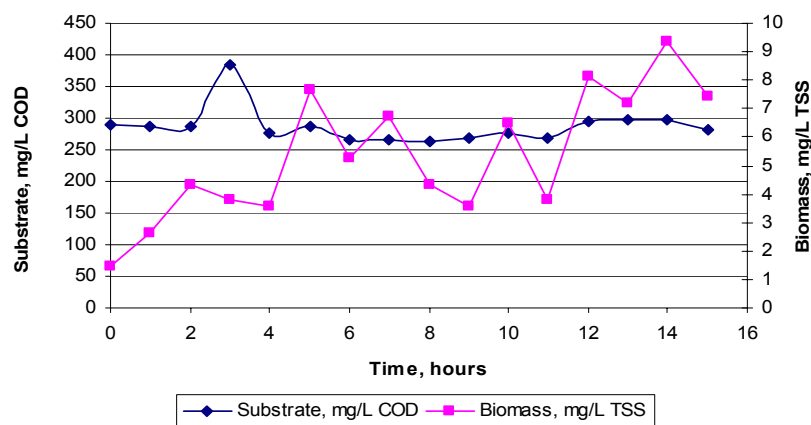


Figure G.1 The whole soluble substrate (COD) and biomass (TSS) versus time for the 200 mg/L glucose media for the first run.

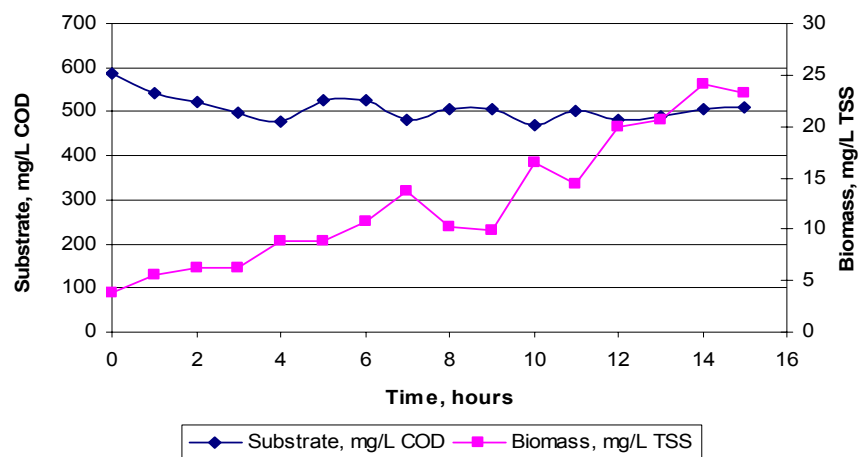


Figure G.2 The whole soluble substrate (COD) and biomass (TSS) versus time for the 400 mg/L glucose media for the first run.

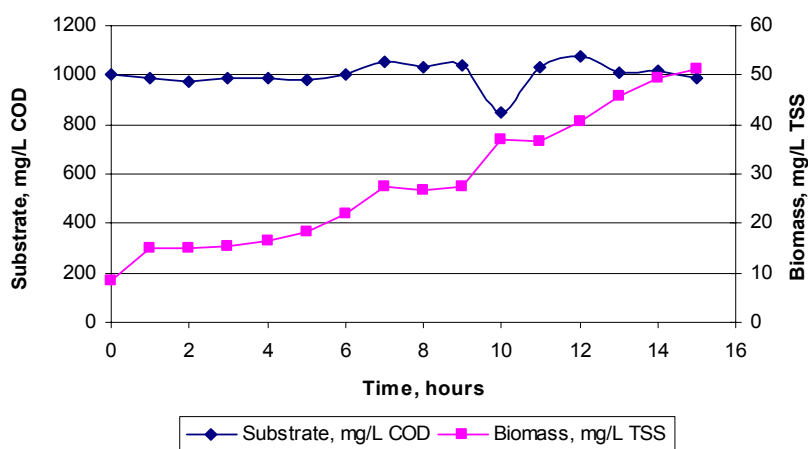


Figure G.3 The whole soluble substrate (COD) and biomass (TSS) versus time for the 1,000 mg/L glucose media for the first run.

The following figures G.4, G.5, and G.6 are from the second run which shows the line trend for soluble substrate measured with COD and the biomass predicted from the OD readings using the calibration curve already mentioned. These figures were used to calculate the biomass yield by breaking the time into five parts or five “time frames”

averaging the biomass (mg/L TSS) and the substrate (mg/L COD) over each five time frames.

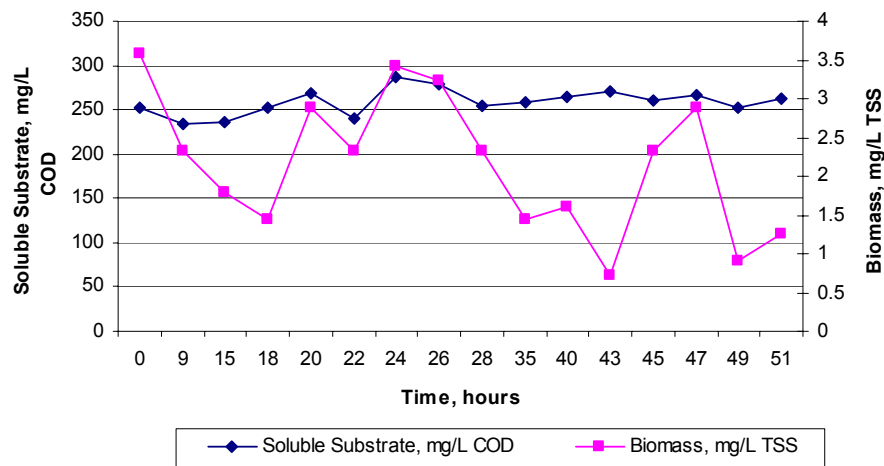


Figure G.4 The whole soluble substrate (COD) and biomass (TSS) versus time for the 200 mg/L glucose media for the second run.

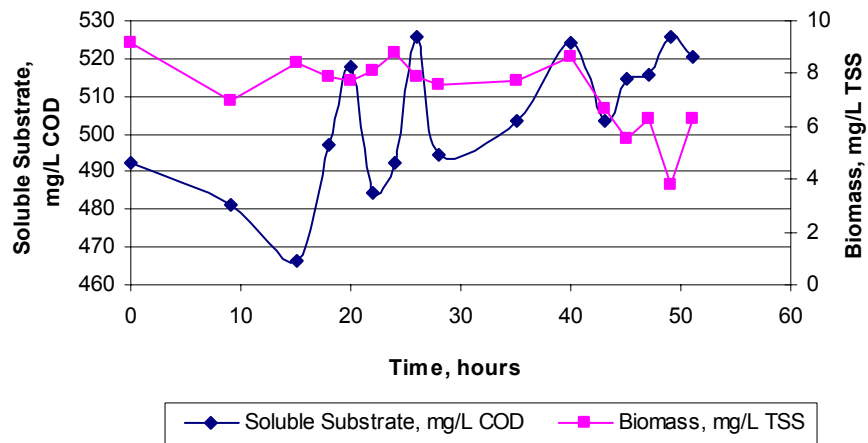


Figure G.5 The whole soluble substrate (COD) and biomass (TSS) versus time for the 400 mg/L glucose media for the second run.

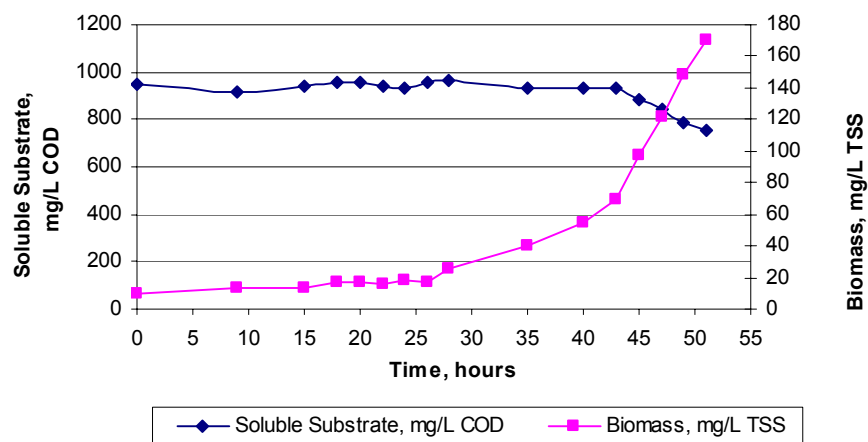


Figure G.6 The entire soluble substrate (COD) and biomass (TSS) versus time for the 800 mg/L glucose media for the second run.

G.2 Anaerobic conditions using the Two-Liter Bioflo® 2000 Fermentors.

The following figures G.7, G.8, and G.9 are for the 5,000, 7,500, and 15,000 mg/L glucose concentrations. The soluble substrate was measured using COD and the biomass TSS predicted from the OD readings using the calibration curve already mentioned. These figures were used to calculate the biomass yield by breaking the time into seven parts or seven “time frames”. The biomass (mg/L TSS) and substrate (mg/L COD) were averaged over each chosen time frame.

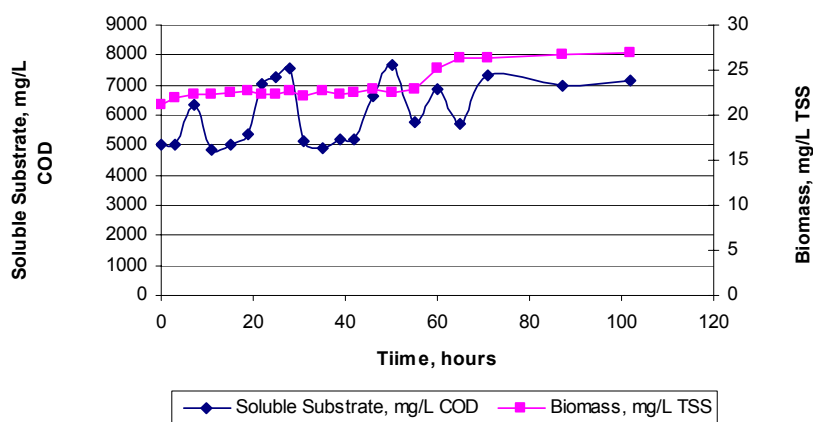


Figure G.7 The entire soluble substrate (COD) and biomass (TSS) versus time for the 5,000 mg/L glucose media.

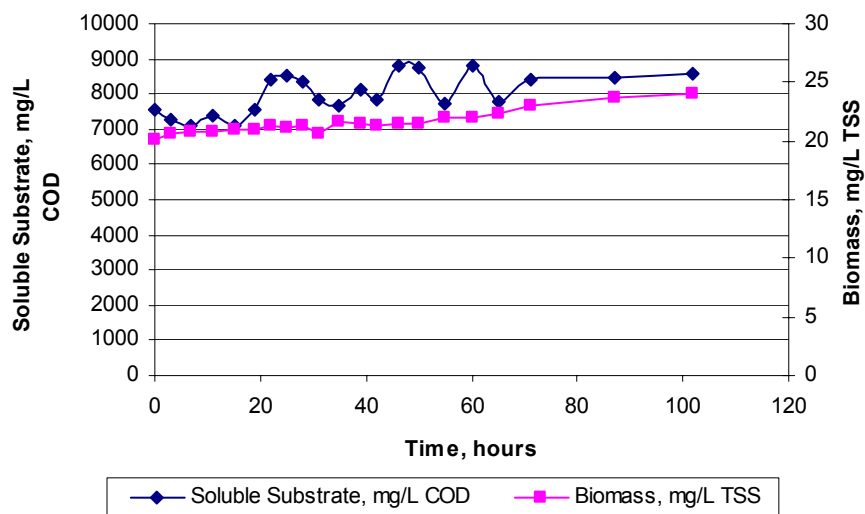


Figure G.8 The entire soluble substrate (COD) and biomass (TSS) versus time for the 7,500 mg/L glucose media.

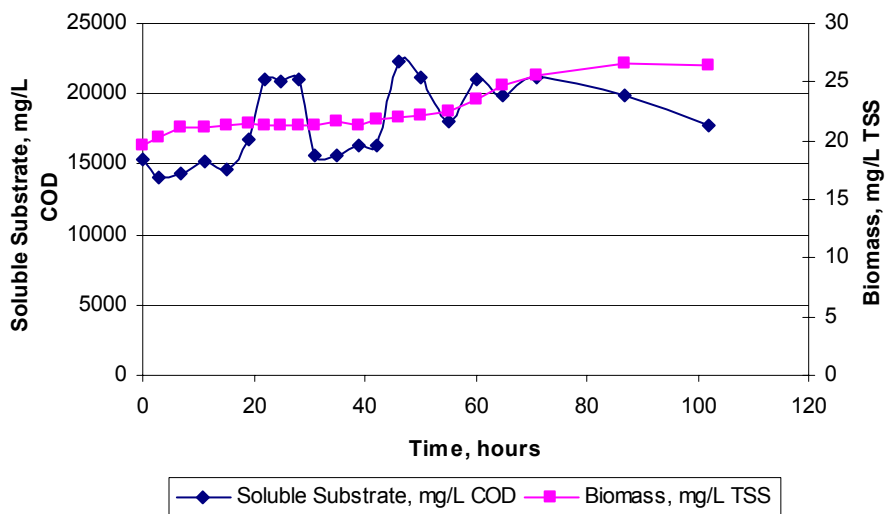


Figure G.9 The entire soluble substrate (COD) and biomass (TSS) versus time for the 15,000 mg/L glucose media.

APPENDIX H

SAS CODE FOR THE AEROBIC EXPERIMENTAL DATA SET USING THE TWO-LITER BIOFLO® 2000 FERMENTORS

H.1 SAS code for the 200, 400, and 1,000 mg/L glucose media experiment

```
title 'SAS Nonlinear Analysis for Kinetic Parameter Determinatiion FOR
aerobic2a august 20 2002.xls file';
*Bioflo2000 Fermentors were used in this experiment with 3 different
substrates;
*the experiment last for 15 hours;
*scod=soluble substrate in mg/L COD units;
*tss=biomass concentration in mg/L TSS units;
```

```
data batch;
input time scod_200 tss_200 scod_400 tss_400 scod_1000 tss_1000;
cards;
0 288.77 0.72 586.82 3.11 1456.73 8.14
1 285.98 2.63 543.18 5.51 1433.84 14.84
2 287.84 4.31 522.75 6.22 1415.00 15.08
3 384.40 3.83 498.61 6.22 1435.19 15.32
4 275.77 3.59 477.25 8.86 1432.50 16.52
5 285.98 7.66 525.53 8.86 1425.77 18.43
6 264.62 5.27 526.46 10.77 1452.69 22.02
7 266.48 6.70 482.82 13.64 1529.43 27.53
8 262.77 4.31 506.04 10.29 1494.43 26.57
9 267.41 3.59 506.96 9.81 1505.20 27.53
10 277.62 6.46 469.82 16.52 1234.59 37.10
11 268.34 3.83 503.25 14.36 1497.12 36.62
12 294.34 8.14 481.89 19.87 1564.44 40.45
13 298.05 7.18 491.18 20.58 1466.16 45.72
14 297.12 9.33 505.11 24.17 1478.27 49.31
15 280.41 7.42 508.82 23.22 1431.15 51.22
;
```

```
*xbo=initial biomass concentration, at time zero;
*so=initial soluble substrate concentration, at time zero;
***y=biomass yield (biomass mg/L TSS)/(substrate mg/L COD);
```

```
data new1; set batch;
xbo=0.72; so=288.7; y=0.11;
s=scod_200;
xb=tss_200;
t=time;
Run;
proc print data=new1;
title2'The logistic equation is applied for the 200mg/L glucose
concentration media';
proc model data=new1;
title2'The logistic equation is applied for the 200mg/L glucose
concentration media';
parms ks umax;
endogenous xb s;
```

```

exogenous t ;
eq.g1=(( (ks*y/(xbo+so*y))+1)*log(xb/xbo)+((ks*y/(xbo+so*y))*log(so/s)))
-t*umax;
eq.g2=(xb-xbo)-y*(so-s);
fit g1 g2;
run;

*xbo=initial biomass concentration, at time zero;
*so=initial soluble substrate concentration, at time zero;

data new2; set batch;
xbo=3.11; so=586.8; y=0.30;
s=scod_400;
xb=tss_400;
t=Time;
Run;
proc print data=new2;
title2'The logistic equation is applied for the 400mg/L glucose
concentration media';

proc model data=new2;
title2'The logistic equation is applied for the 400mg/L glucose
concentration media';
parms ks umax;
endogenous xb s;
exogenous t ;
eq.g1=(( (ks*y/(xbo+so*y))+1)*log(xb/xbo)+((ks*y/(xbo+so*y))*log(so/s)))
-t*umax;
eq.g2=(xb-xbo)-y*(so-s);
fit g1 g2;
run;

*xbo=initial biomass concentration, at time zero;
*so=initial soluble substrate concentration, at time zero;

data new3; set batch;
xbo=8.14; so=1452.5; y=0.29;
s=scod_1000;
xb=tss_1000;
t=Time;
Run;

proc print data=new3;
title2'The logistic equation is applied for the 1,000mg/L glucose
concentration media';

proc model data=new3;
title2'The logistic equation is applied for the 1,000mg/L glucose
concentration media';
parms ks umax;
endogenous xb s;
exogenous t ;
eq.g1=(( (ks*y/(xbo+so*y))+1)*log(xb/xbo)+((ks*y/(xbo+so*y))*log(so/s)))
-t*umax;
eq.g2=(xb-xbo)-y*(so-s);
fit g1 g2;
run;

```

```
quit;
```

H.2 SAS code for the 200, 400, and 800 mg/L glucose media experimental data set for aerobic conditions using the two-liter Bioflo® 2000 Fermentors.

```
title 'SAS Nonlinear Analysis for Kinetic Parameter Determination FOR
aerobic tap september 20 2002. xls file';
*experiment done using the Bioflo 2000 Fermentors;
*3 different substrate;
*scod=soluble substrate in COD units;
*tss=biomass concentration in TSS units;

data batch;
input  time scod_200 tss_200 scod_400 tss_400  scod_800 tss_800;
cards;
0      252.76      3.59 492.52      9.16 946.01      9.87
9      234.18      2.33 481.37      7.00 913.48     13.64
15     235.11      1.80 466.50      8.44 944.15     13.28
18     252.76      1.44 497.17      7.90 953.44     16.69
20     268.56      2.87 517.61      7.72 954.37     16.87
22     239.75      2.33 484.16      8.08 940.43     16.16
24     286.22      3.41 492.52      8.80 933.93     17.95
26     277.86      3.23 525.97      7.90 953.44     17.23
28     253.69      2.33 494.38      7.54 965.52     25.85
35     258.34      1.44 503.67      7.72 929.28     39.67
40     264.85      1.62 524.11      8.62 929.28     54.57
43     270.42      0.72 503.67      6.64 929.28     69.47
45     261.13      2.33 514.82      5.56 880.03     97.83
47     265.77      2.87 515.75      6.28 841.93    121.17
49     251.84      0.90 525.97      3.77 788.96    148.10
51     262.99      1.26 520.40      6.28 751.79    170.18
;
****xbo=initial biomass concentration, at time zero;
****so=initial soluble substrate concentration, at time zero;
****y=biomass yield (biomass mg/L TSS)/(substrate mg/L COD);

data new1; set batch;
xbo=3.59; so=252.76; y=0.30;
s=scod_200;
xb=tss_200;
t=Time;
Run;
proc print data=new1;
title2'The logistic equation is applied for the 200mg/L glucose
concentration media';

proc model data=new1;
title2'The logistic equation is applied for the 200mg/L glucose
concentration media';
parms ks umax;
endogenous xb s;
exogenous t ;
eq.g1=(( (ks*y/(xbo+so*y)) +1)*log(xb/xbo) + ((ks*y/(xbo+so*y))*log(so/s)))
-t*umax;
eq.g2=(xb-xbo)-y*(so-s);
```

```

fit g1 g2;
run;
****xbo=initial biomass concentration, at time zero;
****so=initial soluble substrate concentration, at time zero;

data new2; set batch;
xbo=9.16; so=492.52; y=0.31;
s=scod_400;
xb=tss_400;
t=Time;
Run;
proc print data=new2;
title2'The logistic equation is applied for the 400mg/L glucose
concentration media';

proc model data=new2;
title2'The logistic equation is applied for the 400mg/L glucose
concentration media';
parms ks umax;
endogenous xb s;
exogenous t ;
eq.g1=(( (ks*y/ (xbo+so*y)) +1)*log(xb/xbo)+((ks*y/ (xbo+so*y)) *log(so/s)))
-t*umax;
eq.g2=(xb-xbo)-y*(so-s);
fit g1 g2;
run;

****xbo=initial biomass concentration, at time zero;
****so=initial soluble substrate concentration, at time zero;

data new3; set batch;
xbo=9.87; so=946.01; y=0.81;
s=scod_800;
xb=tss_800;
t=Time;
Run;
proc print data=new3;
title2'The logistic equation is applied for the 800mg/L glucose
concentration media';

proc model data=new3;
title2'The logistic equation is applied for the 800mg/L glucose
concentration media';
parms ks umax;
endogenous xb s;
exogenous t ;
eq.g1=(( (ks*y/ (xbo+so*y)) +1)*log(xb/xbo)+((ks*y/ (xbo+so*y)) *log(so/s)))
-t*umax;
eq.g2=(xb-xbo)-y*(so-s);
fit g1 g2;
run;

quit;

```

APPENDIX I

SAS (VERSION 9.0) PROGRAM FOR “BIOLOGICAL GROWTH KINETIC PARAMETER DETERMINATION ANALYSIS USING MONTE CARLO SIMULATIONS”

I.1 Data Generation and Simulation: step 1.

```
dm'log;clear;output;clear';
options ps=80 ls=132 nocenter nodate nonumber; **** 020304 newest file ***;

libname output 'C:\Erika Reeves - Monte Carlo from Geaghan\Nonlinear e integer Output
020604\';

data ONE Integer; length dataset $ 40;
***** initial values - constants for the program *****;
seed1=8662823; **** only one seed is needed, it changes automatically ****;
NoOfReps = 5000; *** number of replicates ***;
umax = 0.6;
Ks= 50;
Substrate0 = 500;
Biomass0 = 0.5;
dt=0.001;
SEumax = 0.10*umax;
SEks = 0.10*ks;
do SubstrateINIT = 200 to 1000 by 50;
    do rep = 1 to NoOfReps by 1;
        Do time = 0 to 20 by dt;
            If time eq 0 then do; **** create and output time zero only ****;
                substrate0 = substrateINIT;
                SubstrateT = Substrate0;
                BiomassT = Biomass0;
                Yb = 0.5;

                dBiomassT = .; dSubstrateT = .; ksXX = .; umaxXX = .; timePred = .;
                output;
            end;

            if time gt 0 and rep le NoOfReps then do;
                ksXX = ks + rannor(seed1)*seks; **** add random variation to biological
parameter ****;
                umaxXX = umax + rannor(seed1)*seumax; **** add random variation to biological
parameter ****;
                dBiomassT = (((umaxXX*SubstrateT ) / (ksXX + SubstrateT ))) * BiomassT * dt;
                *** change of Biomass over time ****;
                dSubstrateT = (1/Yb)*dBiomassT;
                *** change of Substrate over time ****;
                BiomassT = BiomassT + dBiomassT;
                SubstrateT = SubstrateT - dSubstrateT ;
                Yb = ((BiomassT-dBiomassT)-BiomassT)/(SubstrateT-(SubstrateT+dSubstrateT));
                *** Biomass Yield defenition ****;

                *****this following timePred will be cancelled for the final draft *****;
            end;
        end;
    end;
end;
```

```

t0=0;
timePred = (( ( ((Ks*Yb + Substrate0*Yb + Biomass0)/(Substrate0*Yb + Biomass0)) *
log(BiomassT/Biomass0)) - ((Ks*Yb)/(Substrate0*Yb + Biomass0)) *
log((Yb*Substrate0 + Biomass0 - BiomassT) / (Yb*Substrate0)) ) / umaxXX ) + t0;
*****;
end;

keep time SubstrateT BiomassT Yb dbiomassT dsubstratet rep SubstrateINIT ksxx umaxxx
timepred;

** stop output when substrateT is small(reached 1 or 0.5) or dbiomassT is less than 0 **;
if dbiomassT gt 0 and SubstrateT gt 1 then do;

if ABS(time-int(time)) le 0.0000001 or ABS(time-int(time)) ge 0.9999999 then do;

*if int(time) = fuzz(time) then do;          ** FUZZ to get around rounding error ****;

SEBt = 0.01*BiomassT;          ** 1% sampling error was added ****;
BiomassT = BiomassT + rannor(seed1)*seBt;
**** added sampling error with biomass term ****;

*output one;          **** detailed numerical integration not saved (too big)****;

output integer;

end; end;
end;
end;
end;
retain BiomassT SubstrateT;
run;

data output.Integer5; set integer;
keep time SubstrateT BiomassT Yb dbiomassT dsubstratet rep SubstrateINIT ksxx umaxxx;
run;

quit;

```

I.2 Graphing the substrates generated: step 2.

```

dm'log;clear;output;clear';
options ps=80 ls=132 nocenter nodate nonumber; **** 02-12-2004 separating the integer
substrate for 3 graphs ***;

libname output 'C:\Erika Reeves - Monte Carlo from Geaghan\Nonlinear 021204';

data Integer; set output.Integer5;
if substrateINIT GE 500 and substrateINIT le 700 then Category = 'Medium';
if substrateINIT LE 450 then Category = 'Low';
if substrateINIT GE 750 then Category = 'High';
*vars time SubstrateT BiomassT Yb dbiomassT dsubstratet rep SubstrateINIT ksxx umaxxx;
run;

*proc print data=integer noobs;
*var time timepred SubstrateT BiomassT Yb dbiomassT dsubstratet SubstrateINIT ksxx
umaxxx;

```

```

        *title1 'Generated data';
*run;
proc sort data=integer; by category; run;

options ps=56 ls=132;
*goptions device=win;

proc plot data=integer; by category;
    plot BiomassT*time; title1 'Biomass versus Time'; run;
proc plot data=integer; by category;
    plot SubstrateT*time; title1 'Substrate versus Time'; run;
proc plot data=integer; by category;
    plot BiomassT*SubstrateT ; title1 'Biomass versus Substrate'; run;

quit;

```

I.3 Nonlinear models fitting: step 3.

```

dm'log;clear;output;clear';
options ps=80 ls=132 nocenter nodate nonumber; **** 020304 newest file ***;

libname output 'C:\Erika Reeves - Monte Carlo from Geaghan\Nonlinear e integer Output
020604\';

data Integer; set output.Integer5;
*keep time SubstrateT BiomassT Yb dbiomassT dsubstratet rep SubstrateINIT ksxx umaxxx;
run;

proc Sort data=integer; by SubstrateINIT rep time; run;
options ps=256 ls=132;

***** NONLINEAR METHOD *****;

*****From: Shuler and Kargi's Bioprocess Engineering Book (newest edition)- with
changing BiomassT *****;

***** FIXED *****;
***** GIVEN INITIAL PARAMETERS *****;

proc model data=integer MAXITER=10000 noprint;*CONVERGE=0.001; by SubstrateINIT rep;
title1 'Kinetics model - 6.52 equation with biomassT changing - Fixed';
    parameters mu = 0.6 ks = 50; Substrate0 = SubstrateINIT; Biomass0 = 0.5;
t0=0;
eq.g1 = ((( ( ((Ks*Yb + Substrate0*Yb + Biomass0)/(Substrate0*Yb + Biomass0)) *
    log(BiomassT/Biomass0)) - ((Ks*Yb)/(Substrate0*Yb + Biomass0)) *
    log((Yb*Substrate0 + Biomass0 - BiomassT) / (Yb*Substrate0)) ) / mu ) + t0)- time;
eq.g2=(BiomassT-Biomass0)-yb*(Substrate0-SubstrateT);
fit g1 / outest=ParmEstimates1a;
run;
data ParmEstimates1a; set ParmEstimates1a; Dataset = 'Shuler-fixed-given'; length dataset
$ 30; run;

***** FIXED *****;
***** NOT GIVEN INITIAL PARAMETERS *****;

```



```

proc model data=integer MAXITER=10000 noprint;*CONVERGE=0.001; by SubstrateINIT rep;
title1 'Kinetics model - 6.52 equation with biomassT changing - Fixed';
parms mu ks ; Substrate0 = SubstrateINIT; Biomass0 = 0.5;
t0=0;
eq.g1 = ((( ( ((Ks*Yb + Substrate0*Yb + Biomass0)/(Substrate0*Yb + Biomass0)) *
log(BiomassT/Biomass0)) - ((Ks*Yb)/(Substrate0*Yb + Biomass0)) *
log((Yb*Substrate0 + Biomass0 - BiomassT) / (Yb*Substrate0)) ) / mu ) + t0) -time;
eq.g2=(BiomassT-Biomass0)-yb*(Substrate0-SubstrateT);
fit g1 / outest=ParmEstimates1b;
run;
data ParmEstimates1b; set ParmEstimates1b; Dataset = 'Shuler-fixed-notgiven'; length
dataset $ 30; run;

***** FITTED *****;
***** GIVEN INITIAL PARAMETERS *****;

proc model data=integer MAXITER=20000 noprint;*CONVERGE=0.001; by SubstrateINIT rep;
title1 'Kinetics model - 6.52 - OLS - Float';
parameters mu = 0.6 ks = 50 Substrate0 = 300 Biomass0 = 0.5;
t0=0;
eq.g1 = ( (( ( ((Ks*Yb + Substrate0*Yb + Biomass0)/(Substrate0*Yb + Biomass0)) *
log(BiomassT/Biomass0)) - ((Ks*Yb)/(Substrate0*Yb + Biomass0)) *
log((Yb*Substrate0 + Biomass0 - BiomassT) / (Yb*Substrate0)) ) / mu ) + t0) -time;
eq.g2=(BiomassT-Biomass0)-yb*(Substrate0-SubstrateT);
fit g1 / outest=ParmEstimates2a;
run;
data ParmEstimates2a; set ParmEstimates2a; Dataset = 'Shuler-float-given'; length dataset
$ 30;run;

***** FITTED *****;
***** NOT GIVEN INITIAL PARAMETERS *****;

proc model data=integer MAXITER=20000 noprint;*CONVERGE=0.001; by SubstrateINIT rep;
title1 'Kinetics model - 6.52 - OLS - Float';
parms mu ks Substrate0 = 300 Biomass0 = 0.5;
t0=0;
eq.g1 = ((( ( ((Ks*Yb + Substrate0*Yb + Biomass0)/(Substrate0*Yb + Biomass0)) *
log(BiomassT/Biomass0)) - ((Ks*Yb)/(Substrate0*Yb + Biomass0)) *
log((Yb*Substrate0 + Biomass0 - BiomassT) / (Yb*Substrate0)) ) / mu ) + t0) -time;.
eq.g2=(BiomassT-Biomass0)-yb*(Substrate0-SubstrateT);
fit g1 / outest=ParmEstimates2b;
run;
data ParmEstimates2b; set ParmEstimates2b; Dataset = 'Shuler-float-notgiven'; length
dataset $ 30;run;

***** NONLINEAR METHOD *****;

***** LEE METHOD *****;

***** FIXED *****;
***** GIVEN INITIAL PARAMETERS *****;

```

```

proc model data=integer CONVERGE=0.001 MAXITER=10000 noprint; by SubstrateINIT rep;
  title1 'Lee equation with biomassT and substrateT changing- Fixed';
parameters mu = 0.6 ks = 50; Biomass0 = 0.5; Substrate0 = SubstrateINIT;
parms ks mu Biomass0 Substrate0;
  endogenous BiomassT substrateT;
  exogenous time;
eq.g1=(( (ks*Yb/(Biomass0+Substrate0*Yb))+1)*log(BiomassT/Biomass0)+
  ((ks*Yb/(Biomass0+Substrate0*Yb))*log(Substrate0/SubstrateT)))-time*mu;
eq.g2=(BiomassT-Biomass0)-yb*(Substrate0-SubstrateT);
fit g1 / outest=ParmEstimates3a;
run;
data ParmEstimates3a; set ParmEstimates3a; dataset = 'Lee-fixed-given'; length dataset $
30; run;

***** FIXED *****;
***** NOT GIVEN INITIAL PARAMETERS *****;

proc model data=integer CONVERGE=0.001 MAXITER=10000 noprint; by SubstrateINIT rep;
  title1 'Lee equation with biomassT and substrateT changing- Fixed';
parms mu ks; Biomass0 = 0.5; Substrate0 = SubstrateINIT;
  endogenous BiomassT substrateT;
  exogenous time;
eq.g1=(( (ks*Yb/(Biomass0+Substrate0*Yb))+1)*log(BiomassT/Biomass0)+
  ((ks*Yb/(Biomass0+Substrate0*Yb))*log(Substrate0/SubstrateT)))-time*mu;
eq.g2=(BiomassT-Biomass0)-yb*(Substrate0-SubstrateT);
fit g1 / outest=ParmEstimates3b;
run;
data ParmEstimates3b; set ParmEstimates3b; dataset = 'Lee-fixed-notgiven'; length dataset
$ 30; run;

***** FITTED *****;
***** GIVEN INITIAL PARAMETERS *****;

proc model data=integer CONVERGE=0.001 MAXITER=10000 noprint; by SubstrateINIT rep;
  title1 'Lee equation with biomassT and substrateT changing - Float';
parameters mu = 0.6 ks = 50 Substrate0 = 300 Biomass0 = 0.5;
  endogenous BiomassT substrateT;
  exogenous time;
eq.g1=(( (ks*Yb/(Biomass0+Substrate0*Yb))+1)*log(BiomassT/Biomass0)+
  ((ks*Yb/(Biomass0+Substrate0*Yb))*log(Substrate0/SubstrateT)))-time*mu;
eq.g2=(BiomassT-Biomass0)-yb*(Substrate0-SubstrateT);
fit g1 g2 / outest=ParmEstimates4a;
run;
data ParmEstimates4a; set ParmEstimates4a; dataset = 'Lee-float-given'; run;

***** FITTED *****;
***** NOT GIVEN INITIAL PARAMETERS *****;

proc model data=integer CONVERGE=0.001 MAXITER=10000 noprint; by SubstrateINIT rep;
  title1 'Lee equation with biomassT and substrateT changing - Float';
parms mu ks Substrate0 = 300 Biomass0 = 0.5;
  endogenous BiomassT substrateT;
  exogenous time;
eq.g1=(( (ks*Yb/(Biomass0+Substrate0*Yb))+1)*log(BiomassT/Biomass0)+
  ((ks*Yb/(Biomass0+Substrate0*Yb))*log(Substrate0/SubstrateT)))-time*mu;

```

```

eq.g2=(BiomassT-Biomass0)-yb*(Substrate0-SubstrateT);
fit g1 g2 / outest=ParmEstimates4b;
run;
data ParmEstimates4b; set ParmEstimates4b; dataset = 'Lee-float-notgiven'; run;

***** ROBINSON METHOD with Substrate changing is a permutation of LEE *****;
***** FIXED *****;
***** GIVEN INITIAL PARAMETERS *****;

**From: Dr.Drapcho's master student thesis - with substrateT changing only **;
proc model data=integer CONVERGE=0.001 MAXITER=10000 noprint; by SubstrateINIT rep;
  title1 'Robinson equation with SubstrateT changing - Fixed';
  parameters mu = 0.6 ks = 50; Biomass0 = 0.5; Substrate0 = SubstrateINIT;
  endogenous BiomassT substrateT;
  exogenous time;
  eq.g1=((ks*Yb/(Biomass0+Substrate0*yb))+1)*log((yb*(Substrate0-SubstrateT)+Biomass0)/Biomass0)+
    ((ks*Yb/(Biomass0+Substrate0*Yb))*log(Substrate0/SubstrateT))-time*mu;
  eq.g2=(BiomassT-Biomass0)-yb*(Substrate0-SubstrateT);
  fit g1 / outest=ParmEstimates5a;
run;
data ParmEstimates5a; set ParmEstimates5a; dataset = 'Robinson-fixed-given'; length
dataset $ 40; run;

***** FIXED *****;
***** NOT GIVEN INITIAL PARAMETERS *****;

**From: Dr.Drapcho's master student thesis - with substrateT changing only **;
proc model data=integer CONVERGE=0.001 MAXITER=10000 noprint; by SubstrateINIT rep;
  title1 'Robinson equation with SubstrateT changing - Fixed';
  parms ks mu; Biomass0 = 0.5; Substrate0 = SubstrateINIT;
  endogenous BiomassT substrateT;
  exogenous time;
  eq.g1=((ks*Yb/(Biomass0+Substrate0*yb))+1)*log((yb*(Substrate0-SubstrateT)+Biomass0)/Biomass0)+
    ((ks*Yb/(Biomass0+Substrate0*Yb))*log(Substrate0/SubstrateT))-time*mu;
  eq.g2=(BiomassT-Biomass0)-yb*(Substrate0-SubstrateT);
  fit g1 / outest=ParmEstimates5b;
run;
data ParmEstimates5b; set ParmEstimates5b; dataset = 'Robinson-fixed-notgiven'; length
dataset $ 40; run;

***** FITTED *****;
***** GIVEN INITIAL PARAMETERS *****;

**From: Dr.Drapcho's master student thesis - with substrateT changing only **;
proc model data=integer CONVERGE=0.001 MAXITER=10000 noprint; by SubstrateINIT rep;
  title1 'Robinson equation with SubstrateT changing - Fixed';
  parameters mu = 0.6 ks = 50 Substrate0 = 300 Biomass0 = 0.5;
  endogenous BiomassT substrateT;
  exogenous time;
  eq.g1=((ks*Yb/(Biomass0+Substrate0*yb))+1)*log((yb*(Substrate0-SubstrateT)+Biomass0)/Biomass0)+
    ((ks*Yb/(Biomass0+Substrate0*Yb))*log(Substrate0/SubstrateT))-time*mu;
  eq.g2=(BiomassT-Biomass0)-yb*(Substrate0-SubstrateT);

```

```

fit g1 / outest=ParmEstimates6a;
run;
data ParmEstimates6a; set ParmEstimates6a; dataset = 'Robinson-float-given'; length
dataset $ 40; run;
***** FITTED *****;
***** NOT GIVEN INITIAL PARAMETERS *****;

**From: Dr.Drapcho's master student thesis - with substrateT changing only **;
proc model data=integer CONVERGE=0.001 MAXITER=10000 noprint; by SubstrateINIT rep;
title1 'Robinson equation with SubstrateT changing - Fixed';
parms mu ks Substrate0 = 300; Biomass0 = 0.5;
endogenous BiomassT substrateT;
exogenous time;
eq.g1=((ks*Yb/(Biomass0+Substrate0*yb))+1)*log((yb*(Substrate0-
SubstrateT)+Biomass0)/Biomass0)+
((ks*Yb/(Biomass0+Substrate0*Yb))*log(Substrate0/SubstrateT))-time*mu;
eq.g2=(BiomassT-Biomass0)-yb*(Substrate0-SubstrateT);
fit g1 / outest=ParmEstimates6b;
run;
data ParmEstimates6b; set ParmEstimates6b; dataset = 'Robinson-float-notgiven'; length
dataset $ 40; run;

*****;

data nonlinear1 errors; length dataset $ 20 SubstrateINIT rep _NUSED_ 3 group $ 3 ;
set ParmEstimates1a ParmEstimates2a ParmEstimates3a ParmEstimates4a
ParmEstimates1b ParmEstimates2b ParmEstimates3b ParmEstimates4b
ParmEstimates5a ParmEstimates5b ParmEstimates6a ParmEstimates6b;
if SubstrateINIT = 200 then group='A';
if SubstrateINIT = 250 then group='B';
if SubstrateINIT = 300 then group='C';
if SubstrateINIT = 350 then group='D';
if SubstrateINIT = 400 then group='E';
if SubstrateINIT = 450 then group='F';
if SubstrateINIT = 500 then group='G';
if SubstrateINIT = 550 then group='H';
if SubstrateINIT = 600 then group='I';
if SubstrateINIT = 650 then group='J';
if SubstrateINIT = 700 then group='K';
if SubstrateINIT = 750 then group='L';
if SubstrateINIT = 800 then group='M';
if SubstrateINIT = 850 then group='N';
if SubstrateINIT = 900 then group='O';
if SubstrateINIT = 950 then group='P';
if SubstrateINIT = 1000 then group='Q';

keep Biomass0 Dataset Substrate0 SubstrateINIT _NUSED_ _STATUS_ group ks mu rep;
if _STATUS_ eq '3 Error' then output errors;
else if Ks lt 0 then output errors;
else if Ks gt 1000 then output errors;
else if mu lt 0 then output errors;
else if Substrate0 ne . and Substrate0 lt 0 then output errors;
else if Substrate0 gt 10000 then output errors;
else output nonlinear1;
run;

```

```

data output.nonlinear5; set nonlinear1;
  keep Biomass0 Dataset Substrate0 SubstrateINIT _NUSED_ _STATUS_ group ks mu rep;
run;

data output.Errors5; set errors;
  keep Biomass0 Dataset Substrate0 SubstrateINIT _NUSED_ _STATUS_ group ks mu rep;
run;

*proc print data=nonlinear1;
  *title1 'Individual observations by categories';
*run;

proc sort data = errors; by dataset ;
proc means data = errors ; by dataset ;
  title1 'Means by categories for errors';
  var ks mu ;
  output out=next2 mean= MeanKs MeanMu ;
run;

proc sort data = nonlinear1; by dataset ;

proc means data = nonlinear1 ; by dataset ;
  title1 'Means by categories for nonlinear without errors';
  var ks mu ;
  output out=next1 mean= MeanKs MeanMu ;
run;

proc univariate data=nonlinear1 plot normal NOBYPLOT; by dataset;* SubstrateINIT;
  var ks mu ;
run;

options ps=50 ls=99;
proc chart data=nonlinear1;by dataset;
vbar ks/subgroup=group;
run;

ODS HTML file='C:\ ERIKA Monte Carlo program\linear program e
output'\NonlinearMeans.html'
  Style=Styles.Minimal;

proc print data=next1;
  title1 'Means by categories for nonlinear without errors';
run;

proc print data=next2;
  title1 'Means by categories for errors';
run;
ods html close;

quit;

```

I.4 Linear models fitting: step 4.

```
dm'log;clear;output;clear';
```

```

options ps=80 ls=132 nocenter nodate nonumber; **** 020304 newest file ***;

libname output 'C:\ERIKA Monte Carlo program\linear program e output';

data Integer; set output.Integer5;
***** LINEAR METHOD *****;

ODS HTML file='C:\ERIKA Monte Carlo program\linear program e output\LinearMeans3.html'
Style=Styles.Minimal;

***** LINEAR METHOD *****;

data subset1 subset2 subset3 subset4 Whole; set Integer; length category $ 40;
Title1 "Linearization methods";
  lxbt = log(BiomassT);
  Category='Whole';
  output Whole;
  Category='Exponential2-MiddleTime';
  if time LE 4 then Category='Exponential1-EarlyTime';
  if time GE 8 then Category='Stationary-LateTime';
  output subset1;
  Category='Omit';
  if substrateINIT GE 500 and substrateINIT le 700 then Category = 'MediumSubstrate';
  if substrateINIT LE 400 then Category = 'LowSubstrate';
  if substrateINIT GE 800 then Category = 'HighSubstrate';
  output subset2;
  Category='Omit';
  if SubstrateINIT = 200 then Category = 'Select';
  if SubstrateINIT = 400 then Category = 'Select';
  if SubstrateINIT = 600 then Category = 'Select';
  if SubstrateINIT = 800 then Category = 'Select';
  if SubstrateINIT = 1000 then Category = 'Select';
  output subset3;
  if category = 'Select' then do;
    Category='Select-Exponential2';
    if time LE 4 then Category='Select-Exponential1';
    if time GE 8 then Category='Select-Stationary';
  end;
  output subset4;
end;

run;

data categories; set subset1 subset2 subset3 subset4 whole; length dataset $ 40;
  if Category='Omit' then delete;
run;

proc sort data=categories; by category rep substrateINIT; run;

*****
*****

proc means data=categories noprint ;

```

```

var substrateT;
by category rep substrateINIT ;
output out=linearX mean=submean; *** the submean is the averaged substrate for each time
period **;
Title1 "The Three phases together over the average of the entire substrateT ";
run;
data linearX; set linearX; keep category rep substrateINIT submean; run;
*proc print data=linearX; run;

proc reg data=categories outest=linear2 noprint; by category rep substrateINIT;
title2 "First Fit step1 - plot ln(biomass) versus time to get the slope=mu";
model lxbt = time;
run;

data linear1; merge linear2 linearX; by category rep substrateINIT;
run;
*proc print data=linear1; run;

proc sort data=linear1; by category rep substrateINIT; run;

data linear1; set linear1;
title2 "First Fit step1 - plot ln(biomass) versus time to get the slope=mu";
Mu=time; *** time is the slope in this data set***;
Sub_Mu = submean / Mu; *** The Sub_Mu is the Substrate divided by mu***;
inv_sub = 1 / submean;
inv_Mu = 1 / Mu;
run;

*****;

***** HANES PLOT method *****;
***** Hanes Plot for the categories *****;
*****;

proc reg data=linear1 outest=linear3 noprint; by category rep;
Title2 "Hanes Plot Calculations for the categories";
model Sub_Mu = submean; ***this submean is the real averaged substrate***;
run;
*proc print data=linear3; run;

data linear3; length dataset $ 30; set linear3;
Title2 "Kinetic Parameters Calculations using Hanes Plot for the categories";
MuMax = 1 / submean; ***the submean is the slope from the regression results of
linear2***;
ksXX = MuMax * intercept;
Dataset = 'Hanes Plot';
run;

data Hanes_para; *** the kinetic parameters of Hanes calculations ****;
set linear3;
keep category rep submean MuMax ksXX Dataset;
run;
title2 "Kinetic Parameters Calculations using Hanes Plot for the categories";
proc print data=Hanes_para;

run;

```

```

*****;

***** Lineweaver-Burk Plot method *****;
***** Lineweaver-Burk Plot method for the categories *****;

*****;

proc reg data=linear1 outest=linear4 noprint; by category rep;
Title2 "Lineweaver-Burk Plot Calculations for the categories";
    model inv_Mu = inv_sub;    *** this submean is the real averaged substrate ****;
run;

data linear4; length dataset $ 30; set linear4;
    Title2 "Kinetic Parameters Calculations using Lineweaver-Burk Plot for categories";
    MuMax = 1 / intercept;    *** the substrateINIT is the slope from the regression
results of linear2 ****;
    ksXX = MuMax * inv_sub;
Dataset='Lineweaver-Burk Plot';
run;

data Line_para;    ***kinetic parameters for phase3 using Lineweaver-Burk plot ***;
set linear4;
keep category rep submean MuMax ksXX Dataset;
run;
title2 "Kinetic Parameters Calculations using Lineweaver-Burk Plot for categories";
proc print data=Line_para; run;

*****;
***** MEANS OF THE CATEGORIES *****;
***** output results to permanent SAS datasets *****;

data para;
set Hanes_para Line_para; run;

data linear; set para;run;

proc sort data=linear; by dataset category ; run;
proc univariate data=linear plot normal nobyplot ; by dataset category;
var ksXX muMax;
run;

proc means data = linear noprint; by dataset category;
    title1 'Means by categories for the integer substrates ';
    var ksXX muMax;
output out=new1 mean= MeanKsXX MeanMuXX ;
run;
proc print data=new1;run;

quit;

ods html close;

```


APPENDIX J

J.1 THE PROGRAM USED TO DEVELOP THE HISTOGRAM GRAPHS FOR THE μ_{\max} AND THE K_s MEANS KINETIC PARAMETER ESTIMATIONS FROM THE NONLINEAR OUTPUT

```
dm'log;clear;output;clear';
options ps=80 ls=132 nocenter nodate nonumber; **** 020304 newest file ***;

libname output 'C:\Erika Reeves - Monte Carlo from Geaghan\NONLINEAR 021704';

data nonlinear; set output.nonlinear5;
    *vars Biomass0 Dataset Substrate0 SubstrateINIT _NUSED_ _STATUS_ group ks mu rep;
run;
proc sort data=nonlinear; by dataset; run;

/*
proc univariate data=nonlinear plot normal NOBYPLOT; by dataset;* SubstrateINIT;
    var ks mu ;
run;
*/

GOPTIONS DEVICE=cgm GSFMODE=REPLACE GSFNAME=OUT ftext="Swiss" ftitle="Swiss";
GOPTIONS GSFNAME=OUT3;
FILENAME OUT3 'C:\Erika Reeves - Monte Carlo from Geaghan\NONLINEAR 021704\NLHist1.CGM';

proc gchart data=nonlinear; by dataset;
    vbar ks / type=freq midpoints=0 to 280 by 20 ;
    ***Graphs for the Ks kinetic parameter ***;

    PATTERN C=RED V=S ;
run;

GOPTIONS DEVICE=cgm GSFMODE=REPLACE GSFNAME=OUT ftext="Swiss" ftitle="Swiss";
GOPTIONS GSFNAME=OUT4;
FILENAME OUT4 'C:\Erika Reeves - Monte Carlo from Geaghan\NONLINEAR 021704\NLHist2.CGM';

proc gchart data=nonlinear; by dataset;
    vbar mu / type=freq midpoints=0.48 to 0.8 by 0.02;
    ***Graphs for the mumax kinetic parameter ***;

    PATTERN C=blue V=S;

run; quit;
```

The following Figures from J.1 to J.12 are the histograms for the μ_{\max} determined from the twelve nonlinear combinations using the SAS program. The kinetic parameter,

μ_{\max} , has the x-axis range from 0.5 to 0.96 and the y-axis range is for the frequency that those values appear. The Figure J.1 is for the Lee equation-fixed-given, the Figure J.2 is for the Lee equation-fixed-not given, the Figure J.3 is for the Lee equation-float-given, the Figure J.4 is for the Lee equation-float-not given, the Figure J.5 is for the Robinson equation-fixed-given, the Figure J.6 is for the Robinson equation-fixed-not given, the Figure J.7 is for the Robinson equation-float-given, the Figure J.8 is for the Robinson equation-float-not given, the Figure J.9 is for the Shuler & Kargi equation-fixed-given, the Figure J.10 is for the Shuler & Kargi equation-fixed-not given, the Figure J.11 is for the Shuler & Kargi equation-float-given, and finally the Figure J.12 is for the Shuler & Kargi equation-float-not given.

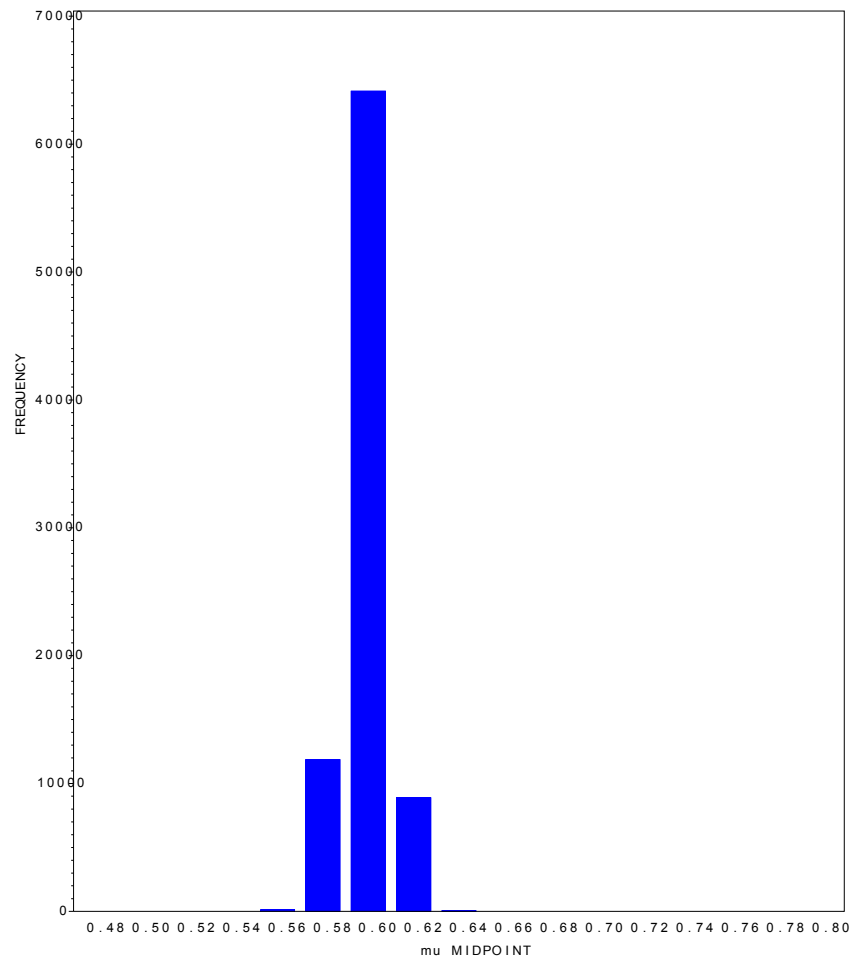


Figure J.1 Lee Equation – Fixed – Given for MuMax

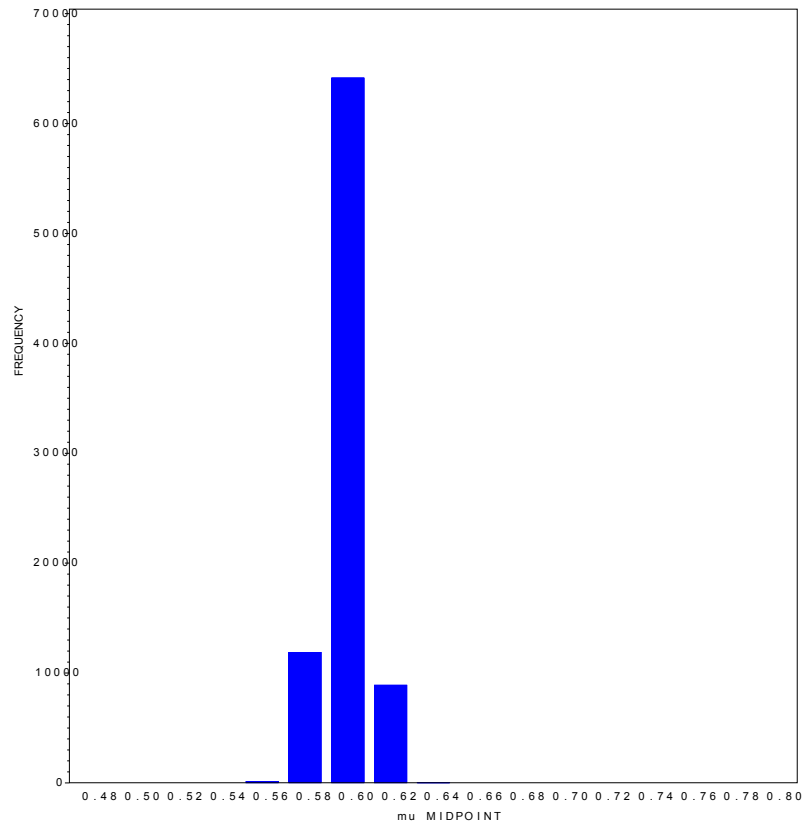


Figure J.2 Lee Equation – Fixed – Not Given for MuMax

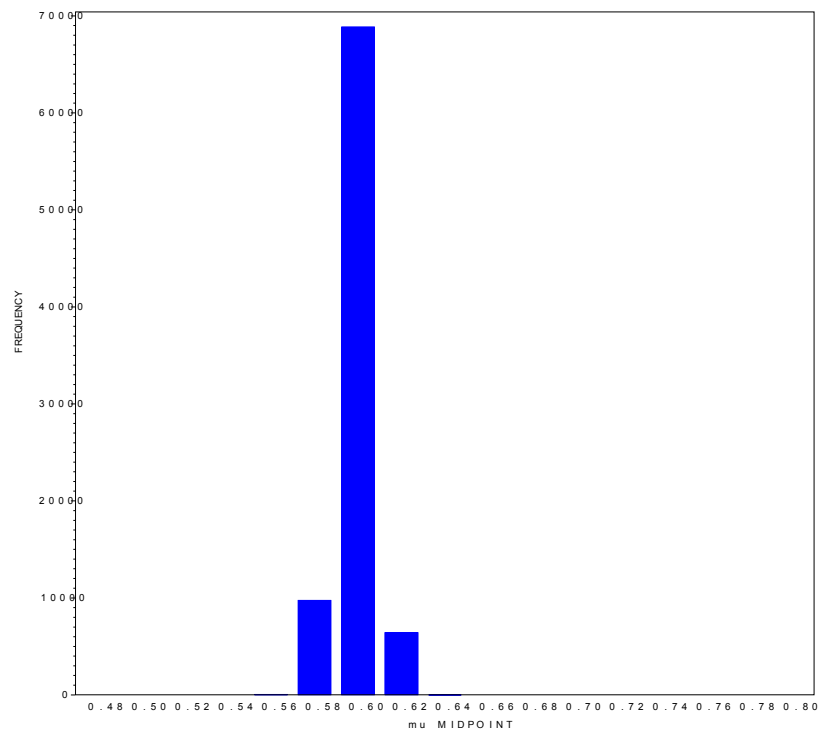


Figure J.3 Lee Equation – Fitted – Given for MuMax

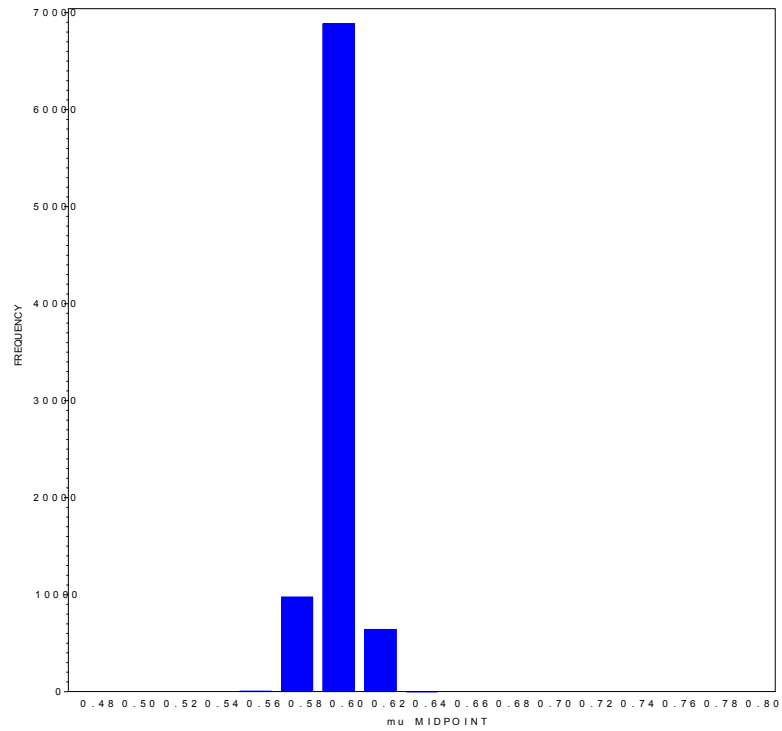


Figure J.4 Lee Equation – Fitted – Not Given for MuMax

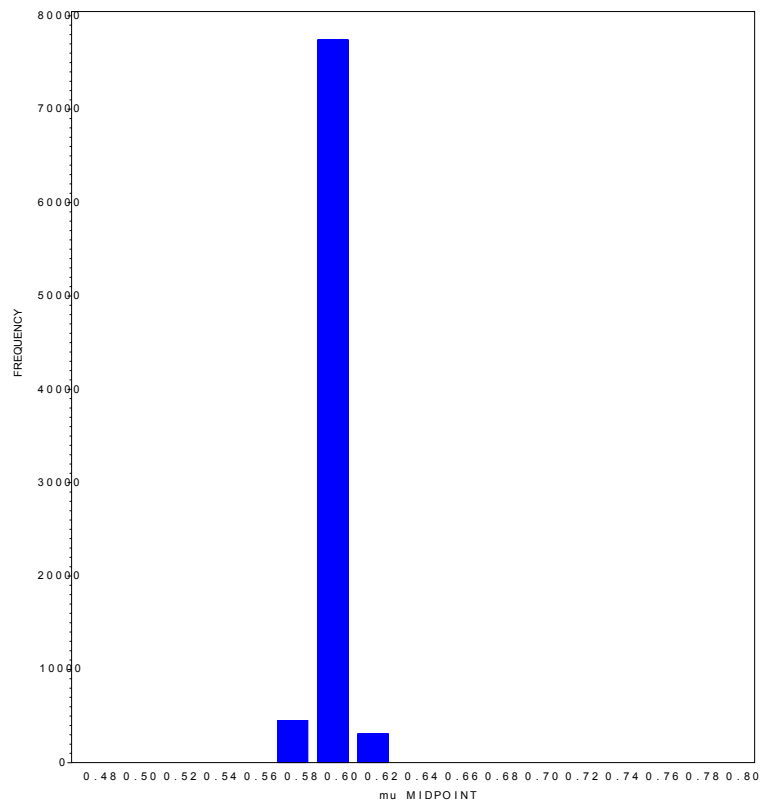


Figure J.5 Robinson Equation – Fixed – Given for MuMax

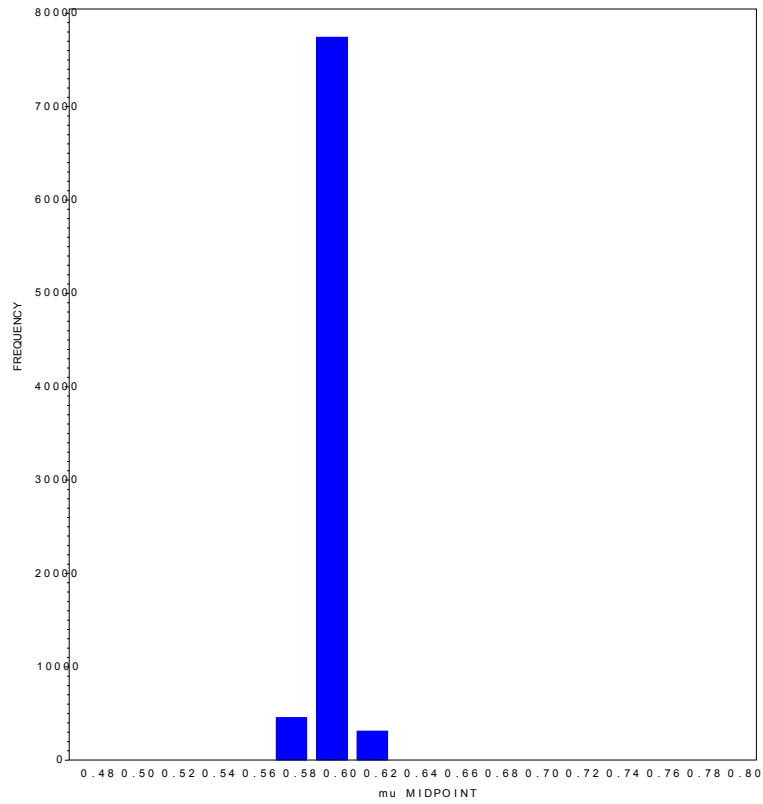


Figure J.6 Robinson Equation – Fixed – Not Given for MuMax

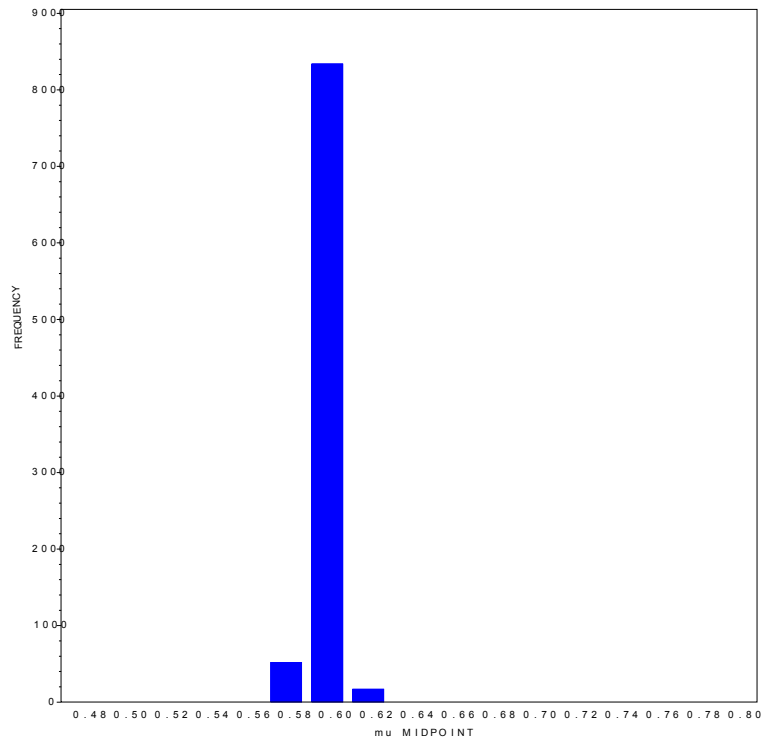


Figure J.7 Robinson Equation – Fitted – Given for MuMax

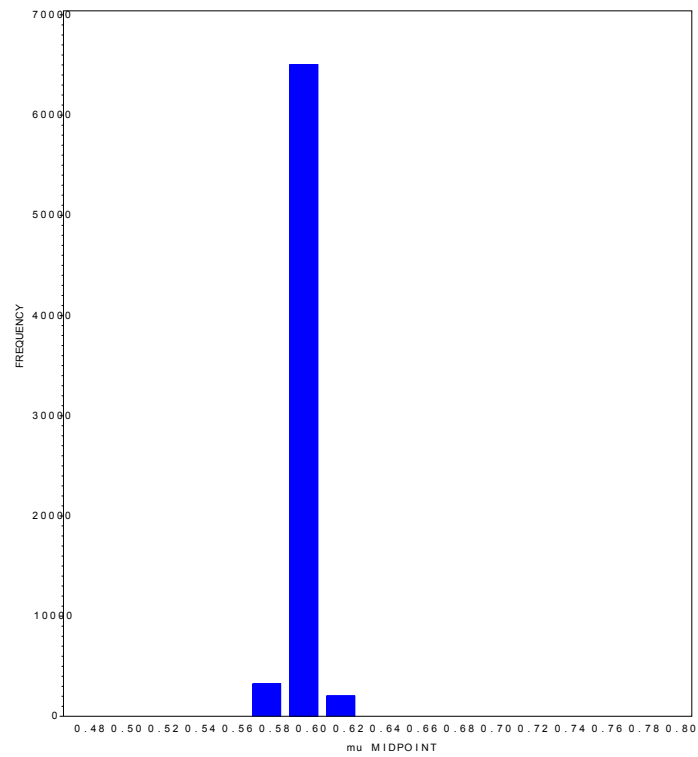


Figure J.8 Robinson Equation – Fitted – Not Given for MuMax

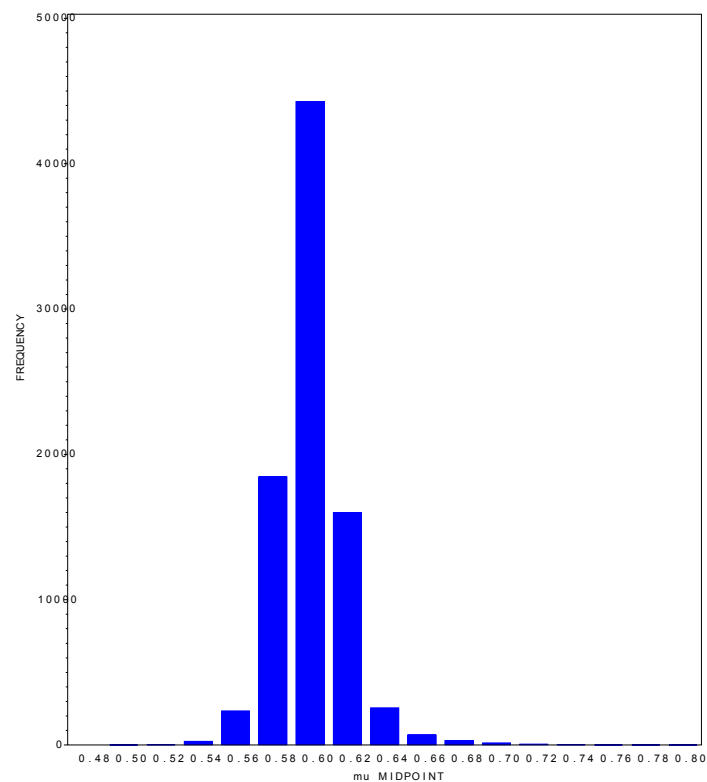


Figure J.9 Shuler & Kargi Equation – Fixed– Given for MuMax

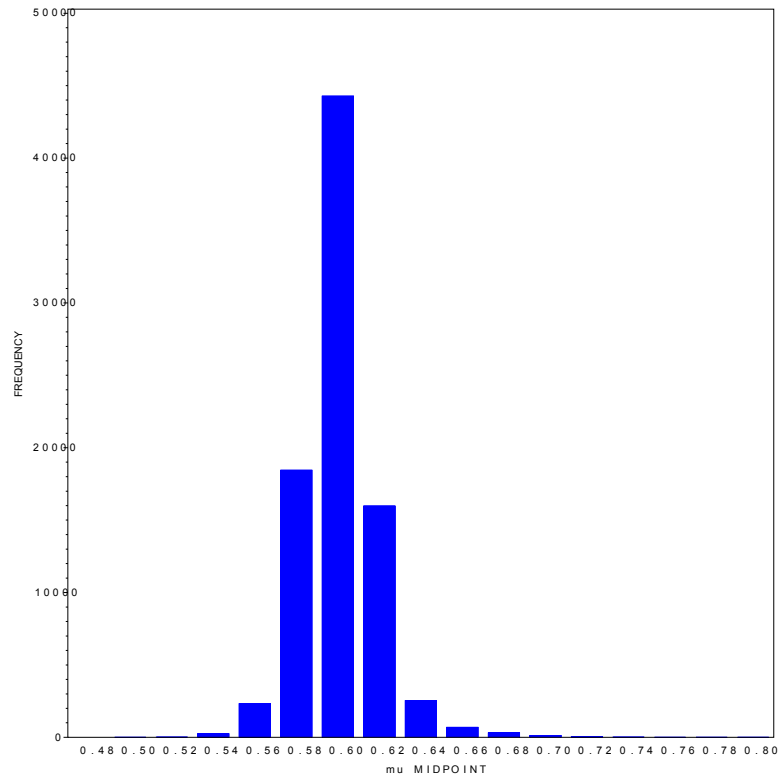


Figure J.10 Shuler & Kargi Equation – Fixed– Not Given for MuMax

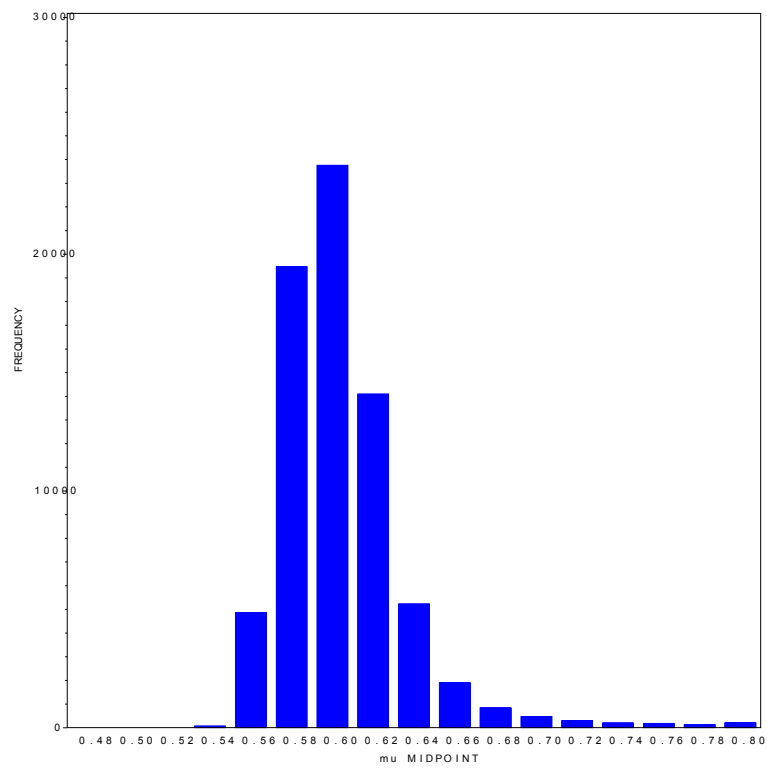


Figure J.11 Shuler & Kargi Equation – Fitted– Given for MuMax

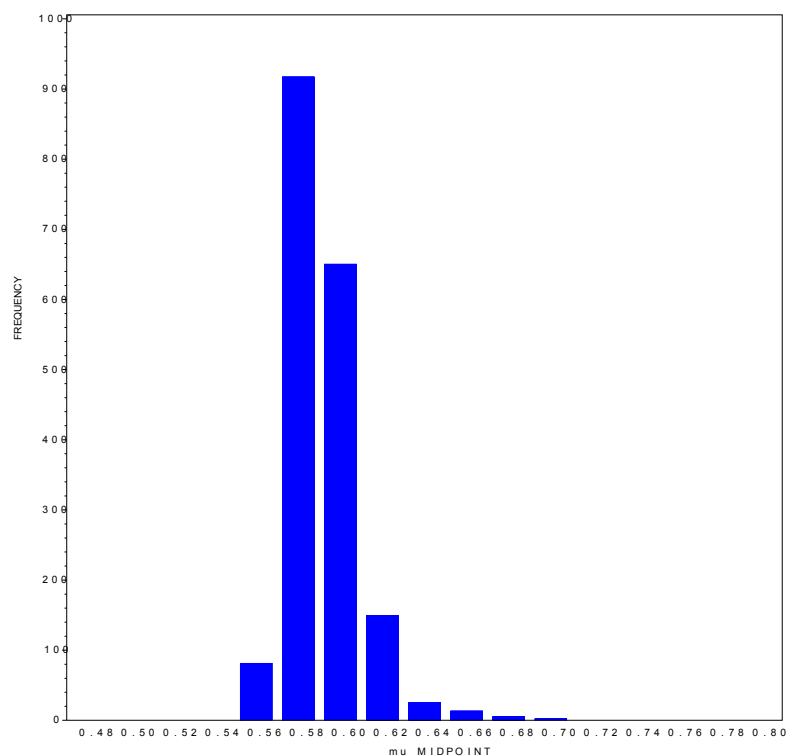


Figure J.12 Shuler & Kargi Equation – Fitted– Not Given for MuMax

VITA

Erika Guimarães Madeira Reeves was born in São Paulo city, São Paulo state, Brazil, on October 27, 1976, to Mr. Ari Madeira and Mrs. Creusa Guimarães Madeira. She attended elementary through high school in Campinas, São Paulo state, Brazil, and in August 1994 she was an exchange student for her senior year at The Dunham School in Baton Rouge, Louisiana. In January 1996 she enrolled in Louisiana State University as an undergraduate and participated in many student organizations; becoming the vice president of “SHPE” (Society of Hispanic Professional Engineers) organization for a year. She was chosen to participate in a minority summer internship research program with the biological sciences department called “LAMP”. During the “LAMP” program she chose to do the summer research with Dr. Arthur Sterling from the Chemical Engineering Department, LSU. Erika received the degree of Bachelor of Science in Biological and Agricultural Engineering in May 2001. She received a second place award for her group senior design project called ‘The Production of Ethanol from Sweet Potato Waste’ at the Institute of Biological Engineering Conference in Sacramento, California state, in August 2001. She is currently enrolled in Louisiana State University as a candidate for the degree of Master of Science in Biological and Agriculture Engineering, which will be awarded in May 2004.